UNIVERSITY OF ALBERTA

Investigation of Animal Models of Copper Storage Disorders

By

Veronica A. Coronado ©

A thesis submitted to the Faculty of Graduate Studies and Research
in partial fulfillment of the requirements for the degree of

Doctor of Philosophy

in

Medical Sciences – Medical Genetics

Edmonton, Alberta
Fall 2006

Library and
Archives Canada

Published Heritage
Branch

395 Wellington Street
Ottawa ON K1A 0N4
Canada

Bibliothèque et
Archives Canada

Direction du
Patrimoine de l'édition

395, rue Wellington
Ottawa ON K1A 0N4
Canada

Your file Votre référence
ISBN: 978-0-494-23008-4
Our file Notre référence
ISBN: 978-0-494-23008-4

NOTICE:
The author has granted a non-exclusive license allowing Library and Archives Canada to reproduce, publish, archive, preserve, conserve, communicate to the public by telecommunication or on the Internet, loan, distribute and sell theses worldwide, for commercial or non-commercial purposes, in microform, paper, electronic and/or any other formats.

The author retains copyright ownership and moral rights in this thesis. Neither the thesis nor substantial extracts from it may be printed or otherwise reproduced without the author's permission.

AVIS:
L'auteur a accordé une licence non exclusive permettant à la Bibliothèque et Archives Canada de reproduire, publier, archiver, sauvegarder, conserver, transmettre au public par télécommunication ou par l'Internet, prêter, distribuer et vendre des thèses partout dans le monde, à des fins commerciales ou autres, sur support microforme, papier, électronique et/ou autres formats.

L'auteur conserve la propriété du droit d'auteur et des droits moraux qui protège cette thèse. Ni la thèse ni des extraits substantiels de celle-ci ne doivent être imprimés ou autrement reproduits sans son autorisation.

In compliance with the Canadian Privacy Act some supporting forms may have been removed from this thesis.

While these forms may be included in the document page count, their removal does not represent any loss of content from the thesis.

Conformément à la loi canadienne sur la protection de la vie privée, quelques formulaires secondaires ont été enlevés de cette thèse.

Bien que ces formulaires aient inclus dans la pagination, il n'y aura aucun contenu manquant.

Canada

ABSTRACT

Copper (Cu) is essential, yet cytotoxic when allowed to accumulate. To date, Wilson disease (WD) is the only human Cu-storage disease for which a gene (*ATP7B*) has been cloned. This thesis focuses on the characterization of genes involved in animal models of Cu-storage to provide insight into the Cu-transport pathway and lead to a better understanding of the molecular defects responsible for human Cu-storage.

The toxic milk (*tx*) mouse is a true model of WD with a mutation in *Atp7b*, but colonies have become virus-infected, reducing their use in animal studies. In 1987, a new mutation (tx^J) arose at the Jackson Laboratories and was shown to be allelic the *tx* mutation. I characterized the *Atp7b* gene in these mice and identified a Gly712Asp mutation, which pinpoints a functionally important region in the Atp7b protein, and allows for genotype testing to distinguish between normal and tx^J mice.

Copper toxicosis (CT) in Bedlington terriers is not due to defects in *ATP7B*. *ATP6H* was excluded as the causative gene in CT, based on data presented in this thesis. With further analysis of candidate genes, I confirmed a *MURR1 (COMMD1)* exon 2-deletion as a potential cause of the disorder in typical affected dogs. However, not all affected dogs in our cohort were homozygous for the *MURR1 (COMMD1)* deletion. Subsequent sequence analysis of *MURR1 (COMMD1)* in these dogs identified no *de novo* mutations, suggesting the participation of additional genes in the etiology of this disorder. We analyzed the potential of canine *ATP7B* acting as a modifier of CT and identified a polymorphism in all Bedlington terriers analyzed. To further characterize MURR1 (COMMD1) and comprehend its role in CT, I propose cell culture experiments and present preliminary data, including antibody production and cellular Cu-toxicity analysis. In hopes of providing supporting evidence for the role of MURR1 (COMMD1) in Cu-

homeostasis, I sequenced 26 patients with Cu-storage of unknown etiology, but failed to identify any mutations in *MURR1 (COMMD1)*. This suggests that *MURR1 (COMMD1)* does not significantly contribute to human Cu-storage disease, which is important information for diagnosis of sibs of patients with Cu-storage disease.

ACKNOWLEDGEMENTS

I would like to start by thanking my supervisor, Dr. Diane Cox, for her constant enthusiasm and support for the "dog project". I am grateful to have had the opportunity to work in her lab and appreciate her belief in my potential. I would like to thank my other committee members, Drs. Walter and Glerum, for their critical analysis of my work and suggestions during my doctoral training, their trust in my abilities, and support for my decisions.

I would like to acknowledge past and present members of the "Cox lab" and thank them for providing a fun and relaxed work environment. Special thanks to: Manoj for his patience while I was learning to follow in his footsteps, Lisa and Susan for answering all my sequencing queries and bringing me goodies from vendor exhibits, Gina and Gloria for their guidance and scientific discussions, and their friendship.

I would like to thank the funding groups that supported my work: Natural Sciences and Engineering Research Council of Canada, Canadian Liver Foundation, Faculty of Graduate Studies and Research, Faculty of Medicine and Dentistry, and Canadian Genetic Diseases Network.

Last, but never least, my family: my husband Richie, my mom and dad, and my in-laws. Though they may not always understand what I am doing, they never fail to provide me with encouragement and support.

Thank you to everyone who told me that I could do it.

TABLE OF CONTENTS

CHAPTER 1 : INTRODUCTION **1**

I. COPPER 2
  i. Essentiality of Copper *2*
  ii. Toxicity of Copper *4*
II. COPPER HOMEOSTASIS 5
  i. Uptake *5*
  ii. Distribution to Tissues *7*
  iii. Intracellular Copper *8*
    a. Cellular Import 8
    b. Copper Chaperones 10
    c. Cellular Export 13
    d. Detoxification 16
  iv. Excretion *17*
    a. Liver Structure 18
    b. Copper in Bile 18
  v. Disruption Of Copper Homeostasis *21*
III. WILSON DISEASE 22
  i. Clinical Presentation *22*
    a. Hepatic 22
    b. Neurologic 23
    c. Psychiatric 23
    d. Other 23
  ii. Pathology *23*
  iii. Biochemistry *25*
  iv. Treatment *26*
  v. Wilson Disease Gene *27*
    a. Mutation Analysis 28
  vi. Wilson Disease Protein *30*
IV. ANIMAL MODELS OF WILSON DISEASE 32
  i. Long-Evans Cinnamon Rat *33*
  ii. Toxic Milk Mouse *35*
  iii. Atp7b Null Mice *37*
V. OTHER COPPER STORAGE DISORDERS 38
  i. Indian Childhood Cirrhosis (ICC) *39*
  ii. Endemic Tyrolean Infantile Cirrhosis (ETIC) *40*
VI. OTHER ANIMAL MODELS OF COPPER STORAGE 40
  i. North Ronaldsay Sheep *41*
  ii. Bedlington terrier *42*
VII. OUTLINE OF THESIS 45

CHAPTER 2 : THE JACKSON TOXIC MILK MOUSE AS A MODEL FOR COPPER LOADING **47**

I. INTRODUCTION 48
II. METHODS AND SAMPLES 50
III. RESULTS AND DISCUSSION 52

CHAPTER 3 : ATP6H, A SUBUNIT OF VACUOLAR ATPASE INVOLVED IN METAL TRANSPORT: EVALUATION IN CANINE COPPER TOXICOSIS **57**

I. INTRODUCTION 58
II. MATERIALS AND METHODS 60
  i. Isolation of Canine ATP6H cDNA *60*
  ii. RT-PCR *60*
  iii. Genomic Southern Blotting *61*

iv. Isolation of Canine ATP6H Genomic Clones ... 62
v. Mapping of Canine ATP6H and C04107ipcr on a Canine Radiation Hybrid Panel ... 62
vi. Mutation Analysis ... 63
III. RESULTS ... 64
i. Genomic Southern Blot Analysis of Canine ATP6H ... 64
ii. Cloning and cDNA Analysis of the Canine ATP6H ... 64
iii. Cloning of the Genomic Region of Canine ATP6H ... 64
iv. Mapping of Canine ATP6H and C04107ipcr on a Canine Radiation Hybrid Panel ... 67
v. Mutation Analysis of the ATP6H Sequence From the Affected Bedlington terrier ... 68
IV. DISCUSSION ... 68

CHAPTER 4 : NEW HAPLOTYPES IN THE BEDLINGTON TERRIER INDICATE COMPLEXITY IN COPPER TOXICOSIS ... 71

I. INTRODUCTION ... 72
II. MATERIALS AND METHODS ... 74
i. Animals and Samples ... 74
ii. Bioinformatics ... 75
iii. Gene Sequencing ... 75
iv. Mutation Analysis ... 77
v. Southern Blot Analysis ... 77
vi. Northern Blot Analysis ... 77
vii. Haplotype Analysis ... 78
viii. RNA Analysis ... 78
III. RESULTS ... 79
i. Analysis of Candidate Genes ... 79
ii. Mutation Analysis of MURR1 ... 80
iii. Haplotype Analysis ... 82
iv. MURR1 Sequence Comparison and Tissue Expression ... 85
IV. DISCUSSION ... 85

CHAPTER 5 : A POLYMORPHISM IDENTIFIED IN CANINE *ATP7B*: CANDIDATE MODIFIER OF COPPER TOXICOSIS IN THE BEDLINGTON TERRIER ... 92

I. INTRODUCTION ... 93
II. METHODS AND MATERIALS ... 95
i. cDNA Library Screening ... 95
ii. Animals and Samples ... 95
iii. Cloning of ATP7B cDNA ... 98
iv. Sequencing of the Canine ATP7B Gene ... 100
III. RESULTS ... 102
i. Canine cDNA Library Screening ... 102
ii. ATP7B Cloning ... 102
iii. ATP7B Sequence Analysis ... 106
IV. DISCUSSION ... 108

CHAPTER 6 : *COMMD1* (*MURR1*) AS A CANDIDATE IN PATIENTS WITH COPPER STORAGE DISEASE OF UNDEFINED ETIOLOGY ... 112

I. INTRODUCTION ... 113
II. PATIENTS ... 114
III. RESULTS AND DISCUSSION ... 116
i. COMMD1 Mutation and Haplotype Analysis ... 116

CHAPTER 7 : PRELIMINARY STUDIES FOR THE FUNCTIONAL CHARACTERIZATION OF HUMAN MURR1 (COMMD1)....119

I. INTRODUCTION....120
II. METHODS AND MATERIALS....122
  i. Construction of MURR1 Expression Vectors....122
  ii. Expression and Purification of Recombinant-MURR1....122
  iii. Generation and Evaluation of Antiserum....124
  iv. Cell Culture....125
  v. MURR1-RNA interference....125
III. RESULTS....127
  i. Expression and Purification of Recombinant-MURR1....127
  ii. Antiserum Characterization....127
  iii. Cell Specific Copper Toxicity....130
  iv. MURR1-RNAi optimization....130
IV. DISCUSSION....132
  ii. MURR1 is a Ubiquitous Protein with Multiple Functions....132
    a. MURR1 and the Copper Pathway....135
    b. MURR1 and the Sodium Pathway....136
    c. MURR1 and the Apoptotic Pathway....137
    d. MURR1 and the NF-κB Pathway....138
    e. MURR1 and Vesicular Trafficking....140

CHAPTER 8 : GENERAL DISCUSSION AND CONCLUSIONS....144

I. THE JACKSON TOXIC MILK MOUSE....145
  i. The Jackson tx Mouse Mutation....145
  ii. The Jackson tx Mouse as a Model of Copper Storage....146
  iii. Future Directions....147
II. COPPER TOXICOSIS: THE ROLE OF *MURR1*....148
  i. Identification of the CT Gene....149
  ii. Not All Dogs Are Created Equal....150
  iii. Human MURR1 Analysis....152
  iv. Making sense of MURR1....154
  v. Future Directions....157
IV. CONCLUDING REMARKS....161

REFERENCES....162

LIST OF TABLES

TABLE 1-1. COPPER IS AN ESSENTIAL COFACTOR IN A NUMBER OF CRITICAL METABOLIC ENZYMES IN MAMMALS. 3

TABLE 2-1. PRIMERS USED FOR RT-PCR, AND AMPLIFICATION AND SEQUENCING OF C3HEB/FEJ NORMAL AND TXJ DNA 51

TABLE 4-1. PRIMERS USED FOR AMPLIFICATION OF CANDIDATE GENE EXONS/INTRONS FROM CANINE GENOMIC DNA FOR SEQUENCE ANALYSIS. 76

TABLE 5-1. CHOSEN COHORT FOR STUDY. 97

TABLE 5-2. DOG SPECIFIC PRIMERS F~~OR CDNA~~ AMPLIFICATION OF ATP7B. 99

TABLE 5-3. INTRONIC PRIMER SETS FOR THE AMPLIFICATION OF THE CANINE ATP7B GENE 101

TABLE 5-4. SUMMARY OF SINGLE NUCLEOTIDE POLYMORPHISMS (SNPS) IDENTIFIED IN BEDLINGTON ATP7B COMPARED WITH THE BOXER GENOME SEQUENCE. 107

TABLE 6-1. COMMD1 SEQUENCING RESULTS IN 26 CLINICALLY AFFECTED PATIENTS WITH COPPER STORAGE OF UNKNOWN ETIOLOGY. 115

LIST OF FIGURES

FIGURE 1-1. COPPER UPTAKE, DISTRIBUTION, AND EXCRETION IN HUMANS AT THE ORGAN LEVEL. 6

FIGURE 1-2. POSSIBLE INTRACELLULAR COPPER PATHWAYS. 9

FIGURE 1-3. CONSERVED DOMAINS AMONG THE HUMAN COPPER-TRANSPORTING P-TYPE ATPASES, ATP7A AND ATP7B. 14

FIGURE 1-4. FUNCTIONAL UNITS OF THE LIVER. 19

FIGURE 2-1. GLYCINE SUBSTITUTION IN EXON 8. 54

FIGURE 2-2. SERINE 107 AND ALANINE 108 ARE CONSERVED AMONG SPECIES. 56

FIGURE 3-1. SOUTHERN BLOT HYBRIDIZATION. 65

FIGURE 3-2. CANINE AND HUMAN ALIGNMENTS OF ATP6H GENE AND PROTEIN. 66

FIGURE 4-1. MURR1 ANALYSIS. 81

FIGURE 4-2. BEDLINGTON TERRIER PEDIGREES SHOWING HAPLOTYPE SEGREGATION AND COPPER TOXICITY STATUS IN DOGS USED FOR THE CURRENT STUDY. 84

FIGURE 4-3. NORTHERN BLOT ANALYSIS OF *MURR1*. 86

FIGURE 5-1. BEDLINGTON PEDIGREE. 96

FIGURE 5-2. CANINE PREDICTED ATP7B PROTEIN COMPARED TO HUMAN PROTEIN. 104

FIGURE 5-3. COMPARISON OF THE PUTATIVE N-TERMINUS OF PREDICTED CANINE ATP7B TRANSCRIPTS AND OTHER SPECIES. 105

FIGURE 6-1. HAPLOTYPE ANALYSIS AT THE WILSON DISEASE (WND) AND COMMD1 LOCI. 117

FIGURE 7-1. EXPRESSION AND PURIFICATION OF RECOMBINANT-MURR1. 128

FIGURE 7-2. CHARACTERIZATION OF ANTISERUM TO RECOMBINANT-MURR1. 129

FIGURE 7-3. CELL SPECIFIC COPPER TOXICITY. 131

FIGURE 7-4. TRANSFECTION REAGENT TESTING. 133

FIGURE 8-1. DIAGRAM OF INTERACTIONS WITH MURR1 AND OVERLAPPING PATHWAYS. 155

LIST OF ABBREVIATIONS, SYMBOLS AND NOMENCLATURE

Cu	copper
bp	base pair
cDNA	complementary DNA
CHO	Chinese hamster ovary cell line
cR_{3000}	centiRay, 3000 radiation dose
CT	copper toxicosis
DAPI	4', 6-Diamidino-2-phenylindole
DNA	deoxyribonucleic acid
DTT	dithiothreitol
EDTA	ethylenedinitrilo-tetraacetic acid
ETIC	endemic Tyrolean infantile cirrhosis
GAPDH	glyceraldehyde-3-phosphate dehydrogenase
GST	glutathione-S transferase
HepG2	human hepatocellular carcinoma cell line
HEK293	human embryonic kidney cell line
ICC	Indian childhood cirrhosis
ICT	idiopathic copper toxicosis
kb	kilo base
kDa	kilo Dalton
LEC	Long-Evans Cinnamon
mRNA	messenger RNA
NCBI	National Center for Biotechnology Information
PAGE	polyacrylamide gel electrophoresis
PBS	phosphate-buffered saline
PCR	polymerase chain reaction
RNA	ribonucleic acid
RNAi	RNA interference
ROS	reactive oxygen species
RT-PCR	reverse transcriptase PCR
SDS	sodium dodecyl sulphate
siRNA	short interfering RNA
SNP	single nucleotide polymorphism
STS	sequence tagged site
TGN	*trans*-Golgi network
TMD	transmembrane domain
tx	toxic milk
WD	Wilson disease

CHAPTER 1 : Introduction

I. COPPER

Copper is an essential metal found in all living organisms that exists in two oxidation states, Cu(I) and Cu(II). Prior to the evolution of dioxygen (O_2) into the atmosphere by prokaryotic metabolism, copper was present in its insoluble Cu(I) state and was not available for life [1]. The advent of O_2 led to the oxidation of copper and the bioavailability of soluble Cu(II). Through its ability to exist in two distinct redox states, copper serves as an important catalytic cofactor in the active site of a number of proteins required for normal biological function. However, this same property can also make copper toxic when it is present in excess due to its readiness to participate in the production of highly reactive oxygen species [2].

1. ESSENTIALITY OF COPPER

The essentiality of copper was first recognized in 1928 when copper was shown to be critical for hemoglobin formation in rats [3]. Copper is a critical component affecting the activity of multiple mammalian enzymes (Table 1-1). Copper can affect enzyme activity, both as a catalytic cofactor and an allosteric effector [4]. In catalytic centres of oxidative and reductive enzymes, copper is essential for electron transfer processes, such as in cytochrome-c oxidase (CCO) and Cu/Zn-superoxide dismutase (SOD). As an allosteric component of enzymes, copper may confer proper protein structure required for enzymatic activity, such as in amine oxidases. The diversity of function and expression of copper-proteins further exemplifies the essentiality for copper in mammalian systems.

Table 1-1. Copper is an essential cofactor in a number of critical metabolic enzymes in mammals.

ENZYME	**FUNCTION**
Cytochrome-c oxidase	Electron transport in mitichondria
Cu/ZnSOD	Free radical detoxification
Metallothionein	Excess metal storage, possible metallochaperone
Ceruloplasmin	Ferroxidase, acute-phase reactant, Cu distribution
Protein-lysine-6-oxidase	Cross-linking of collagen and elastin
Tyrosinase	Formation of melanin
Dopamine-β-monooxygenase	Catecholamines production
α-Amidating enzyme	Modification of hypothalamic peptide hormones
Amine oxidases	Possible inactivation of histamine, serotonin, dopamine, and tyramine
Peptidylglycine monooxygenase	Bioactivation of peptide hormones
Hephaestin	Ferroxidase
CMGP	Ferroxidase/amine oxidase
β-Amyloid precursor protein	Possible brain copper homeostasis
Prion protein	Possible neuronal protection
S-Adenosylhomocysteine	Sulfur amino acid metabolism hydrolase
Angiogenin	Induction of blood vessel formation
Blood clotting factor V and VIII	Blood clotting

Modified from Tapiero et al. [5].

II. TOXICITY OF COPPER

The basis of copper toxicity is its ability to produce reactive oxygen species (ROS), such as the highly reactive hydroxyl radical ($OH^{\bullet}$), by participating in Fenton chemistry and resulting in what is known as the metal-ion catalyzed Haber-Weiss reaction [6]:

$$\begin{array}{lll} & Cu^{2+} + O_2^{-} \rightarrow Cu^{+} + O_2 & \text{(reduction of copper)} \\ & Cu^{+} + H_2O_2 \rightarrow Cu^{2+} + OH^{\bullet} + OH^{-} & \text{(Fenton reaction)} \\ \text{Net:} & O_2^{-} + H_2O_2 \rightarrow O_2 + OH^{\bullet} + OH^{-} & \text{(Haber-Weiss reaction)} \end{array}$$

The hydroxyl radical can react with almost every type of molecule found in living cells, including sugars, amino acids, phospholipids, nucleic acids, and organic acids [2]. Hydroxyl radicals can cleave DNA and RNA molecules by interacting with the aromatic rings of purines and pyrimidines. Damage to proteins and phospholipids, potentially occurs by hydrogen atom abstraction, which leaves behind an unpaired carbon atom. In fatty acids, carbon radicals tend to stabilize by molecular rearrangement, generating a conjugated diene. Unfortunately, this conjugated diene reacts readily with oxygen to produce a secondary radical, setting off a chain reaction of lipid peroxidation. This destructive action of hydroxyl radicals and other ROS on DNA, proteins, and lipids, has been implicated in the development of cancer, aging, and a variety of neurological disorders [6].

In addition to the generation of ROS, copper ions may exert their toxic property by displacing other metals from their binding sites within metalloproteins. For example, the human estrogen receptor contains a zinc-finger DNA binding domain required for binding to its target DNA sequence. It has been shown *in vitro*, that if copper replaces zinc in this domain, the human estrogen receptor is defective in binding to its target sequence [7].

II. COPPER HOMEOSTASIS

Because copper is both essential and potentially toxic, precise regulatory mechanisms must be in place to ensure that copper concentrations are maintained at levels where copper deficiency and toxicity are both avoided. Studies in yeast and bacteria have led to the identification of functionally and structurally homologous mammalian proteins playing key roles in copper homeostasis. However, in complex organisms, copper homeostasis is not only maintained at the cellular level, but also at the level of the tissue and the complete organism (Fig 1-1).

I. UPTAKE

To maintain normal biological function, it is important to obtain sufficient dietary copper on a daily basis. The main dietary sources of copper include shellfish, organ meats, and seeds, including nuts and grains. Drinking water does not usually contribute significantly to intake [8]. In mammals, the major site of copper absorption is at the small intestine and the amount of copper absorbed varies with dietary intake [9]. The adult body contains about 110 mg of copper, with most of it in the liver (10 mg), brain (8.8 mg), blood (6 mg), bone and marrow (46 mg), and skeletal muscle (26 mg) [10].

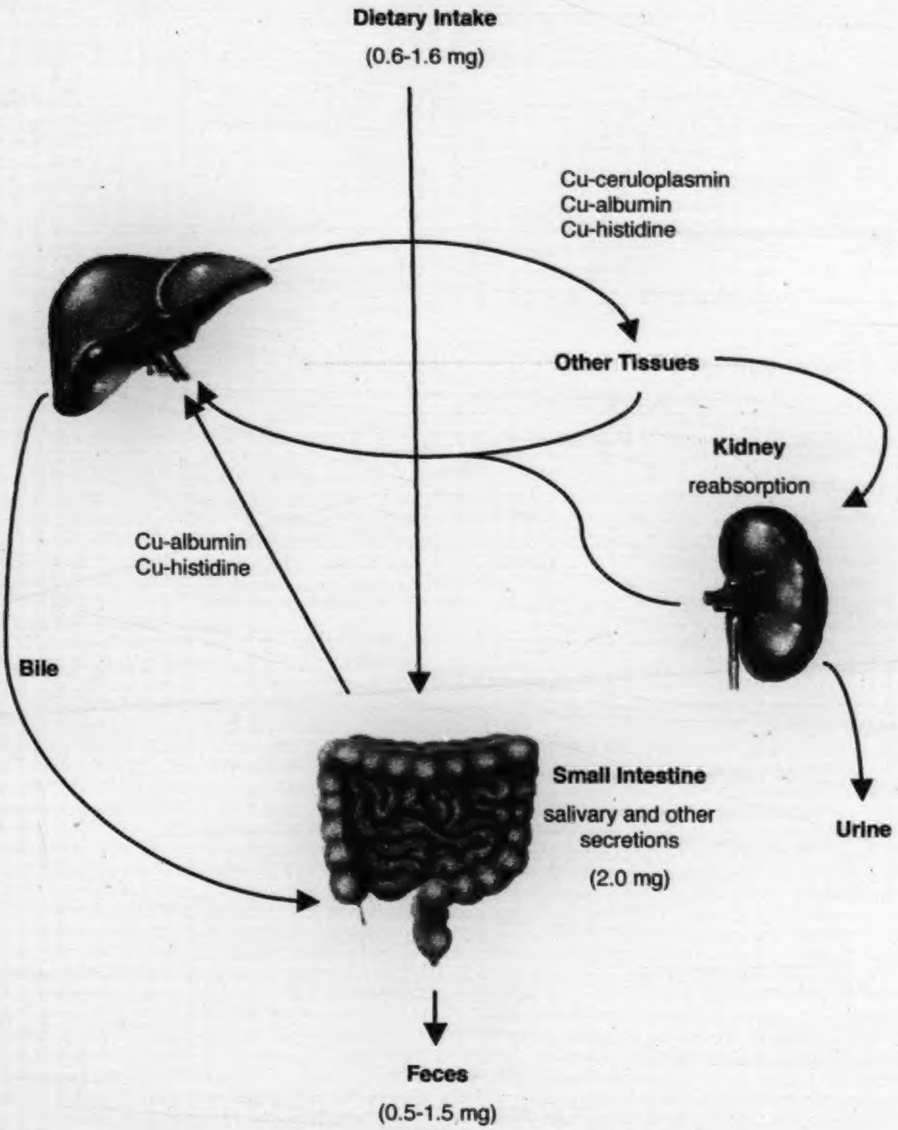
Dietary Intake
(0.6-1.6 mg)
Cu-ceruloplasmin
Cu-albumin
Cu-histidine
Other Tissues
Kidney
reabsorption
Cu-albumin
Cu-histidine
Bile
Small Intestine
salivary and other secretions
(2.0 mg)
Urine
Feces
(0.5-1.5 mg)

Figure 1-1. Copper uptake, distribution, and excretion in humans at the organ level. Dietary copper is mainly absorbed in the small intestine. Once in the portal circulation, copper is carried by albumin and histidine. Copper is rapidly deposited in the liver and incorporated into ceruloplasmin. Ceruloplasmin and the previous carriers, then distribute copper to extrahepatic tissues. Copper is reabsorbed at the kidney, with only negligible amounts excreted in the urine. Most copper is excreted from the liver into bile. Copper values taken from Linder and Hazegh-Azam [8].

Approximately 4.5 mg of copper is secreted daily into gastrointestinal fluids, 2.5 mg in bile and 2.0 mg in other fluids secreted into the digestive tract. However, most of this copper is recycled and recuperated by reabsorption [8]. The average daily intake of copper for a human adult is between 0.6 and 1.6 mg and 55-75 % is absorbed by the small intestine.

II. DISTRIBUTION TO TISSUES

Human serum contains approximately 1 μg copper per millilitre. Although albumin is the most abundant carrier protein in serum, only a small fraction of copper is bound to albumin. The majority of copper in blood is bound to ceruloplasmin; a ferroxidase synthesized in the liver that is involved in mobilizing iron and requires copper in order to be functionally active.

Copper distribution to tissues is suggested to occur in two waves [11]. The first wave delivers copper to the liver and kidney. This wave is primarily mediated by albumin and amino acids such as histidine. Histidine can also form ternary complexes with copper-bound albumin and intermediates of these complexes can exist in equilibrium in blood [12,13]. In the liver, copper becomes incorporated into ceruloplasmin, which is itself secreted into blood. This reemergence of copper from the liver constitutes the second wave of copper distribution. Only when ceruloplasmin, bearing newly incorporated copper, is secreted does appreciable uptake by other tissues begin [14]. However, copper in ceruloplasmin is not considered part of the *in vivo* exchangeable copper pool.

Albumin and its copper-bound complexes are thought to constitute the largest labile pool of plasma copper for tissue distribution and cellular uptake.

III. INTRACELLULAR COPPER

Total body copper homeostasis begins at the cellular level. Intracellular copper homeostasis involves specialized proteins involved in import, distribution, and export (Fig 1-2). Many of these proteins were initially identified in yeast and bacteria, demonstrating the extensive conservation of this pathway across species.

a. Cellular Import

The mechanism of copper transfer across the brush border into intestinal cells is not fully understood. Earlier studies proposed that this process involves a non-energy-dependent saturable transporter active at low copper concentrations, and diffusion at higher concentrations [8]. Two candidate transporters have been proposed for copper uptake at the brush border: copper transporter 1 (CTR1) and divalent metal transporter 1 (DMT1).

Human CTR1 was identified by functional complementation of respiratory defects in yeast defective in copper transport due to mutations in both *CTR1* and *CTR3* [15]. Cell culture experiments confirm that CTR1 is a high-affinity copper transporter, showing a specific preference for Cu(I) [16]. CTR1 mRNA is ubiquitously expressed, with highest expression in the liver, heart, and pancreas, with intermediate expression in the intestine [15], specifically in the villi of the small intestine [17,18]. In intestinal cells, CTR1 localizes primarily to the plasma membrane [18] and exposure to high

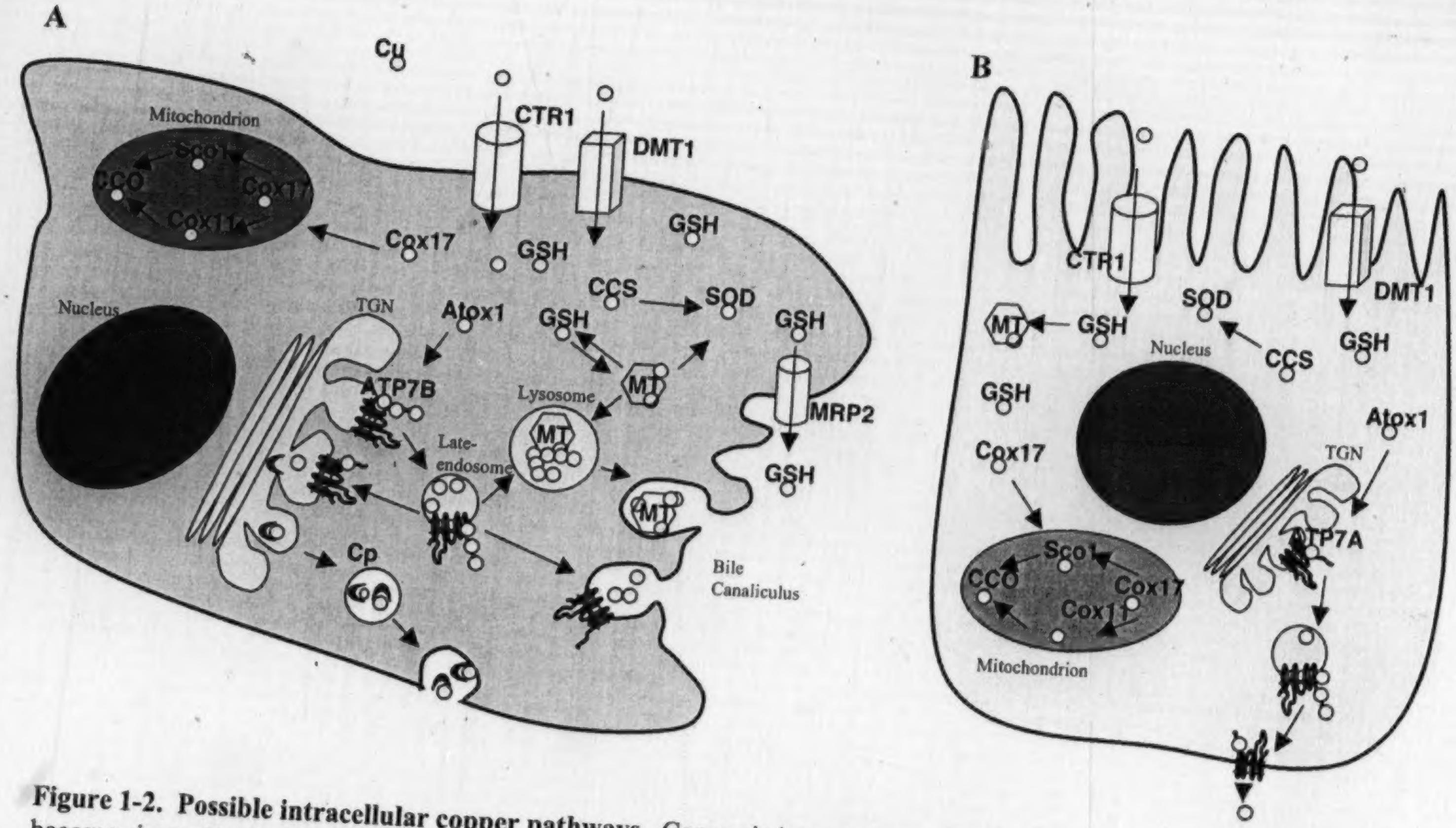
A
Cu
CTR1
DMT1
Mitochondrion
Sco1
CCO
Cox17
Cox11
Cox17
GSH
GSH
Nucleus
TGN
Atox1
CCS
SOD
GSH
GSH
ATP7B
Lysosome
MT
MT
Late-
endosome
MRP2
GSH
MT
Cp
Bile
Canaliculus
B
CTR1
DMT1
MT
GSH
SOD
CCS
GSH
Nucleus
GSH
Atox1
Cox17
TGN
ATP7A
Sco1
CCO
Cox17
Cox11
Mitochondrion

Figure 1-2. Possible intracellular copper pathways. Copper is imported into the cell by CTR1 and DMT1, upon which it becomes immediately bound to glutathione (GSH). Copper is subsequently chaperoned by Atox1, CCS, and Cox17 to their respective targets and sequestered by metallothionein (MT). **(A)** In the hepatocyte, ATP7B incorporates copper into ceruloplasmin (Cp) at the *trans*-Golgi network (TGN) under basal copper conditions. At higher copper concentrations, ATP7B becomes copper loaded and trafficks in vesicular structures towards the apical membrane, fusing with lysosomes in some cells and with the plasma membrane in others. **(B)** In intestinal cells and cells from other tissues, ATP7A is reponsible for mediating copper efflux at the basolateral membrane.

levels of copper, leads to CTR1 internalization [19], providing a point of regulation for intestinal copper absorption. Consistent with previous proposals for copper absorption, uptake by CTR1 is energy-independent and saturable, as well as being stimulated by acidic extracellular pH and high potassium concentrations [16]. CTR1 exists as a symmetrical trimer forming a putative pore for metal transport [20]. The N-terminus of CTR1 is exposed to the extracellular space and contains putative copper binding sites rich in methionine and histidine residues [15,21]. CTR1 appears to be the main copper transporter at the plasma membrane for a variety of different tissues. However cells from CTR1 deficient mice still exhibit residual copper transport activity, suggesting additional transport mechanisms [16].

DMT1 (also known as DCT1 and NRAMP2), predominantly an iron transporter, is expressed in the intestinal mucosa, as well as other cells, and can transport other metals, including copper, with lower affinity [22,23]. Suppression of DMT1 reduces copper transport [24,25] and iron deficiency enhances copper uptake [25,26]. Like CTR1, significant copper uptake by DMT1 is only observed when copper is in the Cu(I) state.

b. Copper Chaperones

Once across the plasma membrane, copper has multiple intracellular chaperones, which form transient complexes with copper and escort the metal ions to and between specific cellular compartments. Because of its potentially toxic nature, free copper ions are virtually non-existent in the cell. The estimated free copper concentration in a cell is less than 10^{-18} M, representing less than one atom of copper per cell [27]. Copper chaperones are necessary for copper transfer in this cellular environment where copper ions are not "free". Delivery of copper by a chaperone is highly specific [28]. Complex formation with target proteins appears to be electrostatically driven, and salt bridging and hydrogen bonding may confer additional specificity at the interfaces [28-30]. At least three mammalian copper chaperones, have been identified through genetic studies in yeast, each involved in distinct copper pathways: CCS, COX17, and ATOX1 (reviewed in [31-34]).

CCS (copper chaperone for SOD, also known as LYS7 in yeast) delivers copper to the Cu/ZnSOD [35]. Three distinct domains have been identified in CCS [36], reviewed in [37]. Domain I contains an MXCXXC copper-binding motif and is homologous to ATOX1. Domain II, in the center of the protein, shows homology to Cu/ZnSOD and contributes to the specific interactions between the chaperone and its target, facilitating protein docking. Domain III, at the carboxy-terminal, is unique to CCS and contains a separate CXC copper-binding motif. This has led to a model in which domain I binds copper, domain II facilitates target recognition, and domain III mediates copper transfer to Cu/ZnSOD. In addition, domain III has also been shown to be important in copper-dependent turnover of CCS [38].

COX17 [39] is unique among the classical chaperones, in that its copper binding involves a labile, binuclear cuprous-thiolate cluster [40]. COX17 is found both in the cytosol and the mitochondrial intermembrane space [41] and is required for delivery of copper for cytochrome-*c* oxidase (CCO) assembly [42], which involves the cooperation of three other copper-binding proteins, SCO1 and SCO2, and COX11 [43]. COX 17 has been shown to be necessary for SCO1 and COX11 copper binding, but not for SCO2 [44,45].

It is generally believed that COX17 crosses the mitochondrial outer membrane already bound to copper to accomplish its function. However, a controversial proposal stemming from studies in yeast, suggests that a mitochondrial copper pool exists that could supply copper to COX17 in the intermembrane space [46].

ATOX1/HAH1 [47] consists of a single protein domain, containing an MXCXXC motif [48]. ATOX1 was originally identified in yeast by its ability to restore anti-oxidant properties in SOD mutants [49]. Although overexpression of ATOX1 prevents oxidative damage in SOD-deficient yeast, at physiological levels the protein does not appear to function as a true anti-oxidant [50]. Human ATOX1 has two docking partners in the secretory pathway and both are copper-transporting P-type ATPases, ATP7A and ATP7B [51,52]. Both ATPases participate in the secretory pathway, transporting copper across the Golgi membrane and delivering copper to copper-requiring proteins. In hepatocytes, ATP7B delivers copper to ceruloplasmin during its synthesis in the *trans*-Golgi network [53]. Although delivery of copper by ATP7A to proteins in the secretory pathway is less well characterized, ATP7A has been shown to play a role in providing copper to tyrosinase [54] and peptidylglycine α-amidating monoxygenase in fibroblasts [55]. ATP7A and ATP7B share similar copper-binding domains with ATOX1, all of which form the same overall βαββαβ fold and are the basis of target recognition by the ATOX1 protein [56,57]. Interaction between ATOX1 and ATP7A or ATP7B involves ionic interactions between the positively charged surface of ATOX1 and the negatively charged surfaces of the copper transporters [57].

c. Cellular Export

In contrast to transfer across the mucosal membrane (cellular import), at normal copper concentrations transfer across the basolateral membrane (cellular export) is energy-dependent and rate-limiting [8]. ATP7A is proposed to transport copper across the basolateral membrane into the blood stream for body distribution. Supporting this hypothesis, ATP7A is expressed in intestinal cells [58] and patients lacking functional ATP7A are copper deficient yet accumulate copper in intestinal cells. ATP7A is also expressed at high levels in muscle, kidney, lung, and brain, but low levels in the placenta and pancreas, and only trace amounts are detected in the liver [59,60], where ATP7B is predominantly expressed [61,62]. Therefore, ATP7A is likely a general copper exporter for most cell types, transporting excess copper across cellular membranes for final removal by hepatocytes and ATP7B.

ATP7A and ATP7B are copper specific P-type ATPases that share 57% identity. Each possesses six amino-terminal MXCXXC copper-binding motifs, an intermembrane CPC motif, a SEHPL motif, and eight transmembrane segments (Fig 1-3) [60,63,64]. They also share various domains conserved among other members of the P-type ATPase family including: a phosphatase domain (TGEA/S), a phosphorylation domain (DKTG), and an ATP-binding motif (TGDN). P-type ATPases are transporters that use energy from ATP-hydrolysis to translocate metal cations across membranes. The copper transport ability of ATP7A and ATP7B has been demonstrated in several systems, including yeast, fibroblasts, and *in vitro* vesicles [65-71]. Copper translocation by ATP7A and ATP7B is believed to involve ATP binding, followed by ATP hydrolysis and subsequent phosphorylation of the invariant aspartate residue in the DTKG sequence [72]. Copper is

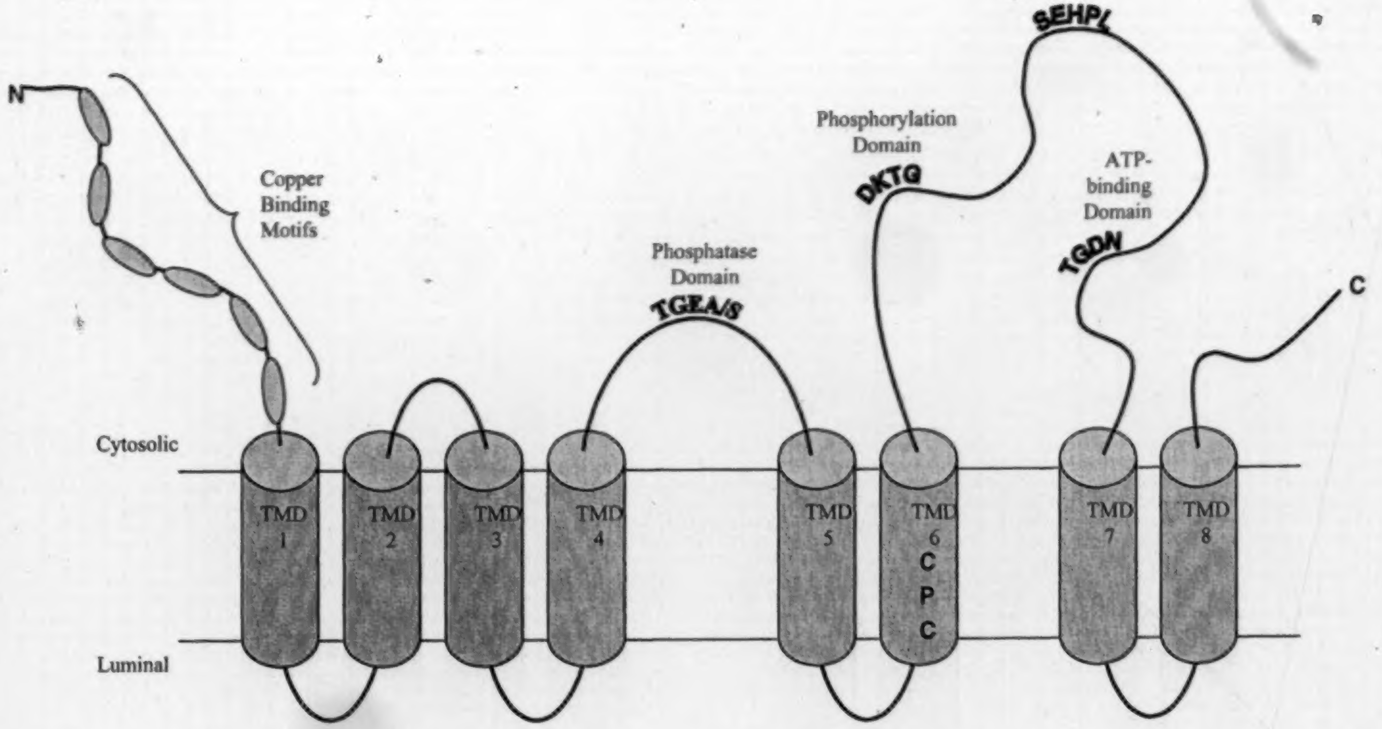

N
Copper
Binding
Motifs
Phosphatase
Domain
TGEA/S
Phosphorylation
Domain
DKTG
SEHPL
ATP-
binding
Domain
TGDN
C
Cytosolic
Luminal
TMD 1
TMD 2
TMD 3
TMD 4
TMD 5
TMD 6
C
P
C
TMD 7
TMD 8

Figure 1-3. Conserved domains among the human copper-transporting P-type ATPases, ATP7A and ATP7B. Eight transmembrane domains (TMD) are predicted for both proteins. Conserved motifs are indicated on the schematic representation. N: amino-terminus, C: carboxy-terminus.

then transferred from the amino-terminus to a high-affinity CPC motif in the transmembrane channel [73,74].

Under normal copper conditions, both ATP7A and ATP7B are predominantly found at the *trans*-Golgi network (TGN) where they participate in the secretory pathway [69,75-78]. Increased copper concentrations induce trafficking of ATP7A and ATP7B to vesicular structures near and at the plasma membrane [68,69,78-80]. Through this mechanism cells are able to regulate copper efflux. When the cell is exposed to high levels of copper, ATP7A redistributes from the TGN to the cell surface, where it is thought to pump copper directly out of the cell [68,81]. However, this has recently been contested by studies in *Atp7a* transgenic mice that suggest ATP7A pumps copper into a vesicular compartment followed by exocytosis to release copper, rather than directly pumping copper across the basolateral membrane [82]. In most liver cells, increased copper levels induce ATP7B movement from the TGN to subapical vesicles, where it most likely fuses with lysosomes for copper excretion into the bile [83]. In hepatocytes surrounding bile capillary networks, ATP7B movement may extend to the canalicular membrane itself [80,84]. The differences in targeting of ATP7A and ATP7B may be related to their particular functions in particular cell types.

In addition to its role as a copper chaperone for ATP7A and ATP7B, ATOX1 may also be involved in regulating the catalytic function of its partners. Apo-ATOX1 is able to strip copper from ATP7B and decrease its activity [85]. Conversely, copper-bound ATOX1 is able to restore ATP7B catalytic activity following copper chelation by bathocuprione disulfonic acid (BCS). In ATOX1-deficient cells, ATP7A trafficking is severely impaired. These findings suggest a role for ATOX1 in establishing the threshold for copper-dependent movement of the copper-transporting ATPases [86].

d. Detoxification

In mammals, very little copper is stored because it is relatively easy to absorb and excrete [14]. However, a hepatic copper pool, most likely regulated by metallothioneins and glutathione, has been described [87]. Within the cytosol, approximately 80% of copper is bound to glutathione (GSH) and metallothionein (MT) [10].

GSH has many important physiologic and metabolic functions in mammalian cells, including metal detoxification. With respect to copper, GSH can limit its reactivity, make it biologically available for apo-cuproproteins, and facilitate its export [88]. GSH is a glutamylcysteinylglycine tripeptide. Cysteine provides the key functional element in GSH through its thiol group. Copper binds to this cysteine and forms complexes with GSH almost immediately upon entering the cell [89], thus limiting its reactivity and protecting the cell against copper toxicity. The reducing ability of GSH allows copper to remain in its biologically active Cu(I) state for its incorporation into apo-cuproproteins. The ability of GSH to transfer copper to other proteins has been demonstrated *in vitro* for MT, Cu/ZnSOD, and ceruloplasmin [90-92]. Due to the lack of any distinguishing target domains, this general chaperone function appears to be non-specific and precludes GSH from being considered an official chaperone. Another mechanism of copper detoxification involves export of copper-GSH complexes directly into bile (see Section iv.b).

The main function of MT is to sequester metal ions into innocuous complexes and protect the cell from their toxic effects. In mammals, two major isoforms, MT1 and MT2, are expressed in most tissues and at most stages of development. Metal toxicity studies in rats report a differential MT response following cadmium toxicity, and propose that MT1 function is associated with metabolism or detoxification of metals such as cadmium, while MT2 is responsible for homeostasis of essential metals such as copper [93]. Increases in copper-MT2 have also been observed in dogs with copper toxicosis [94]. If present in sufficient concentrations, copper will displace other metals with lower affinity for MT, leading to MT induction and subsequent reduced intestinal copper absorption [8]. MT1/2 null cells are sensitive to copper toxicity and fail to induce expression of *Cu/ZnSOD* and *CCS* in response to copper exposure, suggesting that MT may regulate expression of other genes involved in copper metabolism [95]. MT has also been shown to donate copper and zinc to Cu/ZnSOD [96], and function as an antioxidant in cardiac tissue [97].

IV. EXCRETION

Since copper is relatively easy to absorb, it is commonly accepted that copper homeostasis is mainly controlled by regulated excretion. Approximately 85% of absorbed copper is excreted: the majority *via* bile and only negligible fractions in urine. Therefore the liver is critically involved in copper homeostasis, as the organ responsible for biliary copper excretion.

a. Liver Structure

The liver is traditionally separated into four lobes, designated as right, left, quadrate, and caudate (reviewed in [98]). Within a lobe there are numerous individual structural units called lobules (Fig 1-4). Each lobule has at its centre a central vein, with hundreds of hepatocytes radiating from it, and is bounded by four to six portal triads. The portal triad consists of the two blood sources for the liver, the hepatic artery and the portal vein, and the bile duct. The acinus is another physiological unit of the liver, which is divided into three zones (Fig 1-4). Zone 1 (periportal) hepatocytes are generally associated with hepatocyte regeneration, bile duct proliferation, and glucogenesis, while zone 3 (centrilobular) hepatocytes are responsible for detoxification, aerobic metabolism, glycolysis, and hydrolysis [99]. Zone 2 is associated with a mix or zone 1 and zone 3 functions.

b. Copper in Bile

Two main routes of biliary copper excretion have been proposed: one a vesicular pathway involving ATP-dependent transport and lysosomal exocytosis into the bile, and the other involving export of copper-GSH at the canalicular membrane [100]. The chosen pathway appears to be dictated by the mode of copper administration: acute poisoning or loading, normal dietary intake, or chronic accumulation. Excess copper following intravenous copper administration involves rapid phase removal by GSH complexes [101]. Conversely, dietary copper excretion is slow and mediated by a saturable copper-transporting system independent of GSH [101]. Chronic copper loading leads to excretion of copper via a lysosomal pathway [102,103], and may involve the

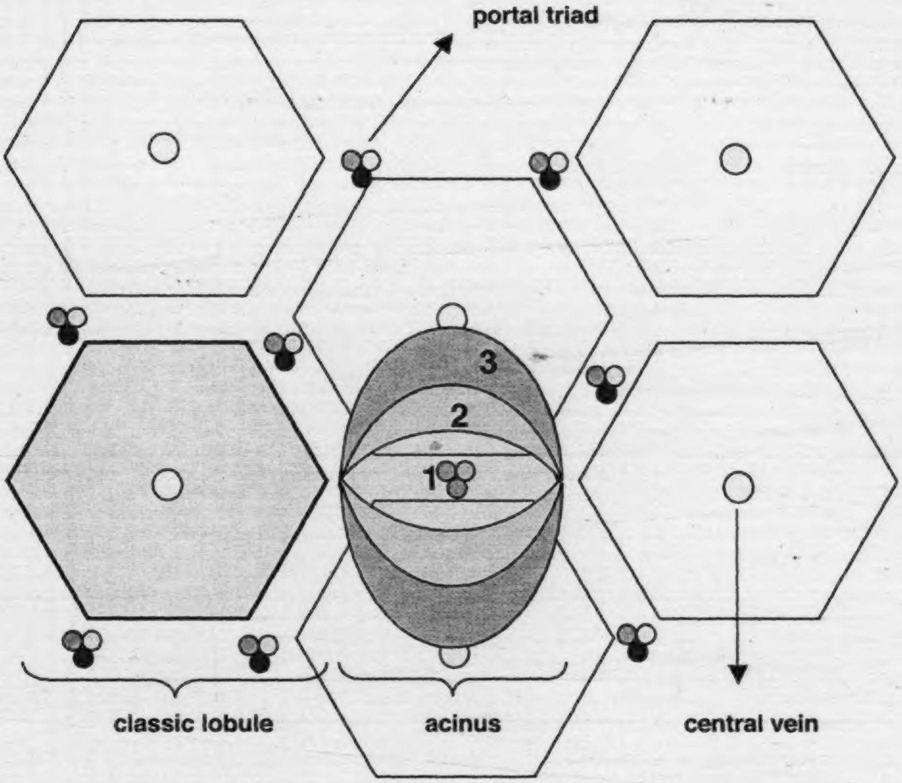
portal triad
3
2
1
classic lobule
acinus
central vein

Figure 1-4. Functional units of the liver. The classical lobule, with the central vein at its centre is bound by four to six portal triads. The portal triad consists of the hepatic artery, portal vein, and bile duct. The acinus is divided into three zones (1-3).

same GSH-independent copper-transporting system. Mutant rats deficient in biliary copper-GSH excretion, exhibit only slow phase copper excretion following intravenous injection of the metal [104]. Rapid phase excretion reaches a plateau, supporting the involvement of a second transporter specific for copper-GSH [103]. This transporter is the multidrug-resistance associated protein 2 (MRP2), also known as the multispecific organic anion transporter (cMOAT) present at the canalicular membrane [101,104]. In accordance with this not being a major route of excretion under physiological copper concentrations, animals lacking MRP2 exhibit decreased amounts of GSH-copper complexes in the bile, but do not accumulate copper in the liver.

The GSH-independent, but ATP-dependent copper transporting system [105,106], can most likely be attributed to ATP7B, a copper-transporting ATPase highly expressed in the liver and defective in Wilson disease, a recessive disorder of copper storage [61,62]. Long-Evans Cinnamon (LEC) rats deficient in Atp7b have decreased biliary copper excretion associated with decreased excretion of lysosomal enzymes, but normal GSH excretion [107]. Further direct evidence of ATP7B involvement in biliary copper excretion has been provided by experiments in these rats, in which introduction of human *ATP7B* cDNA leads to an increase in copper content in lysosomes and bile [108,109]. Under basal conditions, ATP7B is generally believed to localize to the *trans*-Golgi network (TGN) in hepatocytes [69]. Increased copper concentrations cause redistribution of ATP7B from the TGN to subapical vesicles and the canalicular membrane. Copper containing vesicles are thought to fuse with lysosomes for exocytosis into bile or directly with the canalicular membrane.

Within the lysosome, copper excretion is also accomplished *via* degradation of cuproproteins, such as ceruloplasmin and metallothionein (MT). The presence of copper-MT in lysosomes has been widely observed and both radioactive copper from radiolabeled ceruloplasmin and ceruloplasmin fragments have been detected in bile [110,111].

V. DISRUPTION OF COPPER HOMEOSTASIS

The importance of copper homeostasis is underscored by two related, but opposite, disorders of copper transport: Menkes disease [112] and Wilson disease [113]. Menkes disease is an X-linked disorder of copper deficiency that manifests perinatally. Menkes patients suffer from severe neurological and connective tissue dysfunction due to reduced function of copper-dependent enzymes [114]. The underlying defect is failure to export copper from intestinal cells, resulting in copper deficiency of organs and tissues. In contrast, Wilson disease is an autosomal recessive disorder of copper storage.

Cloning and characterization of the Menkes and Wilson disease genes, *ATP7A* and *ATP7B* respectively, has led to a rapid generation of information on copper transport pathways and human copper metabolism. Menkes disease, the ATP7A protein and its properties, have been recently reviewed [115]. Other human diseases involving copper have also been recently reviewed [5,37], including Alzheimer disease, Parkinson disease, amyotrophic lateral sclerosis (ALS), and prion diseases. The remainder of this thesis will focus on disorders of primary copper storage: the human diseases and their animal models.

III. WILSON DISEASE

Wilson disease (WD), also known as Westphal-Strumpell pseudosclerosis, is a rare disorder with an estimated prevalence of one in 30,000 in most populations. In 1912, WD was described in two sets of patients: the first, a family with primary neurological disorder associated with liver cirrhosis [113], and the second, patients with a combination of corneal pigmentation, neuropsychiatric symptoms, and liver cirrhosis [116]. Three decades later, a central role for copper accumulation in the pathogenesis of WD was proposed based on the observation of high concentrations of this metal in tissue from affected individuals [117].

1. CLINICAL PRESENTATION

WD can present with hepatic, neurologic, or psychiatric disturbances, or a combination of these, as well as other features described below. Approximately 45% of patients present with hepatic symptoms, 35% with neurologic, and 10% with psychiatric [118]. Age of onset varies from age three to the sixth decade of life. Symptoms are highly variable, even among family members.

a. Hepatic

Liver disease is the most common presentation of WD, particularly among children and young adults. Liver disease can present as recurrent jaundice, simple acute self-limited hepatitis-like illness, autoimmune-type hepatitis, fulminant hepatic failure, chronic liver disease with hypertension and hepatosplenomegaly, fatty liver, or hemolytic anemia, either acute or chronic [119].

b. Neurologic

Neurologic presentation of WD is often misdiagnosed. Earliest symptoms include changes in personality, difficulty speaking, drooling, and loss of fine motor skills [120]. Symptoms may also include movement disorders: choreic or dystonic [119].

c. Psychiatric

The most common psychiatric disturbance in WD is depression, but neurotic behaviour, such as phobias, compulsiveness, aggression, personality disoragnization, and intellectual deterioration may also indicate psychiatric WD presentation. Psychiatric disturbances usually occur in combination with other symptoms.

d. Other

A common ocular finding in WD patients is the Kayser-Fleisher (KF) ring [121,122]. KF rings form in the cornea as a result of copper deposition in the Descemet's membrane. KF rings are detected in 95% of patients with neurologic symptoms, but only in 50-60% of patients presenting with other symptoms [123]. Clinical symptoms can also result from copper accumulation in other organs, and manifestations may include endocrine abnormalities, cardiomyopathy, renal dysfunction, and arthritis [119].

II. PATHOLOGY

The pathogenesis of WD is a direct consequence of copper accumulation. In the early stages of WD, copper is diffusely distributed throughout the cytoplasm and difficult to stain. In advancing stages of the disease, copper is sequestered into lysosomes, mostly bound to MT and is easily detected by rhodamine (stains for copper) and orcein stains

(stains copper-bound proteins). Prior to the onset of cirrhosis, copper accumulation appears confined to periportal hepatocytes (zone 1). However, once cirrhosis sets in, a more general uneven distribution of copper throughout the nodules is observed [124].

Regardless of the initial clinical presentation, liver abnormalities are consistently found in symptomatic WD patients upon liver biopsy [125]. Severe mitochondrial dysfunction has been observed in the livers of WD patients and an important role for free-radical formation and oxidative damage in WD pathogenesis has been suggested [126]. Copper accumulation in hepatocytes initially causes mitochondrial damage with altered lipid oxidation, resulting in hepatic steatosis [127]. Progression from steatosis to cirrhosis (loss of microscopic lobular architecture, with fibrosis, and nodular regeneration) is variable, but may include necrosis leading to further damage of hepatocytes, ballooning of hepatocytes, Mallory bodies, inflammation, and fibrosis. Fulminant hepatitic failure is often accompanied by copper release into the bloodstream and may result in hemolytic anemia.

Although ATP7B is expressed in the brain, the pathogenesis of neurologic and psychiatric WD is unclear. Gradual accumulation and/or eventual seeping of copper into the plasma ultimately results in copper overload in extrahepatic tissues, including the brain. Patholologic alterations in the brain associated with WD include diffuse brain atrophy and focal abnormalities in the lenticular, thalamice, and caudate nuclei, as well as the brain stem and white matter, and may be due to gliosis, necrosis, or cystic degeneration [128]. Apolipoprotein E (ApoE) isoforms vary in their neuroprotective properties and the ApoEε3 isoform has been suggested to protect against copper toxicity and impact the onset of neurologic symptoms in WD [129]. In addition, the amyloid precursor protein (APP) associated with Alzheimer disease, and the prion protein associated with Creutzfeldt-Jakob disease, both bind copper and may be involved in neuronal copper homeostasis [127]. In fact, homozygosity of the prion 129Met variant has recently been associated with severe neurological symptoms in a small set of German WD patients [130].

Metal overload and oxidative stress have also been linked to the development of hepatocellular carcinoma, however this pathology is extremely rare in WD patients [131]. The low incidence of hepatic cancer in WD may be due to the chelating properties of medications taken for WD clinical management.

III. BIOCHEMISTRY

None of the abnormalities mentioned above are specific to WD, including the hallmark of WD, KF rings, which can also be associated with cholestasis or autoimmune hepatitis. A combination of the above abnormalities is suggestive of WD, but diagnosis should be confirmed with biochemical tests. A scoring system based on a variety of biochemical tests and clinical symptoms, has been proposed by an international panel of experts in the WD field, but has yet to be evaluated [132].

The primary defect in WD is typically recognized as copper retention due to inefficient biliary copper excretion and/or defective incorporation of copper into ceruloplasmin in the liver. Hepatic copper levels are elevated in symptomatic WD patients, but may not be as high in pre-symptomatic patients or patients in the fulminant stage [123]. Due to the inability of the liver to excrete copper *via* bile, urinary copper excretion is also elevated in most symptomatic patients and may support a diagnosis of WD. Low serum ceruloplasmin levels are common in WD [133]. However, normal levels are also observed in 5% of patients with neurologic symptoms, and up to 40% of patients with hepatic presentation [123].

IV. TREATMENT

All of the clinical, biochemical, and histological abnormalities mentioned above can individually occur in diseases other than WD. Diagnosis of WD is a multidisciplinary approach involving all aspects of disease presentation and progression [134]. Early diagnosis of WD is extremely important for the clinical management of the disease as progression of WD can be arrested by chelation therapy. However, not all symptoms can be ameliorated and permanent damage cannot be reversed. Treatment of WD consists of life-long drug therapy. Liver transplantation, which does correct the underlying defect in WD, is only performed on severe cases. Four main therapeutic agents are used for the clinical management of WD: penicillamine, trientine, tetrathiomolybdate, and zinc. Several treatment modalities are effective [134]. Selection of one approach over another depends on physician preferences and patient tolerances. Compliance is a major issue regarding drug therapy and constant monitoring is recommended [135].

Penicillamine [136] and trientine [137] are copper chelators that enhance urinary excretion of copper. Penicillamine is able to bind copper in plasma, mobilize copper from stores, and reduce protein affinity for copper, facilitating binding to the drug and excretion *via* urine. Penicillamine has been shown to ameliorate hepatic and neuropsychiatric symptoms and to prevent disease manifestations in asymptomatic patients. Penicillamine can produce many side effects including skin lesions, systemic lupus erythematodes, and immune complex nephritis, particularly when used long term in high doses [138]. Trientine is also an effective chelator and less toxic than penicillamine [139].

Tetrathiomolybdate has two modes of action. First, it prevents copper absorption by complexing with copper in the intestinal tract. Second, it also forms complexes with copper and albumin in the blood, preventing cellular uptake. Although still in the experimental stage, tetrathiomolybdate appears to be useful as an initial treatment in patients presenting with neurologic symptoms [140].

Zinc induces MT expression, indirectly binding-up copper, preventing its absorption and protecting cells from copper toxicity [141]. Efficacies of zinc and penicillamine are usually similar, but zinc tolerance is much better [135,142].

V. WILSON DISEASE GENE

The autosomal recessive nature of WD was demonstrated in 1960 [143]. Twenty-five years later, the disease was linked to the esterase D locus on chromosome 13 [144] and further refined to 13q14-q21 [145]. Cloning of the *WD* gene, *ATP7B*, was accomplished independently by two groups in 1993 [61,62]. *ATP7B* encompasses approximately 80 kb of genomic sequence. Transcripts are expressed predominantly in the liver, with varying levels of expression among the kidney, placenta, heart, brain, lung, muscle, and pancreas [61,62]. The main transcript expressed in the liver consists of 21 exons [146], however a smaller transcript lacking exon 6 and 7 is also found in liver, as well as kidney, lymphoblasts, and brain [147]. In the brain, other alternatively spliced transcripts are also observed involving different combinations of skipped exons, including exon 6, 7, 8, 12, 13, and 17 [62,146].

The *ATP7B* promoter contains four metal-response-elements (MREs) and six MRE-like sequences (MLSs), as well as other putative regulatory elements, and a transcription start site 335 base pairs upstream of the translation initiation site [148]. Although *ATP7B* does not appear to be upregulated in response to copper, its basal expression does seem to depend on Ku protein binding to MREa [149].

A second promoter is found within intron 8 producing a unique alternative product named PINA, for the pineal night-specific ATPase [150]. The pineal gland belongs to the circadian timing system, which is responsible for establishing rhythmic neuronal signals that dictate our daily sleep cycles. PINA expression is diurnally and developmentally regulated. PINA expression is upregulated at night and occurs in the adult rat pinealocytes and a subset of photoreceptors [150]. In the developing retina, PINA is transiently expressed in the retinal pigment epithelium and ciliary body. A role for PINA in rhythmic copper homeostasis has been suggested, however copper transport by PINA is negligible [150].

a. Mutation Analysis

Molecular genetic testing is playing an increasingly important role in diagnosis of WD and is particularly useful for the identification of asymptomatic sibs. More than 260 mutations in *ATP7B* have been identified, located throughout the gene. The majority of mutations in *ATP7B*, approximately 54 %, are missense mutations and largely confined to the transmembrane domains and conserved functional motifs [151]. Small insertions and deletions, nonsense, and splice site mutations are also highly prevalent. A single large deletion has also recently been identified [152]. A mutation database is maintained at the University of Alberta (www.medicalgenetics.med.ualberta.ca/wilson/ index.php) and curated by Dr. Cox and S. Kenney.

Given the number of possible mutations and the size of the *ATP7B* gene, mutation identification can be challenging and time consuming. Fortunately, some mutations tend to be associated with certain ethnic groups, which can assist in directing mutation screening. For example, H1069Q is the most common mutation in patients of Northern and Eastern European descent [147,153], while R778Q occurs at high frequency in Eastern Asia but has not been reported in European populations [154,155]. However, over half of all known mutations occur only rarely in any given population [120].

Studies have shown that different mutations relate to varying degrees of ATP7B functionality and this variability could contribute to the diversity of clinical manifestations seen in WD [120]. However, genotype-phenotype correlations, to determine the extent to which allelic heterogeneity affects phenotypic diversity, are complicated by the fact that most affected individuals are compound heterozygotes [156]. Mutations that completely prevent the function of the protein tend to produce more severe phenotypes, but even patients with the same homozygous mutations display large variation in age of onset, clinical features, and biochemical parameters [147]. Studies in sibs and identical twins suggest that the WD phenotype is most likely being modified by other factors, either environmental or genetic [120,157], accounting for the observed phenotypic heterogeneity among WD patients.

VI. WILSON DISEASE PROTEIN

Structural analyses of ATP7B have been based on X-ray absorption spectra of purified ATP7B domains [158-160] and molecular modelling using the X-ray structure of a related calcium-transporting P-type ATPase [74,161-164]. Recently the solution structures of the nucleotide-binding domain (N-domain) and a peptide consisting of metal-binding-sites 5 to 6 (MSB5-6) have been resolved [165,166]. These models and structures can be used to predict functional characteristics of ATP7B based on conformational changes induced by ligand binding. In addition, these models and structures allow for theoretical analysis of variations in ATP7B and hypotheses to be made about the disease causing abilities of identified changes prior to functional analysis. Functional analysis of ATP7B and its mutant forms has begun to clarify the molecular pathogenesis of WD and give a better understanding of copper transport in the liver.

In its biosynthetic capacity, ATP7B transports copper for its incorporation into ceruloplasmin in the secretory pathway [53]. Copper incorporation into the six ligand-binding sites of ceruloplasmin does not display any apparent hierarchy for incorporation at any one site and appears to be an all-or-none process [167]. Failure to incorporate copper during ceruloplasmin biosynthesis results in secretion of inactive apoceruloplasmin and severe anemia [168]. A direct role for ATP7B in ceruloplasmin biosynthesis has come from studies in LEC rats deficient in Atp7b, in which ceruloplasmin synthesis is restored upon introduction of human *ATP7B* cDNA [53]. Yeast assays have been created to indirectly test the ability of ATP7B variants to transport copper by measuring the levels of a ceruloplasmin-homologue [69] and observing growth complementation on iron-limited media [66]. Recently, it was also shown that incorporation of copper into ceruloplasmin is chloride dependent, and that the chloride channel family member 4 (ClC4) localizes to ATP7B containing vesicles and stimulates copper incorporation into ceruloplasmin [169].

In its excretory role, ATP7B regulates biliary excretion of copper by trafficking between distinct subcellular locations. In the human liver, ATP7B has been localized specifically to hepatocytes and subcellularly to the *trans*-Golgi network (TGN), with some protein being found at or near the canalicular membrane [77,78]. In primary rat hepatocytes and the polarized human hepatoma cell line *HepG2*, ATP7B was shown to redistribute from the TGN to diffuse vesicular structures and the canalicular membrane after copper exposure [69,77,78,80,170,171]. This process is also completely reversible with the addition of copper chelators. This copper-induced movement from the TGN to subapical and canalicular membranes would allow ATP7B to accomplish both its biosynthetic function (TGN) and its excretory function (bile canaliculi). However, there has been much controversy surrounding the exact subcellular localization of ATP7B, delaying the full elucidation of copper excretion.

In the rat-human hepatic hybrid cell line *WIF-B*, ATP7B distribution partially overlaps with post-TGN and endosomal markers in copper depleted cells, and an apical marker under copper loaded conditions, as well as Rab11, a marker for apical recycling compartments [172]. In agreement with previous studies, this redistribution would allow ATP7B to respond to changes in intracellular copper and have a direct role in its excretion. *In vivo* studies in the LEC rat injected with an ATP7B expression construct have also identified ATP7B both at the TGN and near or at the plasma membrane [173]. However, studies in human hepatoma cell lines *Huh7*, *HepG3B*, and OUMS29 have identified vesicular structures with ATP7B that are positive for late-endosomal markers [174-176]. Furthermore, these studies do not observe any copper-induced trafficking of ATP7B [177]. This localization would still allow for lysosomal fusion in copper excretion and would match well with Wilson disease pathology in which patients with hepatic symptoms accumulate copper in lysosomes, but would not easily accommodate ceruloplasmin biosynthesis at the TGN. Considering the dynamics of vesicular structures and the interconnectedness of pathways, it will be difficult to reach a consensus on the location for ATP7B. The particular liver cell type under investigation also contributes to differences in ATP7B subcellular localization.

These studies support a pathogenic model for WD in which loss of proper ATP7B function in the liver impairs ceruloplasmin biosynthesis and biliary excretion of copper, leading to copper accumulation in lysosomes and other organelles, followed by copper-mediated oxidative damage, cell death, and leakage of copper into the plasma, eventually loading other tissues with copper [156].

IV. ANIMAL MODELS OF WILSON DISEASE

Yeast and bacteria have been instrumental in the identification and characterization of copper proteins. The ability to manipulate cell culture has also provided much understanding of the cellular trafficking of copper, but the single cell is limiting when trying to decipher whole body copper metabolism. Much of what we know about absorption and excretion comes from studies in animals, such as rats. Similarly, animal models of human diseases allow us to study disease pathology and possible treatments at an experimental level not available in humans. Wilson disease has two naturally occurring animal models, the Long-Evans Cinnamon rat and the toxic milk mouse, as well as a genetically engineered *Atp7b* null mouse.

I. LONG-EVANS CINNAMON RAT

The Long-Evans Cinnamon (LEC) rat was established from a closed colony of randomly bred Long-Evans rats [178]. LEC rats accumulate hepatic copper and have markedly reduced levels of serum copper and ceruloplasmin, resembling some WD patients, but Kayser-Fleischer rings have not been observed [179]. Reduced ceruloplasmin levels have been shown to be a consequence of decreased copper incorporation during biosynthesis [180,181], as seen in some WD patients. Copper accumulation in the liver induces DNA strand breaks in LEC rats [182].

At about four months of age, following copper accumulation, LEC rats develop sudden-onset hepatitis associated with severe jaundice, subcutaneous bleeding, oliguria, and loss of body weight [183]. Hepatic iron accumulation observed in LEC rats has been attributed to hemolysis, leading to increasing oxidative damage [184,185]. This may contribute to the development of fulminant hepatic failure from which most animals die. Those that survive go on to develop chronic hepatitis and are highly susceptible to hepatocarcinoma [186,187].

The primary defect in LEC rats appears to be decreased biliary excretion of copper [107,188,189]. Copper deposition in the liver is not uniform, with mosaic patterns of copper accumulation throughout the hepatic lobes [190]. However, copper does tend to preferentially accumulate in periportal (zone 1) hepatocytes [191], consistent with copper accumulation in the liver of WD patients. Approximatelly 75% of copper is present in the cytosol and intracellular distribution is diffuse throughout the cytoplasm most likely bound to MT [189]. Lysosomal copper deposition in hepatocytes is also visible by electron microscopy [190].

The LEC phenotype was determined to be the cause of a single gene mutation inherited in an autosomal recessive manner [183,186]. It was linked to the WD locus on rat chromosome 16 [192,193] and the orthologous *Atp7b* was identified as causative gene [193,194]. Southern blot analysis identified a deletion removing at least 900 bp of coding region at the 3' end and at least 400 bp of the 3' untranslated region [194]. Further characterization of the deletion, placed the proximal breakpoint within intron 15 [195].

Several other pathologies have been described in the LEC rat, including spontaneous porphyria and susceptibility to renal carcinoma and X-irradiation. Other mutant genes have also been identified, such as a mutation in the serotonin N-acetyltransferase (NAT), which controls nocturnal melatonin production [196]. These factors may complicate studies of copper metabolism and may contribute to the differences in phenotype between the LEC rat and WD.

II. TOXIC MILK MOUSE

In 1974, a mutant litter arose out of an inbred DL strain of mice. The entire litter displayed reduced pigmentation, poor growth, tremors, abnormal locomotion, and death by two weeks of age [197]. However, when fostered by normal females, symptoms were mild or absent, suggesting that the milk was a critical agent in producing this phenotype. The new mutant strain was called the toxic milk (*tx*) mouse.

Pups born from *tx* dams display diminished growth rates, apparent one to two days after birth. Pups are hypopigmented, and hair growth is delayed. Coats appear disheveled with distorted individual hairs, and whiskers tend to curl and kink. By day 11, whole body tremors escalate to vigorous lateral shaking, making locomotion difficult. Brains are generally reduced in size with some morphological defects. This phenotype is reminiscent of Menkes disease and suggested copper deficiency as the cause. Atomic absorption spectroscopy of *tx* tissues demonstrated severe copper deficiency. Milk from *tx* dams was also low in copper, a phenomenon not observed in WD mothers.

When *tx* pups are fostered by normal females, pups are fully or partially rescued. If foster-nursed during the first few days of birth, growth rates improve, hair color is restored, and behavioral abnormalities disappear. However, a delay in fostering leads to only partial recovery from symptoms. Fostered pups survive to adulthood, however as they get older they begin to accumulate copper. Most tissues analyzed from seven-week adult *tx* mice exhibit little or no difference in copper compared with normal controls, except the liver.

Livers from *tx* mice show evidence of copper toxicosis with gross morphological, histological, and ultrastructure changes [198,199], leading to hepatic swelling and necrosis [197]. The most notable features are the enlarged livers with irregular surfaces and protruding nodules, swollen large misshapen nuclei, and diffuse cytoplasmic copper staining [198]. Hepatic copper increases 10 to 20 fold and reaches its peak at five months of age. In contrast, plasma copper and ceruloplasmin are greatly reduced. As the mice grow older, other tissues begin to show copper accumulation, including the brain, kidney, and eyes [197]. Therefore, adult *tx* mice are phenotypically similar to WD patients, and the *tx* pup syndrome is the result of failure to accumulate hepatic copper during gestation, which is exacerbated by intake of copper deficient milk postnatally.

By means of various crosses, the *tx* condition was shown to be an autosomal recessive single gene disorder [197]. Although ceruloplasmin levels are reduced in *tx* mice, ceruloplasmin mRNA levels are unaltered, suggesting normal apoprotein production, but failure to incorporate copper during biosynthesis [200]. The excess hepatic copper is associated with MTs in *tx* livers, and levels of MT mRNA are approximately 10-fold higher in *tx* mice [201,202]. However, this effect was concluded to be a secondary consequence of copper accumulation, with the primary defect most likely involving a defect in biliary excretion, similar to WD.

Mapping of the mouse *Atp7b* gene to chromosome 8 and linkage of the *tx* mutation to the same chromosome, supported analysis of the WD gene in *tx* mice [203,204]. Cloning and sequencing of the murine orthologue identified a methionine to valine substitution in the putative eighth transmembrane domain [205]. This methionine is highly conserved across species, supporting the conclusion that this is the causative mutation in the *tx* mouse, making it a true model of WD.

III. ATP7B NULL MICE

In addition to the natural occurring rodent models of WD, a transgenic mouse was created by introducing a homozygous mutation into the murine *Atp7b* in W9.5 embryonic stem cells by homologous recombination [206]. Integration of a neomycin cassette led to alternative splicing and deletion of exon 2, along with a frameshift at the exon 3 junction. Full-length protein was not detected and it was assumed that a null allele for *Atp7b* had been generated. Hepatic copper accumulation is gradual, increasing to 60-fold greater than controls by five months. Intracellular copper accumulation is mostly seen in the cytosol and nuclei [170]. Slight copper increase is also seen in the kidney, brain, placenta, and lactating mammary glands, but no copper deposition is observed in the eye. As in the *tx* mouse, milk produced by mutant dams is low in copper.

Liver pathology develops after five months of age. Despite the lack of steatosis, common in WD livers, the surface of the livers from *Atp7b* null mice appeared irregular with protruding regenerative nodules, indicative of cirrhosis [206]. This pathology develops in stages, progressing from mild necrosis and inflammation, to extreme hepatocellular injury, nodular regeneration, and bile duct proliferation [170]. The accumulation of copper in hepatocyte nuclei is also accompanied by nuclear enlargement [170], similar to that observed in the *tx* mouse [198] and some WD patients [207].

V. OTHER COPPER STORAGE DISORDERS

Although WD can present in childhood, other forms of copper toxicoses exist that are specifically of childhood onset. These include Indian childhood cirrhosis (ICC) and endemic Tyrolean infantile cirrhosis (ETIC). Collectively, along with other cases of non-Indian childhood cirrhosis, this disorder has been called idiopathic copper toxicosis (ICT) [208,209], in an attempt to unify the terminology of non-Wilsonian pediatric liver disease related to primary copper hepatotoxicity.

ICT differs from WD both phenotypically and biochemically. Nervous system abnormalities are absent from ICT and ceruloplasmin levels are often normal or even raised. ICT disease manifestation also appears to depend on environmental copper exposure, whereas WD manifests independent of dietary copper intake. ICT appears in infancy and early childhood as severe liver disease and is histologically defined by hepatocyte necrosis with ballooning and Mallory bodies, pericellular intralobular fibrosis, inflammatory infiltration, absence of steatosis and poor regeneration, with hepatic copper accumulation [210,211]. Copper accumulation is predominantly periportal (zone 1) with panlobular copper staining as the disease progresses [212].

Copper has been implicated as a key environmental factor in the development of ICT. Increased dietary copper has been associated with both ICC and ETIC, in which infants were fed copper-contaminated milk [213,214], and sporadic ICT cases, where copper contamination from water pipes was observed [215]. However, copper ingestion alone does not produce cirrhosis. A genetic component to ICT has been suggested [209,215] and it is proposed that ICT develops when an infant with a genetic susceptibility is exposed to a copper-enriched diet [209,216].

I. INDIAN CHILDHOOD CIRRHOSIS (ICC)

The first of the ICTs to be described, ICC (also known as Sen syndrome), usually presents between the ages of six and 18 months [217]. In addition to the liver pathology described above, sulfur-copper conjugates have been reported in hepatic lysosomes. Approximately 73% of copper is in the nuclear fraction, and there is also evidence of significant DNA fragmentation [218]. Frequency of disease is higher in males, and familial cases are common. Autosomal recessive or X-linked inheritance could not completely explain the appearance of disease, and an environmental source of copper was suggested to be necessary [219]. A retrospective study of ICC patients from Pune showed that infants received cow or buffalo milk heated in brass pots, which may have led to copper contamination [216,220]. Given the preferential treatment given to boys in India, receiving this milk may have been a privilege offered primarily to sons, explaining the high predominance of ICC in male children. ICC has largely disappeared since the use of brass utensils in preparation of milk is no longer common practice.

Two mechanisms for the role of copper in development of disease have been suggested: synergistic toxicity and genetic predisposition [213]. Copper may act synergistically with a second hepatoxoxin, such as pyrrolzidine alkaloids (PAs), which have long been known to be hepatotoxic in cattle. PA toxicity in humans causes veno-occlusion, a clinical feature observed in a small number of children from the Pune series. Milk fed to infants may already be contaminated with PAs and together with copper contamination could produce hepatotoxicity with copper accumulation, as seen in livestock. Alternatively, the high incidence of familial history points towards a genetic component [221].

II. ENDEMIC TYROLEAN INFANTILE CIRRHOSIS (ETIC)

Evidence for a genetic component to ICT came from a large pedigree analysis of infantile cirrhosis identified in the Austrian province of the Tyrol, ETIC [214]. ETIC was clinically and pathologically indistinguishable from ICC and cases of non-Indian childhood cirrhosis. As speculated in earlier reports of ICT, family members confirmed the use of untinned copper and brass vessels for the boiling of milk given to infants. The high frequency of ETIC in the Tyrol suggested a founder effect and the disease was found to be transmitted in an autosomal recessive manner. This study provides strong evidence for genetics in the etiology of ICT, concluding that ICT is an ecogenetic disorder requiring two defective alleles and high levels of copper in order to manifest.

An association study between ETIC and markers at the *ATP7B* locus failed to identify linkage disequilibrium and haplotype analysis did not identify allele sharing among affected chromosomes [222]. Sequencing of the *ATP7B* gene, including all 21 exons and exon-intron boundaries, did not identify any mutations in 23 patients: 12 cases of ICC, one ETIC case, and ten sporadic cases of ICT [223].

VI. OTHER ANIMAL MODELS OF COPPER STORAGE

The molecular basis of ICT has not yet been resolved. Spontaneous animal models of non-Wilsonian copper toxicosis may serve to identify new pathways and lead to the identification of the genes involved in ICT. Not all animals are as tolerant to copper as humans. In general, sheep are more sensitive to high copper intakes and some breeds accumulate copper rapidly. Similarly, other dog breeds have been reported with cases of copper toxicosis, such as Doberman pinschers, Dalmatians, and West Highland white terriers, but none have been as thoroughly studied as the Bedlington terrier.

1. NORTH RONALDSAY SHEEP

Etiological parallels with ICT have been recognized in the North Ronaldsay sheep with copper toxicosis (RCT). The North Ronaldsay sheep are a primitive breed, which have adapted to a copper-poor island environment and low copper seaweed diet [224]. Transfer of this breed onto copper-replete mainland pastures leads to hepatotoxicity, establishing the susceptibility of this breed to copper.

In a restrospective study of livers from mainland-reared adult North Ronaldsay sheep, all samples showed copper accumulation compared to controls [225]. A spectrum of copper accumulation with progressive liver disease falling into four categories (0 to 3) was identified, allowing the investigators to follow the evolution of a distinct pattern of copper-induced liver disease. RCT begins with periportal (zone 1) copper accumulation, which elicits a cellular inflammatory response and cholangioplasia. Subsequent panlobular copper retention with concomitant injury and persistence of inflammation results in an increasingly florid diffuse pericellular fibrosis, with incipient or actual cirrhosis. In contrast, copper accumulation in other sheep breeds is characterized by copper retention predominantly in the centrilobular (zone 3) region with inflammatory focal necrosis [226,227].

Although the liver pathology identified in RCT is similar to that of ICT, neither ballooning of hepatocytes nor Mallory bodies were observed in the study. Because of this major difference, a second study was performed in lambs reared on copper-enriched formula to better mimic ICT conditions [228]. Liver changes were much more uniform than in the adult sheep study. All livers showed copper-positive particles distributed throughout the lobules, and swelling and ultimately ballooning of hepatocytes was observed. Mallory bodies were still absent. The authors suggest that the absence of Mallory bodies in RCT compared with ICT may simply reflect species differences and conclude that the North Ronaldsay sheep is a valid animal model for ICT.

II. BEDLINGTON TERRIER

Large amounts of copper in the livers of Bedlington terriers dying of liver failure were identified in 1975 [229]. Liver disease in these animals seemed to share many features with hepatic manifestations of WD in humans, however several striking differences between the disorders were also noted. Plasma copper and ceruloplasmin levels are generally above normal in the Bedlington disorder [230]. Hemostatic abnormalities are also seen in affected Bedlington terriers. Levels of hemolytic factors VIII, IX, and XI are increased and platelets display hypersensitivity to adenosine diphosphate exposure [231].

Initial reports on Bedlington livers presented very different pathologies. It was soon realized that this is a progressive disorder [232] and each study was presenting the disease at a different stage. Four grades of abnormalities in the Bedlington liver have been identified as the disease progresses [233-236]: pigment granules, mild focal hepatitis, periportal hepatitis resembling chronic active hepatitis, and finally cirrhosis.

When present, inflammatory cells are found primarily in portal tracts, periportal areas, and in randomly distributed microfoci of acute necrosis [234]. Hepatocyte swelling and vacuolization are also observed [236].

Clinical signs of CT are also highly variable, three general groups have been recognized [237]: asymptomatic, acute, and chronic. Dogs in the asymptomatic group show no clinical symptoms, they may be suspected as having CT based on biochemical tests and may have elevated serum glutamic-pyruvic transaminase (SGPT) [235], but can only be confirmed by liver biopsy and increased hepatic copper. The acute form of the disease usually presents in dogs aged two to five years and is often precipitated by a stressful event. Clinical signs include a sudden onset of depression, lethargy, anorexia, vomiting, and fulminant hepatic failure often resulting in death [237]. The majority of dogs display a chronic form of the disease. This form of the disease is progressive and debilitating. Chronic liver damage ultimately leads to cirrhosis, accompanied by polydipsia, polyuria, and chronic weight loss [237]. Hemolytic crisis is often a terminal event in affected Bedlington terriers.

Histologically, copper granules in Bedlington terriers first appear in the cytoplasm of hepatocytes near the central veins (zone 3). With increasing accumulation, midzonal portions of hepatic lobules become involved. In specimens with the heaviest deposits, copper granules can also be detected in the periportal regions (zone 1), however the central regions are always more severely involved in copper accumulation [234,236].

Ultrastucturally, copper accumulates in electron-dense granules in lysosomes [233,234]. Within lysosomes, copper is bound to MT [238,239]. With increasing concentrations of copper, the metal becomes apparent in the nucleus, which leads to DNA damage [240]. Apoptotic bodies have been observed in Bedlington livers [241] and induction of p53, following DNA damage, has been proposed in the pathogenesis of CT [240].

In normal Bedlington terriers, copper decreases with age and is rarely over 500 μg per gram liver dry weight [242]. In contrast, by the age of one, most affected dogs have between 800 and 4000 μg copper per gram liver dry weight. Affected Bedlington terriers continue to accumulate copper, reaching a peak around five to six years of age, after which levels start to decline [230,233,234,242]. Peak levels can be as high as 10,000 μg per gram liver dry weight [242]. Studies also suggest that Bedlington terriers affected by CT begin to accumulate copper *in utero*, as excessive copper accumulation in lysosomes can already be detected at birth [243].

The excessive accumulation of copper in the Bedlington terrier, as in WD, is due to impaired biliary excretion of the metal and there is no evidence of increased copper uptake from the intestinal tract [244]. As a result of hepatic copper overload, renal and urinary copper levels are also elevated [230,245]. Concentrations of copper in other tissues have been reported to be within normal ranges, with elevated brain copper seen in only three older dogs [230]. As in WD, it is speculated that once hepatic copper reaches a certain level copper secondarily rises in the brain. Elevated copper levels in the Bedlington cornea have not been investigated, but Kayser-Fleischer rings have not been seen in dogs.

Inheritance of CT in the Bedlington terrier was shown to be autosomal recessive [246]. Sharing similarities with WD made the *WD* gene an obvious target. In humans and mice, the WD locus is closely linked to esterase D (ESD) and retinoblastoma (RB1). Initial studies proposed that if *WD* and *CT* are homologous genes, linkage of CT to ESD and/or RB1 would likely exist, based on conservation of linkage groups across species maintaining genes in synteny [247]. However, CT failed to display linkage to ESD or RB1. Subsequent linkage of CT to the microsatellite marker C04107 [248], allowed for several candidate genes to be excluded based on mapping data, including *ATP7B* [249,250]. Recently, the *MURR1 (COMMD1)* gene has been implicated in the etiology of CT in the Bedlington terrier [251] and will be discussed in subsequent chapters.

VII. OUTLINE OF THESIS

In addition to answering questions regarding the pathogenesis and treatment of copper-associated diseases, animal models of copper disorders may allow the identification of novel copper proteins that often lead to the identification of human homologues. This thesis focuses on animal models of copper storage and characterization of the genes involved in these disorders in order to gain a better understanding of copper homeostasis and provide new insight into the mechanisms of copper transport.

To this end, in **Chapter 2** I identified the genetic defect in *Atp7b* in a new strain of *tx* mouse, enabling rapid and accurate genotyping of mutant animals. Exclusion of *ATP7B* and other copper genes in Bedlington terrier CT made this disorder particularly interesting for identifying possible novel copper genes. In **Chapter 3** I describe the exclusion of *ATP6H* and confirm a deletion in the *MURR1 (COMMD1)* gene in most CT-affected dogs in **Chapter 4**. Also in this chapter, I identify novel haplotypes in some affected Bedlington terriers, which suggests the involvement of other genes in the etiology of this disorder acting in the same pathway, either independently or as modifiers. **Chapter 5** describes the analysis of *ATP7B* as a possible modifier of CT and identification of a unique polymorphism in *ATP7B* in Bedlington terriers. Searching for supporting data for the involvement of *MURR1 (COMMD1)* in CT, the potential role of the human *MURR1 (COMMD1)* homologue in a series of patients with copper storage, similar to but not molecularly identified as WD, was assessed in **Chapter 6**. I did not identify any mutations in these patients. As a result, I was unable to confirm the role of MURR1 (COMMD1) in copper homeostasis or provide supporting evidence for the role of *MURR1 (COMMD1)* in CT. Therefore further functional analysis of MURR1 (COMMD1) is required, particularly analysis of its function in the copper transport pathway. **Chapter 7** describes preliminary results in the functional characterization of MURR1 (COMMD1), including antibody production and cell culture experiments.

CHAPTER 2 : The Jackson Toxic Milk Mouse as a Model for Copper Loading

Veronica Coronado, Manoj Nanji, Diane W. Cox.

Department of Medical Genetics, University of Alberta, Edmonton, AB, Canada.

Mammalian Genome (2001) **12**: 793-795

For this publication MN provided technical guidance and assisted in experimental protocol.

I. INTRODUCTION

Copper is an essential trace element required for the normal biological function of several prokaryotic and eukaryotic enzymes. However, when present in excess, copper becomes toxic, catalyzing the production of highly reactive oxygen species, including the conversion of hydrogen peroxide to hydroxyl radical [2]. Excessive production of free radicals can result in tissue damage due to oxidative stress. Recently, free-radical induced oxidative stress has been implicated in a variety of neurological disorders, including Alzheimer disease, AD [252], Parkinson disease [253], and amyotrophic lateral sclerosis [254]. In addition, copper has been shown to accumulate in AD-affected brains [255] and amyloid β aggregation, a pathological characteristic of AD, appears to be directly induced by the presence of copper [256]. However, the destructiveness of copper toxicity has been studied primarily in Wilson disease (WD), an autosomal recessive disorder in which ATP7B, a copper-transporting ATPase expressed predominantly in the liver, is defective [61, 62]. Disruption of the copper transport pathway in the liver leads to reduced excretion of copper from the liver into bile and reduced incorporation of copper into ceruloplasmin (reviewed in [257]). As a result, WD patients accumulate copper in the liver, brain, and kidney, leading to chronic liver disease and/or neurological damage frequently associated with kidney malfunction.

Two animal models, with clinical and biochemical features of WD, have been reported to have naturally occurring mutations in their homologous WD genes (*Atp7b*). The Long Evans Cinnamon (LEC) rat has an extensive deletion in the 3' region of this gene [194] and the toxic milk (*tx*) mouse, a 3' missense mutation in the last transmembrane domain [205]. The *tx* mutation first arose in 1974 in the inbred DL strain, and the *tx* condition was ascribed to a single autosomal recessive factor [197]. The *tx* mutation was later identified as an A to G base change at position 4066 resulting in a methionine to valine substitution in the eighth transmembrane region, M1356V [205]. As with WD, the adult toxic milk mouse is characterized by decreased levels of ceruloplasmin and hepatic accumulation of copper eventually leading to liver cirrhosis [198], and can develop haemolysis [199]. Despite these similarities with WD patients, liver morphology of adult *tx* mice shows significant differences from WD livers [198]. Additionally, homozygous *tx* dams produce copper-deficient milk, despite increased copper concentrations in lactating mammary glands [206]. This is due to mislocalization of Atp7b in lactating *tx* mammary glands, preventing delivery of copper into milk [258], a phenomenon not reported in WD. Consequently, litters born of homozygous *tx* dams are severely copper deficient and display growth retardation, hypopigmentation, and death by two weeks of age [197].

In 1987, a new autosomal recessive mutation (tx^J) arose in the C3H/HeJ animal resources colony at the Jackson Laboratory, Bar Harbour, Maine [259]. As with the *tx/tx* mutant, adult homozygous tx^J mice develop cirrhosis, and infant mice are pale coloured, copper deficient, and display early mortality [260] unless fostered by wild-type dams. Allelism tests done by Dr. Harold Rauch at the University of Massachusetts showed the tx^J mutation to be allelic with the original *tx* mutation [259]. tx^J homozygotes have been maintained on the C3HeB/FeJ background, a derivative of C3H/HeJ, at the Jackson Laboratory and are a readily available *tx* strain, but the specific mutation has not been identified. This strain should be particularly useful in the study of neurological diseases in which copper accumulation plays an active role in pathology, such as Alzheimer disease.

Here we report the cloning and sequencing of the *tx^J* mouse *Atp7b* and identify the causative mutation as a glycine to aspartate substitution resulting from a single missense mutation (Gly712Asp) in the second putative transmembrane segment.

II. METHODS AND SAMPLES

Selected tissues from homozygous wild-type C3HeB/FeJ background and homozygous mutant C3HeB/FeJ-Atp7b$^{tx\text{-}J}$ mice (Jackson Laboratory) were removed and snap-frozen in liquid nitrogen. Genomic DNA was isolated by standard phenol/chloroform extraction. RNA was extracted using TRIzol reagent (GIBCO, BRL). Reverse-transcription PCR primers were designed from DL sequence (GenBank accession #U38477) to produce four overlapping fragments of approximately 1.5 kb (Fragment 1: 5' UTR, exon1 and exon 2, Fragment 2: 3' end of exon 2, exons 4-7 and 5' end of exon 8, Fragment 3: 3' end of exon 8 and exons 9-15, Fragment 4: exons 16-21 and 3' UTR). Reverse-transcription of 5 μg RNA was carried out in a 20 μl volume using 200 ng primer (mouse 4R or mouse 2R, Table 2-1) with 200 U SuperscriptII (GIBCO, BRL). Of this reaction, 2 μl were used as template for PCR amplification of fragments 2-4 with 50 ng each of sense and antisense primers, 200 μM each dNTP, and 1.5mM $MgCl_2$ in a final volume of 30 μl. (PCR conditions: 94°C for 30 sec, 30 cycles of 94°C for 30 sec, 60°C for 40 sec, and 72°C for 60 sec). Exon 1 and exon 2 were amplified from genomic DNA. Primers for genomic amplification were designed from sequence of mouse BAC clone 309P13. Exon/intron boundaries were predicted by sequence comparison with human

Table 2-1. Primers used for RT-PCR, and amplification and sequencing of C3HeB/FeJ normal and tx^J DNA.

Primer Name	**Region Amplified**	**Primer Sequence**
mus-ex1F	exon 1	CGATGCCTGAACAGGAGAGACA
mus-int1R	exon 1	GGAACCGAGGAGAAAAGCGCT
mus-ex2R	intron 1	GGACGAGCTGGTGCTGTCCAGA
mus-int1F	exon 2	GCTACGGAAGGATGAAAATTGTT
mouse 1R	exon 2	TGGCTTCTACAGCCGTTCGGAGTTCG
mouse 2F	fragment 2/RT-PCR	TACGACCCCTCCATAGTCAGCTTGG
mouse 2R	fragment 2/RT-PCR	GCTCTTCTCTGCCTTCTCGGCTACG
mouse 3F	fragment 3/RT-PCR	CAAGCCTACAAATCGCTGAGACACAGG
mouse 3R	fragment 3/RT-PCR	GCGTCACTGATGTCACTGGAGATGG
mouse 4F	fragment 4/RT-PCR	GTGATCTGACTGCTCACCCTGTTGG
mouse 4R	fragment 4/RT-PCR	GTGTGATCTCGCCCTCATGAAAAGC
mus-ex8R	intron 7	CCACCAGGATGACCAGGGAGTA
mus-int7fwd	exon 8	CTCCTAGTCCTGAGGCTGGCTCCTC
mus-int8rev	exon 8	ACACACTGCCTTTGGGCTGAGAGTC
mus-int14F	exon 15	ACGCCCTGCTCTTTTGCTTCCA
mus-ex15R	exon 15	CCTGTGGGAGGGTTGCCAACT

Primers for RT-PCR were designed, using the DL mouse sequence (GenBank accession #U38477), to produce overlapping fragments of approx. 1.5 kb. Intronic primers for exon amplification from genomic DNA were designed from sequencing of mouse BAC clone 309P13 (RPCI-23 mouse library). Exonic primers were designed from human *ATP7B* sequence [147]. Except for RT-PCR, all PCR cycles began with a 94°C denaturation for 40 sec followed by 35 cycles of 94°C for 30sec, X°C for 30 sec (40 sec for exon 2), and 72°C for 30 sec (1 min 30 sec for exon 2). X= 65 for exon 1 and 15, 58 for exon 2, and 68 for exon 8, ex: exonic primer, int: intronic primer.

ATP7B [147] and confirmed by sequencing the 309P13 clone. Mouse BAC clone 309P13 was isolated by screening of the C57BL/6J mouse BAC library (RPCI-23) using a 340bp mouse *Atp7b* fragment labeled with α^{32}P-dCTP. DNA from 12 positive BAC clones was isolated and digested with EcoRI (MRC Genome Resource Facility). Subsequent Southern blot analysis (65°C hybridization, room temperature overnight) identified two non-redundant clones. Partial sequencing established clone 309P13 as containing the *Atp7b* gene.

All PCR products were gel purified using GenElute miniprep binding columns (SIGMA). Exon 1 was sequenced directly by ThermoSequenase (Amersham). Fragment 3 cDNA was sequenced directly using LICOR IRD-800 dye-terminators. Exon 2, fragment 2, and fragment 4 were cloned into pGEM-T (Promega) and clones confirmed by restriction enzyme analysis. Clones were sequenced by ThermoSequenase cycle sequencing (Amersham) using M13-IRD labelled primers (LICOR). Multiple clones were sequenced to eliminate any errors inherent to Taq polymerase during PCR. All differences were confirmed by sequencing of exons amplified from genomic DNA. *Atp7b* from the original strain from which the *tx^J* mutation arose (C3H/HeJ; Jackson Laboratory) was sequenced from genomic DNA and confirmed to be identical to the secondary background strain (C3HeB/FeJ).

III. RESULTS AND DISCUSSION

The coding sequence from the *tx^J* mouse *Atp7b* shows divergence with the DL mouse in three exons, exon 2, 8, and 15. Two of these differences, discussed below, are natural polymorphisms in the C3HeB/FeJ strain and are also present in wild-type sequences. The defect in the *tx*^{J} mouse arises from a G to A base substitution at position 2135, causing a Gly712Asp missense mutation in the second putative membrane-spanning domain (exon 8). A change from glycine, a small aliphatic amino acid, to aspartate, an acidic, negatively charged amino acid, is predicted to affect the protein structure of Atp7b, most likely disrupting the formation of the transmembrane domain. Glycine712 is highly conserved among rats, dogs, sheep, and humans (Fig 2-1A), suggesting an important role for this residue in the structure/function of the Atp7b protein at this position. We conclude from this, and the fact that it is the only difference between mutant and wild-type, that this Gly712Asp is the causative mutation in the *tx*^{J} mouse *Atp7b*. Interestingly, the *tx* and *tx*^{J} mutations display homogeneous phenotypes despite being different mutations, whereas in WD there is considerable phenotypic variation among patients.

This specific mutation has not been reported in any human WD patients. However, there is a missense mutation described in WD patients at the corresponding base in exon 8 leading to a glycine to alanine (Gly710Ala) amino acid substitution [261]. There are also two other missense mutations described in this codon where Gly710 (712 in mice) is replaced by serine [262] or arginine [263]. These mutations, all involving the same amino acid and present in diseased patients, further support the conclusion that the Gly712Asp missense mutation in the *tx*^{J} mouse causes the disease phenotype.

Analysis of the *tx*^{J} sequence revealed that the Gly712Asp mutation introduces a novel *Fok I* restriction site and destroys a *Taq II* site. Exon 8 was amplified and digested with *Fok I* and the expected bands were observed (Fig 2-1B). Undigested exon 8 migrated at approximately 360 bp for both samples. Digestion with *Fok I* produced fragments of

A

DL mouse	FLGGWYFYVQAYKSLRHRSANMDVLIVLATTIAYAYSLV
C3HeB/FeJ	FLGGWYFYVQAYKSLRHRSANMDVLIVLATTIAYAYSLV
tx^J	FLDGWYFYVQAYKSLRHRSANMDVLIVLATTIAYAYSLV
Rat	FLGGWYFYVQAYKSLRHKSANMDVLIVLATTIAYAYSLV
Human	LLGGWYFYVQAYKSLRHRSANMDVLIVLATSIAYVYSLV
Sheep	FLGGWYFYVQAYKSLRHGMANMDVLIVLATSIAYVYSLV
Dog	LLGGWYFYVQAYRSLRHRAANMDVLIVLATSIAYTYSLV

DL mouse	ILVVAVAEKAEKSPVTFFDTPPMLFVFIALGRWLEHVAK
C3HeB/FeJ	ILVVAVAEKAEKSPVTFFDTPPMLFVFIALGRWLEHVAK
tx^J	ILVVAVAEKAEKSPVTFFDTPPMLFVFIALGRWLEHVAK
Rat	ILVVAIAEKAEKSPVTFFDTPPMLFVFIALGRWLEHVAK
Human	ILVVAVAEKAERSPVTFFDTPPMLFVFIALGRWLEHLAK
Sheep	ILVVAVAEKAERSPVTFFDTPPMLFVFIALGRWLEHVVK
Dog	ILVVAVAERAERSPVTFFDTPPMLFVFIALGRWLEHIAK

B

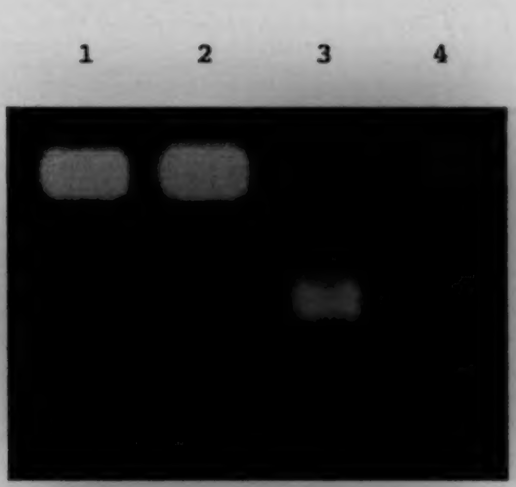

Figure 2-1. Glycine substitution in exon 8. (A) Glycine 712 is conserved among species. Amino acid sequence of mouse exon 8 compared with corresponding sequence in other species. DL: background strain for original *tx* mutation, C3HeB/FeJ: background for Jackson *tx* mutant (*tx^J*). **(B)** Restriction endonuclease analysis of exon 8. Exon 8 was amplified from genomic DNA and digested with *Fok I* enzyme (7 µl exon 8 PCR sample, 2 µl buffer, 1 µl enzyme, 10 µl water, 37°C for 1.5 hrs). 1: undigested C3HeB/FeJ, 2: undigested *tx^J*, 3: digested C3HeB/FeJ, 4: digested *tx^J*. Undigested bands: 360 bp; digestion produces 180 bp bands and an additional 80 bp band for *tx^J*.

approximately 180 bp in both wild-type and *tx*^{J} samples, as well as an additional 80 bp band in the *tx*^{J} sample. This information allows for a rapid test to distinguish between normal and *tx*^{J} mice.

As noted above, sequencing of the *tx*^{J} showed divergence with the DL strain in exon 2 and exon 15 of the *Atp7b* gene. C3HeB/FeJ wild-type and mutant cDNAs both contain T instead of C at position 3268 and 3288 in exon 15. These base transitions do not lead to amino acid changes. We also observed these two variants in the C57BL/6J mouse *Atp7b* BAC clone RPCI-23 309P13 which was originally partially sequenced to design intronic primers. Sequence differences in exon 2 also affect two amino acids, but involve four base mismatches. The net effect is a Lys107Ser and a His108Ala substitution. Amino acid comparison with rat, human, and sheep shows that the serine-alanine combination is actually more highly conserved than the DL lysine-histidine combination (Fig 2-2).

The *tx*^{J} mouse model will be useful for studies of the pathology of copper toxicity in man, as well as the evaluation of potential new therapies.

DL mouse	RISSLKGIVNIKVSLEQG**KH**TVRYVPSVMNLQQICLQIEDMGFEASAAE
C3HeB/FeJ	RISSLKGIVNIKVSLEQGSATVRYVPSVMNLQQICLQIEDMGFEASAAE
tx^J	RISSLKGIVNIKVSLEQGSATVRYVPSVMNLQQICLQIEDMGFEASAAE
Rat	RISSLKGIVSIKVSLEQGSATVKYVPSVLNLQQICLQIEDMGFEASAAE
Human	RISNLKGIISMKVSLEQGSATVKYVPSVVCLQQVCHQIGDMGFEASIAE
Sheep	RVSSLKGIVSIKVSLEQSSAEVRYVPSVVSLMQICHQIEDMGFQASVAE

Figure 2- 2. Serine 107 and alanine 108 are conserved among species. Comparison of amino acid sequence from a section of exon 2. DL: background strain for original *tx* mutation, C3HeB/FeJ: background for Jackson *tx* mutant (*tx*^{J}).

CHAPTER 3 : ATP6H, a Subunit of Vacuolar ATPase Involved in Metal Transport: Evaluation in Canine Copper Toxicosis

Manoj Nanji, Veronica A. Coronado and Diane W. Cox
Department of Medical Genetics, University of Alberta, Edmonton, Alberta, Canada.

Mammalian Genome (2001) **12**: 617-621

For this publication MN designed the overall experiment, isolated RNA and synthesized *ATP6H* cDNA, conducted Southern blot analysis, and wrote the first manuscript draft.

I. INTRODUCTION

Canine copper toxicosis (CT) is an autosomal recessive disorder of copper transport, common in Bedlington terriers [230]. In normal Bedlington terriers, the mean level of hepatic copper is 200 μg/g dry weight. In Bedlington terriers affected with copper toxicosis, the mean value of hepatic copper is 6000 μg/g dry weight, with a range of 1900-12000 μg/g [230]. In affected dogs, the accumulation of copper in the liver results from the failure of the liver to excrete excess copper into bile [244]. This results in chronic hepatitis and eventually liver cirrhosis. CT is phenotypically and biochemically similar to Wilson disease (OMIM 277900) and can be treated with agents that are effective for the treatment of Wilson disease, such as zinc acetate or penicillamine [264].

Wilson disease and its rodent models result from mutations in the gene encoding a copper transport P-type ATPase, *ATP7B* in humans [61,62] and *Atp7b* in the toxic milk mouse [205] and the Long-Evans Cinnamon rat [194]. The CT locus in Bedlington terriers has been mapped to canine chromosome region CFA10q26 by fluorescence *in situ* hybridization (FISH) [249] using a BAC clone containing C04107, a microsatellite marker closely linked to CT [248]. In this mapping study, *ATP7B* was excluded as a candidate gene for CT, as it mapped to canine chromosome region CFA22q11.
In addition to ATP7B, the copper transport pathway characterized in humans provides several other candidate genes for CT in Bedlington terriers. CTR1, CTR2, and a group of small proteins termed metallochaperones also play a role in copper homeostasis in mammalian cells. CTR1 is thought to be responsible for high affinity cellular uptake of copper and CTR2 for the low affinity uptake of copper [15]. Metallochaperones deliver copper to distinct intracellular targets [265]. Currently, three metallochaperones have

been characterized: human CCS (yeast Lys7p), which delivers copper to superoxide dismutase 1 (Sod1p) in the cytosol [35], Cox17p, which directs copper to the mitochondria for activation of cytochrome oxidase [39,42] and human ATOX1 (yeast Atx1p), localized within late trans Golgi network [47] which carries copper specifically to the secretory pathway for incorporation into ATP7B. BAC clones containing canine *CTR1* and *CTR2* were mapped by FISH on dog chromosomes [249]. *CTR1* and *CTR2* were excluded as candidate genes for CT, as they both mapped to canine chromosome region CFA11q22.2-22.5. Recent mapping studies and molecular characterization of *ATOX1* in Bedlington terriers have also excluded *ATOX1* as a candidate gene underlying CT [250,266].

The region including the canine CT locus has a syntenic gene cluster on human 2p21 [267]. The gene, *ATP6H*, encoding the vacuolar proton-ATPase subunit M9.2 [268], has been mapped to chromosome 2p21 and has been suggested as a candidate gene for CT [250]. ATP6H contains a conserved sequence motif CSVCC [268], similar to those of metal binding proteins (MTCXXC). A further reason for considering ATP6H as a good candidate is that yeast defective in vacuolar ATPase have abnormal copper and iron homeostasis [269]. Comparative mapping between human and dog genomes has refined the CT-candidate region in humans between the SPTBN1 and SLC1A4 genes, a region of approximately 30 cR_{3000} in the dog [270]. In the same study, *ATP6H* was excluded as a candidate gene underlying CT based on human radiation hybrid (RH) mapping of the gene outside the specified region. However, comparing chromosome between species often shows regions of discontinuity within syntenic clusters. Mapping of *ATP6H* outside the region in the human does not guarantee the same order of genes in the dog, especially since the CT region is estimated to be 9 Mb [270]. For these reasons, we undertook cloning and characterization of *ATP6H* in the dog in order to map this gene on a canine RH panel and conduct mutation analysis in CT affected Bedlington terriers. We also report the identification of two canine *ATP6H* pseudogenes. Our results unequivocally exclude *ATP6H* as a candidate gene underlying CT in Bedlington terriers.

II. MATERIALS AND METHODS

I. ISOLATION OF CANINE ATP6H CDNA

Preparation of RNA: Total RNA was prepared from liver, kidney and fibroblast samples from a normal dog and a fibroblast sample from a obligate heterozygote (mother of an affected) Bedlington terrier respectively, using TRIzol reagent (GIBCO, BRL). Homozygous normal dogs were distinguished from heterozygotes based on microsatellite marker analysis of C04107 [248]. The affected dogs were diagnosed by a high liver copper as determined from a biopsy sample, and pedigree analysis.

II. RT-PCR

From cDNA sequence of human *ATP6H*, primers were designed to allow reverse transcription and PCR amplification of the canine *ATP6H* homolog from each of the total RNA preparations above. 5 μg of total RNA was mixed with 500 ng of 3' RACE Adapter Primer (GIBCO, BRL) and the mixture was heated at 70°C for 10 min and snap chilled on ice. First strand synthesis was carried out in a final volume of 20 μl for 50 min at 42°C with SuperscriptII RNaseH-RT (GIBCO, BRL). For PCR, 2 μl of RT reaction was amplified in 50 μl containing 200 nM each, forward (M9.2F):

ATGGCGTATCACGGCCTCACTGTGCCTCT and Universal Adapter Primer (GIBCO-BRL), 200 µm each dNTP, 50 mM KCl, 1.5 mM MgCl, 20 mM Tris-HCl (pH 8.5) and 5 U of AmpliTaq DNA polymerase (Perkin Elmer). The thermal cycling protocol was 94°C for 1 min, followed by 30 cycles at 94°C for 40 sec, 56°C for 40 sec and 72°C for 1 min carried out in a thermocycler (PTC-100-96V; MJ Research, Watertown, USA). PCR products were purified with a Qiaquick spin column (Qiagen), and cycle sequenced (Thermosequenase, Amersham) using the sense PCR primer. The remaining product from the first strand cDNA synthesis was purified and dC tailed according to manufacturers instructions (GIBCO, BRL). Standard PCR using one fifth of the tailed cDNA was performed as described above in 50 µl using 200 nM each, of reverse primer (M9.2R) and the 5' RACE Abridged Anchor Primer (GIBCO, BRL). The PCR product was purified with Qiaquick spin column (Qiagen), and cycle sequenced (Thermosequenase, Amersham) using the antisense PCR primer.

III. GENOMIC SOUTHERN BLOTTING

Total genomic DNA was isolated from blood [271] collected from normal and affected Bedlington terriers. 5 µg each, of genomic DNA from a normal Bedlington terrier, was digested with *EcoRI*, *BamH1* and *EcoR1/BamH1* respectively, electrophoresed through 1% agarose gel and blotted onto the Hybond-N+ nylon membrane (Amersham). The blot was probed with canine *ATP6H* cDNA labeled with α-^{32}P-dCTP using a T7 Quick Prime kit (Pharmacia Biotech). Hybridization was carried out in 7% SDS, 0.5 M phosphate buffer pH 7.2 and 10 mM EDTA at 65°C overnight. Final washing conditions were at 65°C in 0.1X SSC and 0.1% SDS. Autoradiography was done with Kodak film at -70°C, overnight.

IV. ISOLATION OF CANINE ATP6H GENOMIC CLONES

BAC clones were isolated by screening eight high density filters of a total canine genomic BAC library, RPC81 [272] using canine *ATP6H* cDNA as a probe, labeled with α-^{32}P-dCTP using a T7 Quick Prime kit (Pharmacia Biotech). The screening followed by Southern blot analysis of DNA from BAC clones revealed fifteen positive BAC clones of three different types. From each of the three different types of BAC clones, one was used to determine the sequences of *ATP6H* loci.

BAC DNA from 100 ml overnight culture was isolated by alkaline lysis method using a Qiagen midi plasmid kit (Qiagen) as described by the manufacturer. Double stranded BAC DNA was cycle sequenced using the Thermosequenase kit (Amersham) according to the manufacturer. Primers for sequencing, shown 5' to 3', were designed from the canine *ATP6H* cDNA sequence and were: A: ATGGCGTATCACGGCCTCACTGTG CCTCT, B: AAGAGATAGCAGCAAACTGAACA, C: TGTTCAGTTTGCTGCTAT CTCTT, D: CTGTGGTCCAAAGAGAGGGTTGA, E: ATGATACCTGAGGTACCA GATG, F: TCAACCCTCTCTTTGGACCACAG, G: CATCTGGTACCTCAAGTATC AT, H: CATCTTCAAATTCACAGGTTCCA, I: TCTGAACATGCTCTCCTACTG.

V. MAPPING OF CANINE ATP6H AND C04107IPCR ON A CANINE RADIATION HYBRID PANEL

A 193 bp single copy probe, C04107ipcr, which lies next to the CA polymorphic marker linked to canine copper toxicosis (C04107) [249], and a 137 bp probe, spanning the exon 1/intron 1 splice junction of canine *ATP6H*, were each amplified by PCR from genomic DNA of a Bedlington terrier and from the canine radiation hybrid panel RHT08.02, containing 91 canine/hamster hybrids (Research Genetics). Primer sequences used were: C04107ipcr: forward primer GTATGTACGTGAGTGTGATGTGG, reverse primer CCTAGAAGAATACAAGCCTGAGAC [249]. For *ATP6H*, forward primer, CF1 and reverse primer, C1IR, shown above, were used. A second reverse primer from exon 3 of *ATP6H* (M9.2R: TCAAGGCCAATGATACTTCAGATACCAG) amplified a 242 bp product, plus or minus insertions or deletions, from intronless pseudogenes. For PCR, 25 ng of genomic DNA from a normal Bedlington terrier and from each of the hybrid clones was amplified in 10 μl reactions containing 200 nM each sense and antisense primers for C04107ipcr and *ATP6H* probes, respectively, 200 μM each dNTP, 50 mM KCl, 1.5 mM MgCl, 20 mM Tris-HCl (pH 8.5) and 2 U of AmpliTaq DNA polymerase (Perkin Elmer). The thermal cycling protocol was 94°C for 1 min followed by 30 cycles at 94°C for 40 sec, 60°C for 40 sec and 72°C for 1 min (thermocycler: PTC-100-96V; MJ Research, Watertown, USA). PCR products were run in a 1% agarose gel, stained with ethidium bromide and photographed. Canine specific PCR products were scored for their presence or absence in the hybrid clones.

VI. MUTATION ANALYSIS

For PCR, 25 ng of genomic DNA from each normal and affected Bedlington terriers was amplified, in 50 μl reactions containing 200 nM each sense and antisense primers for each of the four exons, 200 μm each dNTP, 50 mM KCl, 1.5 mM $MgCl_2$, 20 mM Tris-HCl (pH 8.5) and 5 U of AmpliTaq DNA polymerase (Perkin Elmer). The thermal cycling protocol was 94°C for 1 min followed by 30 cycles at 94°C for 40 sec, 58°C for 40 sec and 72°C for 40 sec (thermocycler: PTC-100-96V; MJ Research, Watertown, USA). PCR products were purified with Qiaquick spin column (Qiagen) and cycle sequenced (Thermosequenase kit,

Amersham). Primer sequences used: Exon 1: forward, C1F: ATGGCGTATCACGGCCT CACTGTGCCTCT; reverse, C1IR: GTCCTTCCCAAGGCGGGCCCCTA; Exon 2: forward, C2F: GCTTAAGCCATCCGACAATG, reverse, C2R: AAGTGTGCTCTTCCC TCTTAGG; Exon 3: forward, C3F: AGGTGTGCTTGTGAACATGG; reverse, C3R: CACCAATGTGAAAGGTTGAGG.

III. RESULTS

I. GENOMIC SOUTHERN BLOT ANALYSIS OF CANINE ATP6H

Canine *ATP6H* cDNA was hybridized to each of *EcoRI*, *BamH1* and *EcoR1/BamH1* digested genomic DNA from a normal dog (Fig 3-1). Multiple *EcoR1* and *BamH1* bands were observed, suggesting the presence of multiple *ATP6H* loci in the canine genome.

II. CLONING AND CDNA ANALYSIS OF THE CANINE ATP6H

The canine *ATP6H* cDNA was isolated by RT-PCR using 5' and 3' RACE primers and primers designed from human *ATP6H* cDNA sequence. The canine *ATP6H* cDNA contained an open reading frame of 246 bp encoding a protein of 81 amino acid residues (Fig 3-2A). The deduced amino acid sequence showed 99% identity with human ATP6H. The potential metal binding site, CSVCC and a glycosylation site, NET are conserved in each of the sequences (Fig 3-2 B).

III. CLONING OF THE GENOMIC REGION OF CANINE ATP6H

We cloned the genomic region of canine *ATP6H* by screening the total canine genomic BAC library, RPC81. Sequence analysis of the BAC inserts showed that the BAC clone

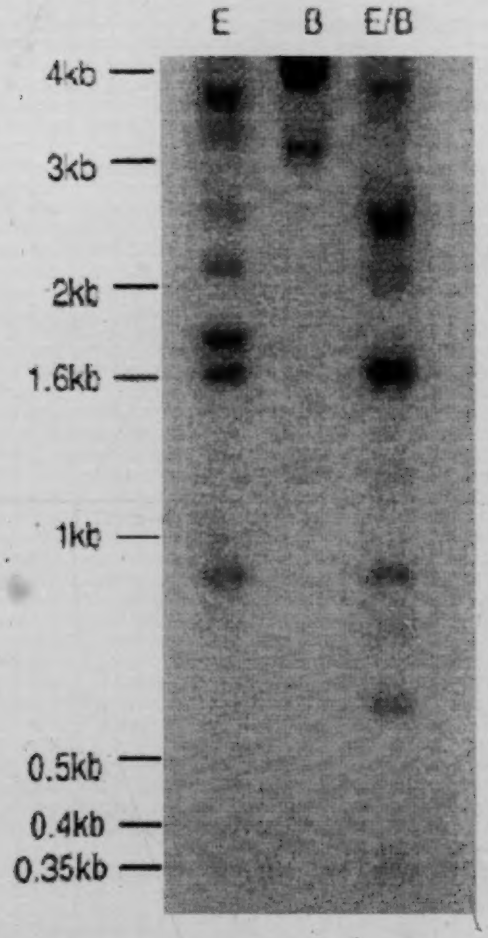
E
B
E/B
4kb
3kb
2kb
1.6kb
1kb
0.5kb
0.4kb
0.35kb

Figure 3-1. Southern blot hybridization. *ATP6H* cDNA was used to probe dog genomic DNA digested with *EcoR1* (E), *BamH1* (B), or *EcoR1/BamH1* (E/B).

A

```
ATP6H        C-AGG-GG-CTT--GCGC---CTCCGCGGCAGCCATGGC-GTATCAC-GGCCTCACTGTGCCTCTCATCGTG
ΨATP6H-1     C-ATG-GG--TT---CGCAG-CTCCGTGGCAACCATGCCTGTA--AC-GGCCTCACCGTGCCTCTCATCGTG
ΨATP6H-2     CCAGGTGGACCGAAGAG-AGGCGCTG-GGCAGCCATGGC-GTA-CAATGGC-TCACTGTGCCTCTCATCATG

                                                                            1↓2
ATP6H        ATGAGCGTGTTCTGGGGCTTCGTCGGCTTCTGCGTGCCCTGGTTTATCCCTAAGGGTCCCAACCGGGGAGTT
ΨATP6H-1     ATGAGCACGTTCTGGGGCTTCGTCGGCTTCTGCGTGCCCTGGTTCATACCTAAGGGTCCCAACCGGGGAGTT
ΨATP6H-2     ATAAGCGTGTTCTGGGGCTTTGTCGGCTTCTGCGTGCCCTGGTTTATCCCTAAGGGTCCCAACCGGGGAGTT

                                               2↓3
ATP6H        ATCATCACCATGTTGGTAACCTGTTCAGTTTGCTGCTATCTCTTTTGGCTGATTGCAATTCTGGCCCAACTC
ΨATP6H-1     ACCATCACCATGTTC--A-C-T-TT--G----CTACTATCTCTTTTGGCTGATTGCAATTCTGGCCCAACTC
ΨATP6H-2     ATCATCACCATGTTGGTAACCTGTTCAGTTTGCTGCTATCTCTTTTGGCTGATTGCAATTCTGGCCCAACTC

ATP6H        AACCCTCTCTTTGGACCACAGTTGAAAAATGAAACCATCTGGTACCTCAAGTATCATTGGCCTTGAGGAGGA
ΨATP6H-1     AACCCTCTCTTTGGACCACAGTTGAAAAATGAAACCATCTGGTACCTCAAGTATCATTGGCCTTGAGGAGGA
ΨATP6H-2     AACCCTCTCTTTGGACCACAGTTGAAAAATGAAACCATCTGGTACCTCAAGTATCATTGGCCTTGAGGAGGA

                                  3↓4
ATP6H        AGACCTGCTCTCCAGCGCTCAGTCACTGAGGTCACGAAGAGAATTCCTCTAGATGCAAAATCAACTCCAAAC
ΨATP6H-1     AGACCTGCTCTCCAGCGCTCA-T---TGAGGT
ΨATP6H-2     AGACCTGCTCTCCAGCGCTCAGTCATTGAGGT

ATP6H        CCAGACCGCCTTCTTTGACTTGCCTATTTTGGCCATCAGCTGCCTTAAACATTCACACCATATTTGAATAT
             CTTATTCTACAATGCAGTATTTTTTCCTGTTGCCTTTTTTTACATTTTGATGAATTATGTGCCTACTTAAACTG
             TGCTGACTCCATAAAATGTTTATGCACTCTTCTGAGATAGAGGGTGCTATTCTTCTGAGAAATACATTGCTCTC
             TCCTTGGAACCTGTGAATTTGAAGATGACTCCTGCCTGGTCACAACATGAGAATCAGCAAAGTGTTTAAAAACT
             GTCACAAGACAAGGCAGTCAGTAGGAGAGCATGTTCAGAGGGAATATCTGTCCCAACAGAATTACACCAAAGTA
             TATTTTCAGGATGGCTTTCTTATTTCTGCCATCTACTGGAATAAATTATTTTTCAGCTTTCTGTGG
```

B

```
cATP6H       MAYHGLTVPLIVMSVFWGFVGFCVPWFIPKGPNRGVIITML
hATP6H       MAYHGLTVPLIVMSVFWGFVGFLVPWFIPKGPNRGVIITML

cATP6H       VTCSVCCYLFWLIAILAQLNPLFGPQLKNETIWYLKYHWP
hATP6H       VTCSVCCYLFWLIAILAQLNPLFGPQLKNETIWYLKYHWP
```

Figure 3-2. Canine and human alignments of *ATP6H* gene and protein. (A) Alignment of normal canine *ATP6H* cDNA and the pseudo-*ATP6H* sequences. The start and stop codons are underlined and shaded, single nucleotide changes are indicated in bold and deletions by dashes. The position of introns in the normal *ATP6H* sequence are indicated by an arrow and the poly (A) signal is shaded. **(B)** Alignment of deduced amino acid sequence of canine ATP6H with human ATP6H. The potential metal binding motif, CSVCC and the glycosylation site, NET are shaded.

411G18 contained the genuine *ATP6H* gene. The canine *ATP6H* is organized into four exons of 104, 48, 130 and 475 bp respectively. The 246 bp open reading frame is contained within the first three exons. The genomic structure of the *ATP6H* human ortholog has not been reported. Two other BAC clones, 416P16 and 267G14, contained sequences homologous to that of *ATP6H* and also showed characteristics of pseudogenes by lacking introns and by the presence of deletions, base substitutions and insertions (Fig 3-2A). The cDNAs corresponding to the two pseudogenes were not identified by RT-PCR on total RNA from the dog liver, kidney and fibroblast samples, indicating that the two pseudogenes are unlikely to be transcribed.

IV. MAPPING OF CANINE ATP6H AND C04107IPCR ON A CANINE RADIATION HYBRID PANEL.

C04107ipcr and canine intronic *ATP6H* DNA fragments were analyzed on a canine radiation hybrid panel by PCR and scored for the presence (+) and absence (-) of each probe in the hybrid clones. Out of 91 hybrid clones, 34 were positive for C04107ipcr, and 20 were positive for canine *ATP6H*. Out of all positive hybrid clones, 9 were positive for both C04107ipcr and canine *ATP6H*. Hybrid clones positive for C04107ipcr were 3, 4 ,5, 15, 17, 18, 19, 20, 22, 24 , 26, 34, 35, 37, 38, 41, 50, 51, 58, 60, 61, 63, 66, 67, 68, 78, 79, 80, 81, 87, 88, 89, 90, and 91. Hybrid clones also positive for *ATP6H* were 17, 19, 34, 50, 51, 61, 88, 89, and 90, and for *ATP6H* only were 10, 11, 13, 21, 29, 47, 59, 64, 70, 72, and 85. These results indicate that it is unlikely that canine *ATP6H* and C04107ipcr, the canine copper toxicosis marker, are closely linked. When exonic primers were used, 47 hybrid clones were amplified, of which 23 were shared with marker CO4107 ipcr, compatible with the presence of one or more pseudogenes in addition to the functional gene, as suggested by results of the Southern blot.

V. MUTATION ANALYSIS OF THE ATP6H SEQUENCE FROM THE AFFECTED BEDLINGTON TERRIER

Mutational analysis was carried out as an independent confirmation of conclusions from the mapping results. Sequence analysis of the PCR products from the coding regions including intron/exon boundaries of *ATP6H* from the genomic DNA of an affected Bedlington terrier did not show any changes as compared with the normal *ATP6H* sequence. These results were confirmed by sequencing of *ATP6H* cDNA amplified from total RNA isolated from a fibroblast sample from an obligate heterozygote terrier.

IV. DISCUSSION

We identified the canine *ATP6H* cDNA with an open reading frame of a 246-bp encoding a protein of 81 amino acid residues. The potential metal binding motif (CSVCC) and a potential glycosylation site, NET, were conserved in each of the sequences indicating functional similarity.

Southern analysis of genomic DNA from normal dog using the canine *ATP6H* cDNA as a probe showed multiple *EcoR1* and *BamH1* bands, suggesting the presence of multiple *ATP6H* loci in the canine genome. We cloned canine *ATP6H* and two *ATP6H* pseudogenes and determined their genomic structure. The sequences of *ATP6HP1* and *ATP6HP2* showed characteristics of pseudogenes by lacking introns and by the presence of deletions, base substitutions and insertions. Pseudogenes derived from the retrotransposon of a processed mRNA are known to be abundant in the mammalian genome [273]. Typical features of these pseudogenes are the lack of introns and the presence of stop codons and other deleterious mutations that accumulate over time in the absence of selective pressure and indicate non-functionality. There are, however, a few examples of retrotransposons that lead to functional intronless genes [274]. However, *ATP6HP1* and *ATP6HP2* messages were not identified by RT-PCR analysis of cellular RNA from the dog fibroblasts, kidney and liver samples indicating that they are apparently not transcribed.

Sequence analysis of the PCR products from the coding regions including intron/exon boundaries of *ATP6H* from the genomic DNA of the affected Bedlington terrier did not show any changes in comparison with the normal *ATP6H* sequence. We have also shown, using the canine radiation hybrid panel, that the 193 bp single copy amplimer, C04107ipcr, which lies next to the CA polymorphic sequence marker C04107 [249], and the 137 bp amplimer spanning the intron 1/exon 1 junction sequence of canine *ATP6H* are not closely linked. Use of the intron-spanning probe has ensured mapping of the true gene. We were unable to specify the location of the two pseudogenes because all three transcripts were mapped together using a probe that detected pseudogenes, and the radiation hybrid panel cannot identify specific chromosome regions. However, the fact that the pseudogene probe shared more positives with C04107 on the canine RH panel than the true gene probe (spanning intron junction), suggests that the *ATP6H* 'gene' previously mapped to this region [270] is a pseudogene. In fact, after submission of this manuscript, human *ATP6H* was re-localized to human chromosome 5 (GDB accession #9958045), independently confirming our results. Our previous experience with pseudogenes in the dog [266] and the results presented here emphasize the dangers of getting misleading mapping results without the knowledge of the true gene sequence.

Autosomal recessive idiopathic childhood cirrhosis is biochemically similar to copper toxicosis (CT) in Bedlington terriers, but clinically much more severe [209]. *ATP7B* has also been excluded as a candidate gene underlying this disorder in humans [222]. Although idiopathic childhood cirrhosis and CT share certain features with Wilson disease, several differences also exist. Most Wilson disease patients usually show reduced levels of serum ceruloplasmin [275]. In some Wilson disease patients, copper accumulation in the brain and cornea leads to neurologic symptoms and occurrence of occular Kayser-Fleischer rings. In idiopathic childhood cirrhosis and CT, there is no reduced level of ceruloplasmin [208] and neurologic damage and Kayser-Fleischer rings have not been reported [94,233].

Our data provide strong evidence to exclude canine *ATP6H* as a candidate gene underlying canine copper toxicosis. The gene responsible for this disease in dogs remains to be identified and its identification may lead to the discovery of a novel human gene defective in human copper storage diseases where the cause is not known, such as idiopathic childhood cirrhosis.

CHAPTER 4 : New Haplotypes in The Bedlington terrier Indicate Complexity in Copper Toxicosis

Veronica A. Coronado, Deepti Damaraju, Ritva Kohijoki* and Diane W. Cox.
Department of Medical Genetics, University of Alberta, Edmonton, AB, Canada.
*The Finnish Bedlington Club, Finland.

Mammalian Genome (2003) **14**: 483-491

For this publication DD assisted in first round genotyping using microsatellites. RK provided samples and pedigree information.

I. INTRODUCTION

Copper toxicosis (CT) in the Bedlington terrier was first observed by Hardy et al. [229] as a hereditary hepatic cirrhosis associated with elevated copper concentrations. CT is an autosomal recessive genetic disorder prevalent among Bedlington terriers [246] and occurs due to the toxic accumulation of copper in the liver as a result of impaired biliary excretion [244]. These characteristics are similar to those of Wilson disease (WD) in humans, and CT was originally thought to be a model of WD. In CT, copper accumulates in the centrilobular and midzonal hepatocytes [235], specifically within electron-dense granules in lysosomes [234]. Four grades of liver abnormalities are observed as the disease progresses: pigment granules, mild focal hepatitis, periportal hepatitis, and finally cirrhosis [233]. Although not all dogs become clinically ill, the disease is usually fatal unless treated. Treatment of CT consists of life-long medication with a copper-chelating agent, such as penicillamine, or with zinc acetate, which inhibits absorption of dietary copper [264]. At one time approximately 66% of Bedlington terriers in the US [276], 25% in the Netherlands [237], and 37% in Europe [277] were affected. This high gene frequency, along with the difficulty of early diagnosis, has made CT a difficult disease for breeders to eliminate.

Diagnosis of CT is traditionally based on hepatic copper concentration measurements and histological changes in the liver. This requires that a liver biopsy be taken, typically when the animal is one year of age. Until recently, some breeders have been using test-mating strategies to reduce disease frequency, where an animal of unknown status is mated to an affected animal. In 1997, a closely linked microsatellite marker, C04107, was identified [248]. Strong linkage disequilibrium was observed between allele 2 of

C04107 and the disease, and all dogs were thought to contain the identical mutation by descent. As a result, diagnosis has been shifting away from biopsy and towards interpretation of alleles. However, CT affected 1-1 homozygotes and 1-2 heterozygotes have been observed [278], suggesting recombination between the marker and the disease gene. Therefore, the marker alone cannot be used to reliably predict an individual dog's disease status. The DNA marker test is only 90-95 percent accurate [248] and even then results must be interpreted based on pedigree analysis.

The CT locus was mapped to canine chromosome region 10q26 using the strong linkage disequilibrium observed between C04107 and CT [249]. Subsequent FISH mapping [249,250] excluded several known copper genes as the cause of CT: *ATP7B*, responsible for WD in humans [61,62], *ATOX1* [47], which encodes a copper chaperone that interacts with ATP7B [51], *CTR1*, encoding a high affinity copper transporter [279], and *CTR2*, which encodes a possible low affinity transporter [280]. Therefore, CT suggested the presence of another component involved in copper homeostasis in mammals, which may account for a copper transport disorder phenotypically similar to WD, but not defective in *ATP7B*.

The search for other candidate genes led to comparative mapping between the dog and human, where canine chromosome region 10q26 was found to have a conserved region of syntenic genes at human chromosome region 2p13-21 [249]. Further comparative mapping refined the "CT-candidate region" to a region of synteny between the genes *SPTBN1* and *SLC1A4* on human chromosome 2 [270] and positional cloning allowed for the identification of *MURR1* as the CT gene [251]. Mutational analysis revealed a genomic deletion encompassing exon 2 of the *MURR1* gene in all affected dogs.

Screening candidate genes in our collection of Bedlington terriers, we independently discovered a deletion of exon 2 of the gene *MURR1* in our affected 2-2 homozygous dogs. However, our collection of dogs also included affected C04107 1-1 homozygotes and 1-2 heterozygotes, suggesting recombination. Interestingly, these affected dogs were not recombinants, as they did not have the homozygous deletion of exon 2. Here we describe two novel haplotypes identified using two previously established markers, C04107 and C04107B, and two new SNPs within *MURR1* intron 1. Results from haplotype analysis and deletion screening raise doubts as to the causative role of *MURR1* in copper toxicosis.

II. MATERIALS AND METHODS

I. ANIMALS AND SAMPLES

Blood was collected from 10 Finnish Bedlington terriers (5 affected, 3 carriers, 2 unaffected). Total genomic DNA was isolated according to Miller et al. [271] by phenol/chloroform extraction. Additional samples (16 Finnish, 23 Canadian) were obtained by cheek swabs provided by private breeders. DNA from swab samples was isolated using a QIAamp DNA blood kit (Qiagen). Copper levels from liver biopsies were obtained from breeders, when available. All dogs with mean copper levels over 1000 μg/g were classified as affected. Pedigrees were constructed for individual kindreds for four to six generations.

II. BIOINFORMATICS

Sequence searches were performed using NCBI's human genome resources (http://www.ncbi.nlm.nih.gov) and genes/ESTs were chosen for analysis based on their position on human chromosome 2. Gene orthologues were found through links on NCBI databases and through searches in BLAST (http://www.ncbi.nlm.nih.gov). Amino acid alignments were constructed with ClustalW courtesy of BCM Search Launcher (http://searchlauncher.bcm.tmc.edu). Genes were also predicted using the gene prediction programs: HMMgene (http://www.cbs.dtu.dk), Genscan (http://genes.mit.edu), and GrailEXP v3.3 (http://compbio.ornl.gov) and then compared with ESTs on NCBI.

Human sequences for all three *MURR1* exons, including flanking intronic sequence, were obtained through BLASTN searches on the Celera public database (http://publication.celera.com). Structural motifs for *MURR1* were analyzed using ExPASy (http://www.expasy.ch).

III. GENE SEQUENCING

By comparing orthologous sequences between human and mouse, primers were designed from conserved regions using Primer3 Input (http://www-genome.wi.mit.edu). Genomic structures were predicted by sequence comparison and when possible primers were designed to span introns of short length. Primers were designed for *CCT4* (AF026291), *CRM1* (D89729), *PEX13* (AF048755), KIAA0729 (AB018272), KIAA0570 (AB011142), and *MURR1* (D85433). A list of primers and conditions is given in Table 4-1. Amplified products were isolated by gel electrophoresis and purified using a QIAquick gel extraction kit (Qiagen). Fragments were sequenced directly using LICOR

Table 4-1. Primers used for amplification of candidate gene exons/introns from canine genomic DNA for sequence analysis.

Amplification Product	Forward Primer	Reverse Primer	Annealing Temperature
Exon 12 of *CCT4*	5'GCAGGAGGTGGTGCTCCAGAAATAG	5'CCTGGGCATGCCGGTTTCTTAGTT	65
His repeat of KIAA0570	5'TCGACAATTTATTGGTCCACA	5'AGATAATCTCTGTACCCAACATGG	56
Exon/intron 12 of *CRM1*	5'CCAGAGGAAGTATTGGTTGTAG	5'ACTAATGGAGCCTATTGCCC	56
Exon/intron 13 of *CRM1*	5'TGGGCAATAGGCTCCATTAG	5'ATGCATGAATTCGAACAGCT	56
Exon/intron 14 of *CRM1*	5'AAGCTGTTCGAATTCATGCA	5'CACAAGCCATATCCTGGACTC	50
Exon 4 of *PEX13*	5'CCCAAAGTGCGTGGTTGGCTTC	5'CAAAGGCAGCTTCCTGTTCATCCA	65
Exon/intron 18 of KIAA0729	5'GACCTGAGGGCACTCGCTTTGC	5'CAGAAGTGCTCGTTGGGGTCAGG	58
Exon 1/splice sites of *MURR1*	5'CCGAGCTCGAGGGCTCCAAG	5'CGGTACCTTAAGGATGCCCCT	63
Exon 2/splice sites of *MURR1*	5'CCTGCAGTTAAGAAGCTGGGTTT	5'TTTCCAGCTCCATTATGGCAACA	62
Exon 3/splice sites of *MURR1*	5'CAGCTTCTCACGTGCCTCATCA	5'GGAGGGATCATGAACACCTTTGC	62

IRD-700/800 dye-terminators or radioactive dideoxynucleotides and ThermoSequenase (Amersham), depending on length.

IV. MUTATION ANALYSIS

Homozygous deletions of exon 2 of canine *MURR1* were identified by PCR amplification using primers listed above. Presence or absence of exon 2 product was visualized by gel electrophoresis and ethidium bromide staining. Fragments were purified (Qiagen) and sequenced by ThermoSequenase (Amersham). *MURR1* point mutations in the affected 1-1 homozygote were also screened by sequencing all exons and intronic boundaries as described above.

V. SOUTHERN BLOT ANALYSIS

Genomic DNA (5 μg) from selected normal, affected, and carrier Bedlington terriers and canine BAC 27N21 was digested with *EcoRI* and *BamHI* and separated on a 0.7% agarose gel, then blotted onto Hybond-N^+ nylon membrane (Amersham). The blot was probed with a canine fragment containing exon 2, exon 1, or iPCR (described below). Probes were labeled with $[\alpha\text{-}^{32}P]$dCTP using the *redi*prime™ II random prime labeling system (Amersham). Hybridization was carried out in 7% SDS, 0.5 M phosphate buffer pH 7.2, and 1 mM EDTA at 65°C overnight.

VI. NORTHERN BLOT ANALYSIS

A human multiple tissue RNA blot (Origene) was probed with the *MURR1* human STS, WI-16949, labeled with $[\alpha\text{-}^{32}P]$dCTP using *redi*prime™ II (Amersham). This probe contains exon 3 coding and 3' untranslated sequences. Hybridization was performed using ExpressHyb^{TM} as described by the manufacturer (Clontech). An actin probe was used as a control.

VII. HAPLOTYPE ANALYSIS

The following were amplified from each DNA sample: C04107 [248], C04107B [281], iPCR [249], and exon 2 of *MURR1*. C04107 primers were obtained from the FHCRC dog genome project site (http://www.fhcrc.org/science/doggenome/dog.html). The microsatellite was amplified in 1.5 mM magnesium with an annealing temperature of 58°C. C04107B primer sequences were obtained from Koskinen and Bredbacka [281], and the microsatellite amplified in 2 mM magnesium and annealed at 58°C. Both microsatellite reactions were radioactively labeled with [α-^{33}P]dATP using ThermoSequenase (Amersham) and separated by PAGE for analysis of alleles. The iPCR fragment was amplified in 1.5 mM magnesium using 60°C as the annealing temperature with primers TATGTACGTGAGTGTGATGTGG and CTAGAAGAATACAAGCCTGAGAC [249]. Exon 2 of *MURR1* was amplified as described above. Both iPCR and exon 2 fragments were separated on agarose gels and purified (Qiagen) then directly sequenced with ThermoSequenase (Amersham). All PCR and sequencing reactions were done in triplicate.

VIII. RNA ANALYSIS

Whole blood was collected in PAXgene^{TM} blood RNA tubes (PreAnalytiX) according to the manufacturer's instructions and RNA isolated using the PAXgene^{TM} blood RNA kit (PreAnalytiX). First-strand cDNA synthesis was carried out using Superscript II RNaseH-RT (Gibco, BRL) with an oligo(dT) primer. For PCR, 10% of the RT reaction was used to amplify *MURR1* double-stranded cDNA, using primers CCCAGGAAGCTTTCCACGG [251] and GGAGGGATCATGAACACCTTTGC in 1.75 mM magnesium at an annealing temperature of 66°C.

III. RESULTS

1. Analysis of Candidate Genes

Using positional data from van de Sluis et al. [270] and exploiting the conserved synteny between CFA10q26 and HSA2p13-21, we screened candidate genes around the CT marker, C04107. The equivalent position of C04107 on human chromosome 2 was determined by sequence searches within the NCBI human genome database using human *MURR1* [282] as the query, since partial sequencing of the canine BAC containing C04107 (BAC 27N21) had previously yielded a homology match to an exon of human (D85433) and mouse (D85430) *MURR1* [249]. BLAST results showed a partial match to UniGene cluster Hs.339669, within AC018462. Predicted genes in AC018462 also matched the 3' end of *MURR1*. Therefore, despite incomplete sequence information telomeric to AC018462, these results were sufficient to indicate the probable location of *MURR1*. *MURR1* was added as a candidate and additional candidates were chosen within the 1.5 Mb region above *MURR1*.

CCT4 (chaperonin containing TCP1 subunit 4), *PEX13* (peroxisome biogenesis factor 13), and *CRM1* (chromosome region maintenance, exportin 1) were chosen mainly for their position within the 1.5 Mb region. Partial sequence analysis of these genes revealed no differences between affected and unaffected dogs (data not shown). KIAA0729 and KIAA0570 were also in the region and contained possible metal-binding motifs.

KIAA0729 has two putative CXXC metal-binding motifs and KIAA0570 contains a stretch of 12 histidine residues (cat[cac]$_6$cat[cac]$_4$ in humans, cat[cac]$_7$cat[cac]$_3$ in dogs). Histidines are common to zinc-finger motifs, but have also been known to bind copper [283]. Partial sequences obtained for KIAA0729 and KIAA0570 showed no differences between affected and unaffected dogs and no variation in repeat length was observed within the histidine repeat (data not shown). When *MURR1* was amplified from genomic DNA, no product was detected for exon 2 from all 2-2 affected dogs, despite altering various conditions (Fig 4-1A). Unaffected Bedlington terrier samples produced the expected 330 bp fragment, as did dogs with carrier status. BAC 27N21 containing *MURR1* exon 2 and 3, and C04107, was used as a positive control.

II. MUTATION ANALYSIS OF MURR1

Homozygous deletions of exon 2 of canine *MURR1* were initially identified by PCR amplification. A positive control PCR reaction was electrophoresed with every sample to ensure that negative results were not due to poor DNA quality. Deletions of exon 2 were confirmed for chosen samples by Southern blot analysis. Genomic DNA from affected, carrier, and unaffected dogs was hybridized with canine specific *MURR1* exon 1, exon 2, and exon 3 probes. All dogs analyzed showed the same banding pattern on Southern blots when probed with exon 1 (not shown). All affected dogs genotyped 2-2 for C04107, showed a homozygous deletion of a 1.5 Kb *EcoRI* fragment when their DNA was probed with exon 2, while C04107 heterozygotes had one copy of the fragment (Fig 4-1B). Exon 3 hybridized to a 6 Kb *BamHI* fragment in all 1-1 homozygote dogs, but 2-2 affected animals showed a homozygous band shift consistent with the observed deletion (data not shown). Heterozygous animals carried one copy of the 6 Kb and the upper

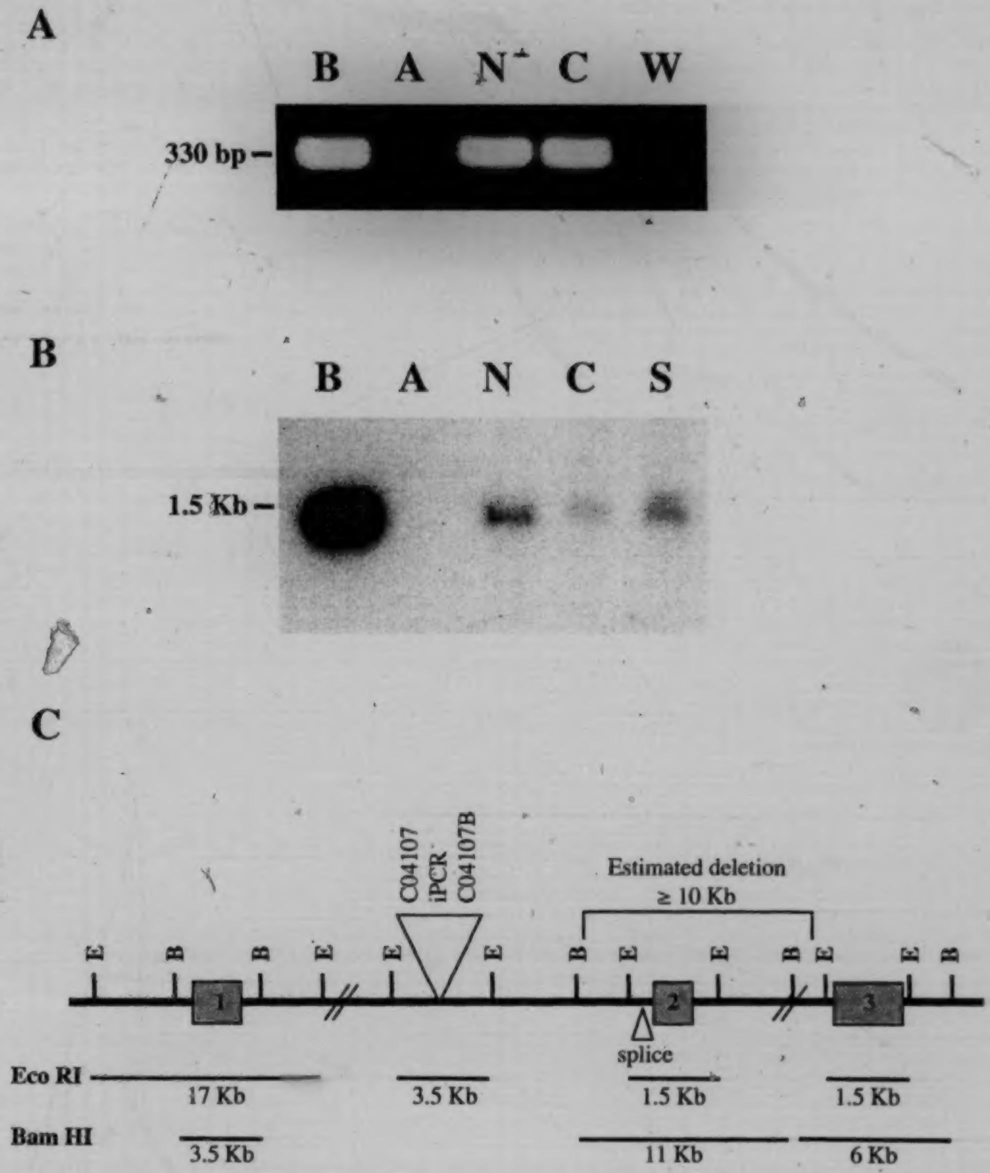
A
B A N C W
330 bp
B
B A N C S
1.5 Kb
C
C04107
iPCR
C04107B
Estimated deletion
≥ 10 Kb
E B B E E E B E E B E E E B
1
2
3
splice
Eco RI
17 Kb
3.5 Kb
1.5 Kb
1.5 Kb
Bam HI
3.5 Kb
11 Kb
6 Kb

Figure 4-1. ***MURR1* analysis.** **(A)** PCR amplification of exon 2 of *MURR1* using dog specific primers. **(B)** Southern blot analysis. Canine genomic DNA was digested with *EcoRI* and hybridized with canine specific probe for exon 2 of *MURR1*. For **(A)** and **(B)**; B refers to BAC 27N21; A, affected dog sample; N, normal/unaffected; C, carrier; S, splice homozygote; W, water. **(C)** Schematic representation of the structural organization of the *MURR1* gene. *BamHI* and *EcoR*I restriction fragments are shown.

shifted 6.7 Kb band. Two dogs, reported as affected with copper levels over 1000 μg/g, were genotyped as 1-1 and 1-2 for C04107 and did not carry the homozygous deletion of exon 2.

All exons and intronic boundaries were sequenced in the affected 1-1 homozygote and compared with an unaffected 1-1 homozygote. This revealed a single base pair difference in intron 1 within the acceptor site of exon 2. Affected and unaffected 1-2 heterozygotes, related to the 1-1 affected dog, displayed the same single nucleotide polymorphism (SNP). This SNP was added to the marker list for genotyping to determine possible correlations.

Because the SNP was identified within a splice site, *MURR1* cDNA was analyzed on an agarose gel for dogs with different genotypes and disease status (data not shown). Affected dogs genotyped as 2-2 for C04107 showed the expected truncated message consistent with the observed homozygous deletion of exon 2, compared with the full-length cDNA from dogs homozygous for the typical normal chromosome (noted below). Dogs heterozygous for the deletion and a normal chromosome showed both lengths of the message. When dogs, affected and unaffected, carrying homozygous and heterozygous splice variations were analyzed, no obvious change in length of message was observed, suggesting that the splice site SNP does not interfere with pre-mRNA splicing.

III. HAPLOTYPE ANALYSIS

The C04107 microsatellite repeat, $(GT)_6GA(GT)_x$, has 2 alleles in the Bedlington terrier, where x=11 for allele 1 (162 bp) and x=13 for allele 2 (166 bp). The microsatellite repeat

C04107B was isolated on the same plasmid as C04107 (V. Yuzbasiyan-Gurkan, personal communication) and has three alleles in the Bedlington terrier, designated *a*, *b*, and *c*. The microsatellite consists of a (CT)-dinucleotide repeat, with allele *a* (130 bp) having 11 repeats and allele *b* 12 repeats, totaling 132 bp. Allele *c* (139 bp) has 11 repeats, but also includes a 9 bp insertion immediately following the dinucleotide repeat.

iPCR is a non-redundant sequence fragment adjacent to C04017 (Fig 4-1C). It was originally generated by inverse PCR for screening a canine BAC library in order to isolate the C04107-containing BAC (27N21) for mapping of the CT locus [249]. We sequenced this 193 bp fragment and discovered a SNP halfway through the fragment. A single base pair transition was observed, G to A, and all 2-2 dogs were homozygous for the G allele. As noted above, sequencing of exon 2 also yielded a SNP among our collection of dog DNA. This SNP occurs within the 3' acceptor consensus sequence for exon 2. Therefore, three possibilities for exon 2 were encountered: a C, or an A at the splice site, or a complete deletion of exon 2.

Four pedigrees were constructed (Fig 4-2). All dogs were genotyped for both microsatellites, and both SNPs and the information placed on the pedigree. Dogs with less than four markers on the pedigree were not tested in our laboratory, but existing marker information was provided by private breeders along with paternity results. Four distinct haplotypes were observed: one typical unaffected (haplotype A: 1-G-*a*-C), one typical affected (haplotype B: 2-G-*b*-Δ), one uncommon unaffected (haplotype C: 2-G-*b*-A), and one splice variant (haplotype D: 1-A-*c*-A). Pedigrees A and B show both typical haplotypes and complete segregation of allele 2 with the disease. This same segregation

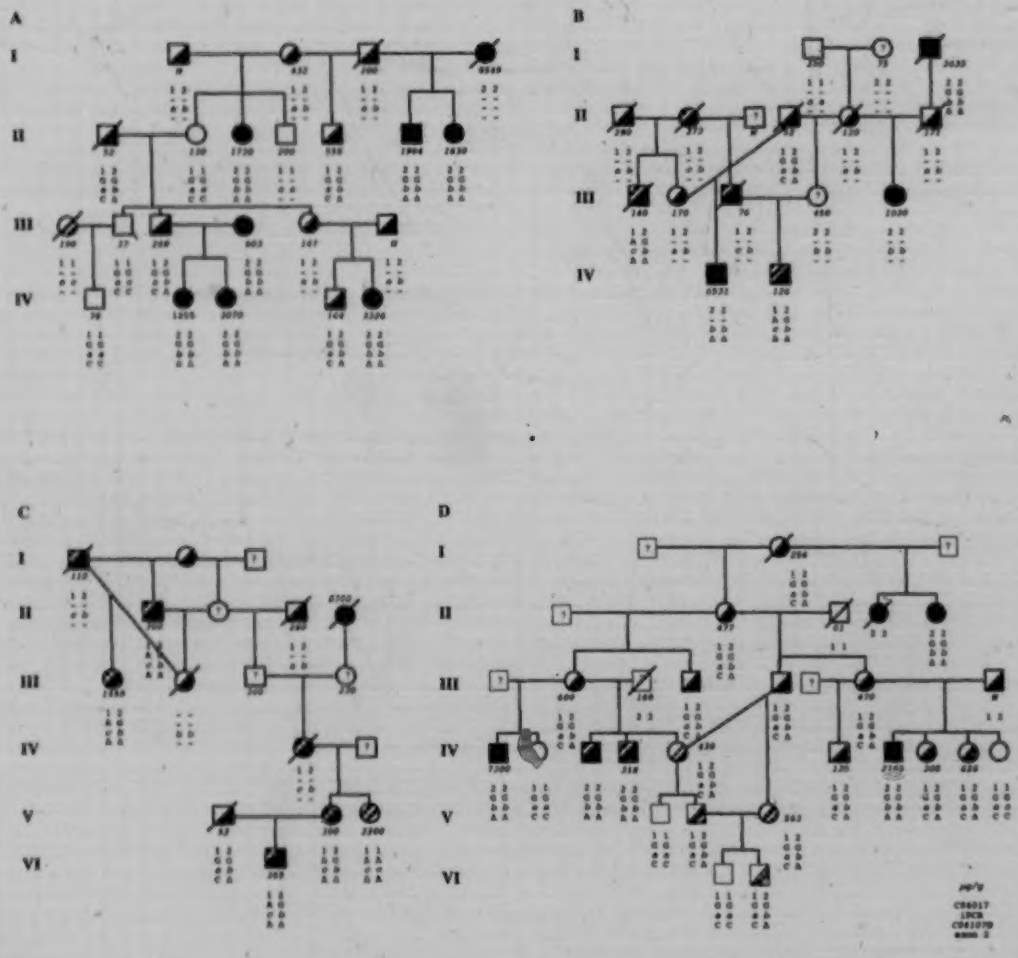

Figure 4-2. Bedlington terrier pedigrees showing haplotype segregation and copper toxicity status in dogs used for the current study. Legend lower right; copper measurements are listed in µg/g dry weight, alleles for C04107 (1 or 2), iPCR (G or A), C04107B (*a*, *b*, or *c*), exon 2 (deletion (Δ), A, or C). Filled symbols represent two copies of the deletion. Half filled symbols represent one copy of the deletion. Hatched symbols, full or half, represent homozygotes and heterozygotes, respectively, for the splice variation.

is observed in most of pedigree D. However, the newly introduced haplotype appears in generation IV and continues through the next two generations. Segregation of allele 2 with the disease is also lost in pedigree C with the appearance of the splice variant haplotype, which is present in one homozygous affected (V:3), one heterozygous affected (III: 1), and other heterozygous unaffected dogs, including III:1 and IV:2 from pedigree B.

IV. MURR1 SEQUENCE COMPARISON AND TISSUE EXPRESSION

Sequence comparison between human, mouse, and dog revealed that *MURR1* consists of three exons, with an ATG start codon in exon 1 and a TAG stop codon in exon 3. Database searches identified only mammalian orthologues and no homology was identified between the predicted protein and any other protein or functional domain. Protein analysis using links from ExPASy predicted a 21 kDa protein with some possible phosphorylation and glycosylation sites, but no transmembrane segments.

Northern blot analysis of a multiple human tissue RNA blot probed with a human specific probe revealed a single transcript present in all tissues (Fig 4-3). Visually correcting for controls, highest expression of *MURR1* was observed in the liver, brain, and heart, with moderate expression in the kidney. Lower level expression was visible in the spleen and leukocytes.

IV. DISCUSSION

Diagnosis of CT is complicated by two major issues. First, although the onset of C04107 genotyping has reduced the level of CT worldwide because a higher percentage of

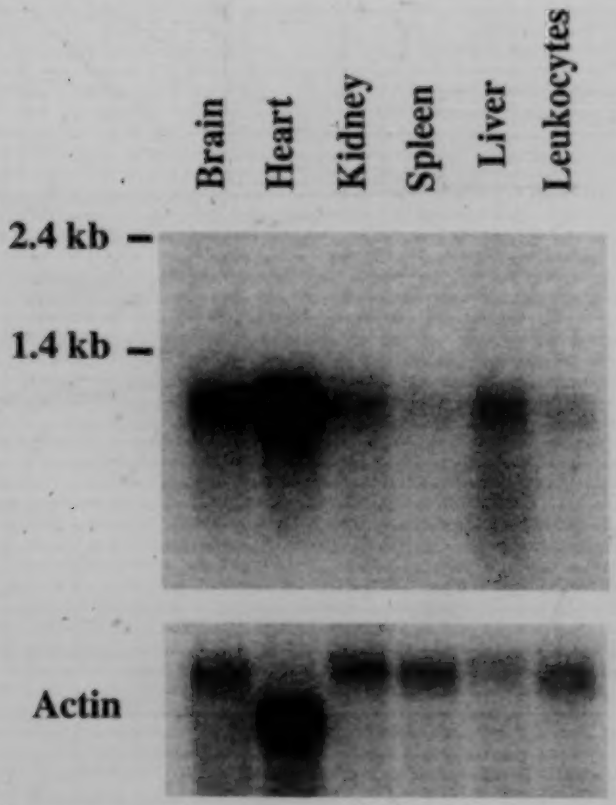
Brain
Heart
Kidney
Spleen
Liver
Leukocytes
2.4 kb
1.4 kb
Actin

Figure 4-3. Northern blot analysis of *MURR1*. Human multi-tissue RNA blot (Origene) probed with *MURR1* human STS WI-16949. Hybridized with actin for loading controls.

carriers can be identified, the test is not 100% accurate. However, some breeders still do not subject their dogs to biopsy and rely solely on C04107 genotyping. Second, there is disagreement on existing cut-off ranges for copper measurements in affected animals. Certain groups maintain that liver copper in excess of 400 µg/g dry weight plus histochemical evidence of copper deposition is characteristic of CT and sufficient for diagnosis [284,285]. However, a study at Helsinki University re-evaluated mean copper levels in healthy and affected Bedlington terriers by comparing values in their study with those of three previously published studies [242]. The conclusion was that unaffected dogs had a mean copper level of less than 500 µg/g dry weight and affected animals exhibited values greater than 800 µg/g. In response to this study, the Finnish Bedlington Club established its limit for affected animals as above 1000 µg/g dry weight and unaffected below 440 µg/g dry weight, criteria that we used in this study. These biopsy results are then used in conjunction with pedigree analysis and marker genotyping to determine the disease status of an animal. However, there still remains a large grey area of undiagnosed dogs. The hope was that identifying the gene and the defect involved in CT would solve this ambiguity.

The CT-candidate region was recently refined to a 9 Mb region in the dog between markers FH2523 and C10.602 [270], which corresponded to approximately 10 Mb between the genes *SPTBN1* and *SLC1A4* on human chromosome 2p (NCBI build 26). Using this positional data, we screened candidate genes, limiting the search to a 3 Mb region around the "CT-marker" based on the low number of recombinants observed in data from the literature. Following the identification of the microsatellite C04107, several studies were performed in different countries to establish phase in certain pedigrees and determine if microsatellite testing was a viable means of diagnosis. Allele 2 completely segregated with the disease in all 25 affected dogs tested in the USA [248]. Complete linkage disequilibrium between the marker and the CT was also observed among 25 Dutch, German, and Belgian affected dogs tested in the Netherlands [277] and eight affected Danish dogs [286]. However, in the UK, Holmes et al. [278] reported the first assumed recombinant event, where two out of 13 affected dogs showed a C04107 genotype other than 2-2. van de Sluis et al. [270] reported another recombinant 1-1 affected animal among nine English dogs. Assuming no dogs tested were duplicated, we estimated that approximately 3% recombination was occurring in these animals.

We identified a homozygous deletion of exon 2 of *MURR1* in 2-2 affected dogs, also identified by van de Sluis et al. [251]. *MURR1* was first described by Nabetani et al. [282], who characterized the region around the imprinted gene U2af1-rs1 in the mouse. They localized U2af1-rs1 within an intron of a gene they called *MURR1*, for the gene that locates within the mouse U2af1-rs1 region. The human *MURR1* orthologue was isolated, but did not contain U2af1-rs1. *MURR1* itself was not imprinted and no further consideration was given as to the function of the gene. We could not identify any homology between the predicted MURR1 protein and any other protein or functional motif. Although we did observe high levels of *MURR1* transcript in the liver, *MURR1* was widely expressed in all other tissues, albeit at varying levels. This pattern disagrees with Northern analysis from van de Sluis et al. [251], which showed highest expression of *MURR1* in the liver and lower levels in skeletal muscle, followed by heart, kidney, and placenta, with no expression in the brain, spleen, or leukocytes. However, our observed ubiquitous expression is consistent with their later results from multi-tissue RT-PCR and discrepancies may be due to the use of different hybridization probes. The function of MURR1 remains to be elucidated, particularly its connection to copper homeostasis in humans.

Based on C04107 genotyping and copper biopsy measurements, we identified four dogs in our cohort as containing possible recombinant chromosomes (III:1 and V:3 in pedigree C, IV:3 and IV:4 in pedigree D). The two dogs in pedigree D were 2-2 homozygous for C04107, but had copper levels in the normal range. These dogs had only one copy of the deletion. The other chromosome showed separation of C04107 from the disease and contained an intact exon 2. This chromosome was introduced into the pedigree by III:3, who originated from the United States, and represents a previously uncharacterized haplotype in the Bedlington terrier (haplotype C). The other two possible recombinants were genotyped 1-1 and 1-2 for C04107, but had copper levels well over 1000 μg/g. We screened for the deletion, the 1-1 homozygote had two copies of exon 2 (no deletion) and the heterozygote had only one copy of the deletion, dispelling the theory that these dogs arose from recombination, and presenting yet another haplotype into this population of dogs (haplotype D). This was unexpected, since the assumption up to now has been that all Bedlington terriers would have the same mutation inherited by descent due to decades of inbreeding. However, considering that the C04107 microsatellite has been placed within intron 1 of *MURR1* [251], low recombination would be anticipated.

We sequenced *MURR1* exons and intronic boundaries for any other possible mutations, and discovered a non-coding single base difference in the exon 2 splice site. Using this SNP and the remaining markers to genotype all dogs in our collection, haplotype analysis revealed that this SNP is associated with the two novel haplotypes mentioned above. The nucleotide variation occurs within the 3' acceptor consensus sequence for exon 2. In eukaryotes, a 3' acceptor sequence generally consists of (T/G)N(C/T)AG [287]. In the typical unaffected chromosome (haplotype A), position N is occupied by a cytosine, while the splice variant chromosome (haplotype D) has an adenine at this position. Although this change occurs in a non-conserved (wobble) position, possible explanations for the 1-1 or 1-2 affected dogs could be that this single base change affects pre-mRNA splicing of *MURR1* or that it affects the levels of functional MURR1 protein produced. cDNA amplification showed no obvious differences in length of message under the test conditions used between dogs with or without the splice variant. We also do not see any affected animals with haplotype C in the Canadian pedigree, which share this splice variant allele. Only two out of the six dogs with this haplotype C have had liver biopsies, but both have copper levels within the normal range and appear to be unaffected. Therefore, the splice variant appears to be a common polymorphism that does not affect splicing. Further investigations regarding levels of transcription may be more informative.

In conclusion, we have shown that copper toxicosis in the Bedlington terrier is not always associated with a *MURR1* exon 2 deletion, raising doubts as to the causative nature of defects in this gene. We have also shown that the Bedlington breed is not as homogeneous as originally predicted. We identified two novel haplotypes that may have contributed to false estimates of recombination between C04107 and the CT mutation. Within our cohort, we identified typical normal 1-1 dogs (haplotype A), affected 2-2 dogs with a homozygous deletion of exon 2 of *MURR1* (haplotype B), unaffected 2-2 dogs where allele 2 is not linked to the deletion (haplotype C), and 1-1 and 1-2 affected dogs without the homozygous deletion, but with another novel haplotype (haplotype D). The data presented here indicate that the ultimate test for CT diagnosis is still unavailable. Although a homozygous deletion of exon 2 of *MURR1* may be positive proof for a CT diagnosis, a negative result should not be interpreted as clear status. In addition to our two non-conforming dogs, two 1-2 affected dogs have been reported to only have one copy of the deletion [251], and we have recently identified an English 1-1 affected dog without deletions. A second mutation, either in the promoter or an intron of *MURR1*, is a possibility, but unlikely. Alternatively, some other gene may be involved in this disorder.

CHAPTER 5 : A Polymorphism Identified in Canine *ATP7B*: Candidate Modifier of Copper Toxicosis in the Bedlington terrier

Veronica A. Coronado[1], Brian O'Neill[1], Manoj Nanji[2] and Diane W. Cox[1]

[1]Department of Medical Genetics, University of Alberta, Edmonton, Alberta, Canada.

[2] Department of Biology, University College London, London WC1E 6BT, UK

Unpublished

For this publication BO assisted with primer design, sequencing, and analysis. MN conducted cDNA library screening and cloned *ATP7B*.

I. INTRODUCTION

Inherited canine copper toxicosis (CT) was first described in the Bedlington terrier in 1975 [229], but similar diseases affect a variety of other canine breeds including the West Highland white terrier [288], Doberman pinscher [289], and Dalmatian [290,291]. These disorders are generally associated with primary copper accumulation ultimately leading to liver injury and cirrhosis [236,244,292-294]. The disease is of particular interest because of the similarity to human disease. The fatality and high frequency of CT in Bedlington terriers has resulted in intense interest and support for the study of this disorder from breeders and kennel clubs worldwide, which have provided samples and pedigrees from their dogs. Linkage, followed by mapping and positional cloning, led to the identification of a *MURR1* exon 2 deletion as the cause of CT in the Bedlington terrier [248,249,251,270]. However, recent studies have raised certain doubts as to whether the CT phenotype in the Bedlington is in fact due to a single gene [295,296].

CT in the Bedlington was initially linked to the microsatellite marker C04107 [248], initiating prediction of disease status based on strong linkage between the disease and C04107 allele 2. However, our collection of dogs, as well as another collection from Australia [296], includes affected 1-1 homozygotes and 1-2 heterozygotes. Interestingly, these affected dogs are not simple recombinants, as they are not homozygous for the *MURR1* deletion. This is surprising since it has long been assumed that all affected Bedlington terriers would have the identical mutation inherited by descent due to decades of inbreeding. Sequencing all exons and exon-intron boundaries identified no *de novo* mutations in the coding region of *MURR1* in these dogs [295]. However, it did identify two novel single nucleotide polymorphisms (SNPs) within intron 1 of *MURR1*, which were used along with C04107 to conduct a *MURR1* haplotype analysis in our entire cohort. Pedigree analysis indicated that there are two typical haplotypes, one typical-unaffected and one typical-affected, maintaining tight linkage between C04107 allele 2 and the deletion in most pedigrees. We also identified a recombinant haplotype, where allele 2 has lost its association with the deletion and is linked with an intact exon 2, and a fourth haplotype containing a novel splice site variant. These findings suggest that deletion of exon 2 in *MURR1* is not the sole contributor to CT in this breed. In certain cases, CT may arise from yet unidentified *MURR1* mutations, either in the promoter or regulatory regions, or mutations in other genes acting independently in affected dogs with two intact copies of *MURR1*, or as modifiers in conjunction with *MURR1* haploinsufficiency in affected dogs carrying one copy of the deletion.

Wilson disease in humans is an autosomal recessive disorder of copper storage, similar to CT, caused by mutations in *ATP7B*, a gene encoding a copper-transporting ATPase expressed predominantly in the liver [61]. Located in the *trans*-Golgi membrane, ATP7B incorporates copper into ceruloplasmin [53] and trafficks to the apical membrane in hepatocytes to excrete excess copper into bile [80]. MURR1 has recently been shown to interact with ATP7B and is proposed to facilitate ATP7B trafficking [297]. *ATP7B* was originally excluded as the causative gene for CT based on mapping data [249]. However, full sequence characterization of *ATP7B* in the dog has not been published.

Here, we investigate the possibility that *ATP7B* is acting as a modifier of CT allowing for copper accumulation in Bedlington terriers with either one or two intact copies of *MURR1*. In this paper we describe cloning of the *ATP7B* gene, its structure, and sequence analysis in a Bedlington pedigree that does not show complete linkage between C04107 and CT.

II. METHODS AND MATERIALS

I. cDNA Library Screening

Using the canine liver cDNA library, DL1007A (Clontech), cDNAs were synthesized with a mixture of oligo-dT and random primers. These cDNAs were cloned into phage λgt10 vector and propagated in *E.coli* strain Y1090. Library screening was done according to standard procedures using a mixture of human and rat *ATP7B* cDNA probes spanning the entire coding region of the gene. Positive recombinant bacteriophage λ cDNA clones were subcloned into pBSK plasmid vector (Stratagene) for restriction mapping and sequence analysis. Plasmid DNA was sequenced using universal and sequence-derived oligomers.

II. Animals and Samples

For cloning of *ATP7B* cDNA, cultured fibroblasts were obtained for a female Bedlington terrier with known carrier status for copper toxicosis. Blood and/or buccal samples for *ATP7B* sequencing were previously collected and genomic DNA isolated as described [295]. All chosen animals belonged to one extended Finnish Bedlington terrier pedigree (Fig 5-1). Hepatic copper levels were determined by biopsy and values obtained directly from breeders. Dogs with a mean copper level over 1000 μg/g were considered affected, while animals with a copper level below or just above 400 μg/g were classified as unaffected. Animals for this study were chosen to include all *MURR1* haplotypes associated with affected animals (Table 5-1). Where possible affected dogs were

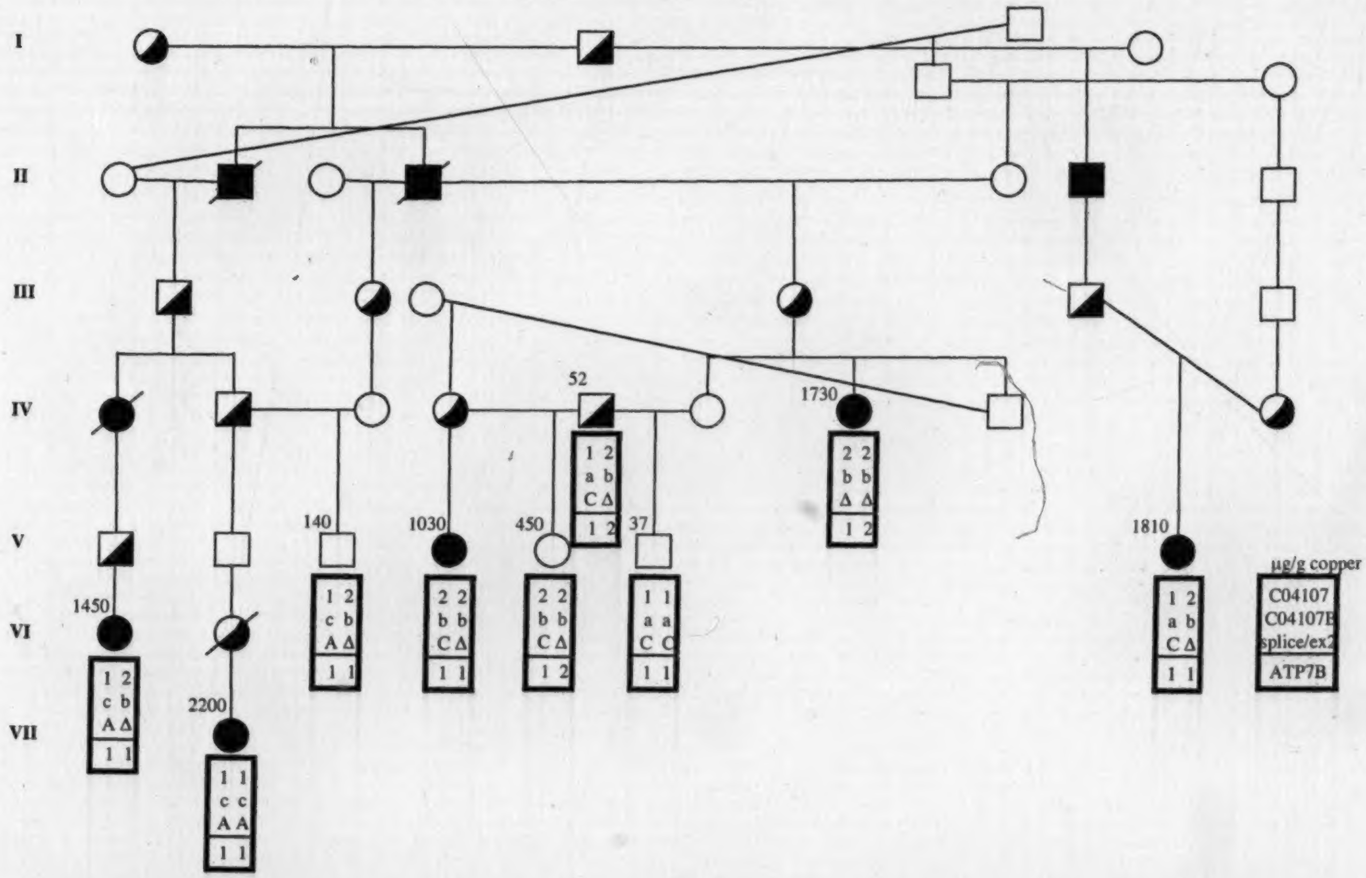
I
II
III
IV
V
VI
VII
52
1 2
a b
C Δ
1 2
1730
2 2
b b
Δ Δ
1 2
140
1 2
c b
A Δ
1 1
1030
2 2
b b
C Δ
1 1
450
2 2
b b
C Δ
1 2
37
1 1
a a
C C
1 1
1810
1 2
a b
C Δ
1 1
µg/g copper
C04107
C04107B
splice/ex2
ATP7B
1450
1 2
c b
A Δ
1 1
2200
1 1
c c
A A
1 1

Figure 5-1. **Bedlington pedigree.** Pedigree shows relationship of each dog chosen for study. Listed for each chosen dog: copper level (µg/g), alleles at *MURR1* locus (microsatellite C04107: 1 or 2; microsatellite C04107B: a, b, or c; exon 2 SNP: A, C, or deletion Δ [295], *ATP7B* haplotype: 1 or 2.

Table 5-1. Chosen cohort for study.
Dogs are listed by haplotype at the *MURR1* locus; includes alleles for microsatellites C04107 (1, 2) and C04107B (a, b, c), and polymorphism at the exon 2 splice site (A, C, deletion Δ). Dogs are identified by generation numbers corresponding to the pedigree in Figure 5-1. Disease status is determined from the given copper levels and whether or not the animal has had affected pups.

Haplotype	Dog	Copper (μg/g)	Status
1 2 a b C Δ	V:vii	1810	Affected
	IV:v	52	Unaffected Carrier
1 2 c b A Δ	VI:i	1450	Affected
	V:iii	140	Unaffected
2 2 b b C Δ	V:iv	1030	Affected
	V:v	450	Unaffected
2 2 b b Δ Δ	IV:vii	1730	Affected
1 1 c c A A	VII:i	2200	Affected
1 1 a a C C	V:vi	37	Unaffected

matched with unaffected dogs sharing identical haplotypes. *MURR1* haplotypes have been previously described [295] with the addition of a fifth Bedlington haplotype (2-b-C, Fig 5-1) also observed by Hyun et al. [296]. Additional canine DNA samples were isolated to confirm results: Doberman RPCI-81 bacterial artificial chromosome (BAC) 57N9 DNA was extracted using a plasmid midi kit (Qiagen), Maltese genomic DNA was isolated from buccal swabs (QIAamp DNA blood kit, Qiagen).

III. CLONING OF ATP7B CDNA

Total RNA was extracted from cultured fibroblasts from a Bedlington terrier using Trizol (Gibco, BRL). Total cDNA was synthesized by reverse transcription using a First-strand cDNA synthesis kit (Pharmacia) and random hexamers. This was followed by PCR using dog-specific primers for *ATP7B* (Table 5-2). PCR fragments were subjected to electrophoresis and gel purified (QIAquick gel extraction kit, Qiagen) for cloning and cycle sequencing using ThermoSequenase (Amersham). A total of 8 overlapping fragments were amplified to cover the entire coding region plus 3' UTR sequence. Fragments A, B, and D were amplified initially using dog-specific primers based on sequence obtained from positive clones identified above. Fragments A and B were amplified directly from total cDNA, while fragment D was obtained by nested PCR (Table 5-2). Dog cDNA sequence obtained from fragments A, B, and D was subsequently utilized to design additional primers for amplifying fragments C, E, F, and G. Fragment C is also a product of nested PCR and fragment E is a product of semi-nested PCR using BDR4 as the 3' primer in the second round. Fragment G is also a product of a semi-nested PCR with dog-specific primers only on the 5' end. Primers for the 3' end of fragment G contain degenerate nucleotides and their design was based on

Table 5-2. Dog specific primers for cDNA amplification of ATP7B.
N signifies degenerate nucleotide, Y denotes pyrimidine.

Designation	Sequence 5' to 3'	Amplified Segment
BDF3	ATCACAGGCATGACCTGTGC	Fragment A
BDR3	ACCTTGTGGTCCAAGTGATG	
BDF4	CGCATCACTTGGACCACAAG	Fragment B
BDR1	TACCAACTTCACGATCTGAG	
BDF5-1	CCACGTGGGCAACGATACCA	Fragment C
BDR5-1	TGGCTGTCTTCCGGTTGTCN	
BDF1	YGTCTGTGNGGGACNATG	1st round fragment D nested
BDR4	CTCTATGTTGGACACACAGG	
BDF1-1	CATGACCTGCCAGTCCTGTG	2nd round fragment D nested
BDR4-1	CAGGATGCACAGGTCATGCC	
BDF10	CAAGTGTCCTTGGAGAACA	1st round fragment E semi-nested
BDR4-2	ACGCCTGCTTCTTTCTGCAG	
5BDF1	YGTCYGTGNGGGACNATG	Fragment F
5BDR1	CTTGCCTTYGATGGAGCTGA	
3BDF1	CGTGAATGGATGAGGCGCAA	1st round fragment G nested
3BDR1	GCACCTCGGCCTGCCCNGG	
3BDF2	TGTGCTGTGCGGGATGATCG	2nd round fragment G nested
3BDR2	ATGGGCATGAAGACACCTGC	
3BDF5	TTCATCTCTCCAAGAGGACN	Fragment H
3BDR3	AGGCCCGTCTGGAAGGAGCN	

conserved sequences between *ATP7B* sequences from rat, human, and mouse. Primers used for amplifying fragment H were designed completely based on sequence conservation.

Fragments were sequenced with the same primers used in amplification as well as some additional primers: Fragment B, B2F: CACGAGCATCGCCTACACC, B3F: GCGATGT CATCAAGGTGGTC, and BDSC1: GGTGTAGGCGATGCTCGTG; Fragment C, C2F: CTCATCAAAGGAGGCAAGC, C3F: CGGAGGCCAGCAGCGAGCAC, C2R: CTCT TGAGCATGTGCAGAGC, and C3R: GCGTCTCATCTGTTTCCTCG.

Species comparison of putative proteins was accomplished using Clustal W (1.83) multiple sequence alignment program (www.ebi.ac.uk/clustalw/).

IV. SEQUENCING OF THE CANINE ATP7B GENE

The *ATP7B* cDNA was compared with genomic sequence available on the public databases of NCBI (http://www.ncbi.nlm.nih.gov) and Ensembl (http://www.ensembl.org) to determine intron/exon boundaries. Predicted transcripts used for comparison (XM_534107, ENSCAFT00000006859, ENSCAFT00000006864) were all derived from the dog genome draft July 2004. Intronic primers (Table 5-3), generated by Primer3Input (http://www.genome.wi.mit.edu), were designed from genomic sequence to avoid amplification of the *ATP7B* pseudogene [249]. All exons, except exon 2, were amplified using standard PCR conditions and treated with ExoSAP-it (USB) prior to direct sequencing on a 3130xl Genetic Analyzer (Applied Biosystems) using the same primers for sequencing as those used for amplification. Exon 2, because

Table 5-3. Intronic primer sets for the amplification of the canine ATP7B gene.

Amplified Segment	Primer Sequence 5' to 3'	Amplified Segment	Primer Sequence 5' to 3'
Exon 2	F: GTGCCAGACCAGCCAGGATA	Exon 12	F: ATGCCTGTGCTGGCGTATTT
	R: CCCGGACACATTCAACACAC		R: CAATCCCAGAAATGGCCAAA
Exon 3	F: GTGTGCCCTGCCTCTGGTT	Exon 13	F: TGACACGGAAGCAGAGTGGA
	R: TGGACTTGCTGCCAGGGTAT		R: AGCTGCTTTCAAGCCACGTC
Exon 4	F: CCAAGCATGGGGAGTGGTAA	Exon 14	F: CACCATCATACCCCCAGCAC
	R: CAAACCCAGGCTCTGGACAC		R: GAGCTGCACCTCCAACTGGT
Exon 5	F: ACGAAAGCCCATCACTGTCA	Exon 15	F: TCTTGAGAGCCTCCGAGCAG
	R: CGGACACACGGTGTCACATT		R: CTGCAGTGTGCTGCCACCTA
Exon 6	F: AGCCATTGCCAAGAAACCAA	Exon 16	F: CACGTCTCCCTGGTCCTTTG
	R: AGAGGTGGCCATTTCCATGA		R: GGGTGACTGAACCTGGCTTG
Exon 7	F: TGCGGGTCCCTACGACATTA	Exon 17	F: TCTGGAAACTGTCCGGTAGCA
	R: TTGATCACCGACAGCCCTCT		R: CGACGAATCATCCCCATCAT
Exon 8	F: GAGGGGCCTCTGGGTCTCTA	Exons 18-19	F: ACGCTGCTCCCCTTTTCTTC
	R: CACAATGCGCCTCAACAAAG		R: GCACCCTCTCTGCAGCTTTC
Exon 9	F: TTTAGCGTGGCAATGACGTG	Exon 20	F: GTCCCAGGAAGGCCAGAGTT
	R: CCTCTGCATTCTGGGGACAC		R: GCATGGCATTTTCACAAGCA
Exons 10-11	F: CTGCCCAGTGTGAAGTGCAG	Exon 21	F: ACTTTGCCCACCTGCAAAA
	R: ACTCGGCAAAATCGGCCTAA		R: CCTGGGGATCCTAAGGCAAG

of its size, was subjected to electrophoresis after PCR amplification and gel purified (QIAquick gel extraction kit, Qiagen) prior to sequencing. In addition, sequencing of exon 2 was accomplished in three sections using the original two primers used for amplification and four additional primers: BTex2R1: GACCCGGACTCTTGCTACCC, BTex2F2: CAGCGTTGCAGAAGGAAAGG, BTex2R2: AAGTTCCCTGGTGGGAG AGC, and BTex2F3: AACTCCCCGGGGTTCAGAAT.

III. RESULTS

I. CANINE cDNA LIBRARY SCREENING

Approximately 2.5 x 10^6 clones were screened, nine of which were carried through the tertiary screening and were plaque-purified. Sequences obtained from both ends of the inserts were compared with human and rat *ATP7B* cDNA sequences. Only two clones, one with a 0.25 kb insert and the other with an insert of 1.4 kb, contained DNA sequence with similarity to the published human and rat sequence. Sequence from these two clones was used to design dog-specific primers for RT-PCR of *ATP7B* from total Bedlington cDNA.

II. ATP7B CLONING

Most fragments corresponded well to published *ATP7B* cDNA sequences, encoding the entire predicted protein. Certain fragments contained high levels of sequence heterogeneity, including small insertions and deletions, and the complete deletion of exon 12, suggesting the presence of both a functional gene and pseudogene. This sequence information allowed us to distinguish between BACs containing "real" and "pseudo" copies of *ATP7B*. These BACs were used for mapping the functional *ATP7B* gene to canine chromosome 22 and the pseudogene to canine chromosome 4 [249].

Exons were given the same numbering as the human gene based on sequence conservation. However, compared with the human cDNA sequence, canine exon 1 did not align with human exon 1 and the first methionine that led to a predicted in-frame ATP7B protein was in the corresponding exon 2. Since we could not identify a homologous exon 1 in the canine sequence, we began our cDNA numbering with exon 2 based on sequence alignment with the human cDNA. All subsequent exons (3 to 21) aligned well with the human sequence.

Beginning translation from exon 2, the predicted canine protein shares 85.6% identity with the human protein (Fig 5-2). It is interesting to note that, an alternative sheep *ATP7B* transcript (AF118225) has an extended 5' end which does not align with mouse, rat, human, or the main sheep transcript sequence. The Ensembl predicted dog transcript, ENSCAFT00000006859, also has an extended 5' end. Compared to the alternative sheep transcript, the 5' end of the Ensembl predicted protein shares 53% identity at the protein level over the aligned region (Fig 5-3). This Ensembl canine prediction however, incorrectly splits up exon 2 (ENSCAFT00000006859 exon 3) into two (exons 3 and 4), leaving a 42 bp intron. This sequence encodes a small repeat pattern, which was identified in our canine liver cDNA.

```
                                                                                    Cu1
C: ILSKLSLPTRAWEPVMKQSFAFDNVGYEGGLDSVCPP-QTATSTISILGMTCQSCVRSIEGRISSLKGIVSIKISLEQGNATVKYMPSILSLPQV   94
H: ILSKLSLPTRAWEPAMKKSFAFDNVGYEGGLDGLGPSSQVATSTVRILGMTCQSCVKSIEDRISNLKGIISMKVSLEQGSATVKYVPSVVCLQQV  112
   **************.**:***************.: *. *.****: **********:***.***.****:*:*:*****.*****:**::.* **
                                                                              Cu1
C: CRHIEDMGFEASVAEGKAASWPSRSSPGLEAVVRLRVEGMTCQSCVSSIEGKLGKLQGVARVRVSLSTQEAVITYQPYLIQPQDLRDHVNDMGFE  189
H: CHQIGDMGFEASIAEGKAASWPSRSLPAQEAVVKLRVEGMTCQSCVSSIEGKVRKLQGVVRVKVSLSNQEAVITYQPYLIQPEDLRDHVNDMGFE  207
   *::* *******:*************. ****:*****************: ** ***.**:****.**************:***********
                                          Cu2
C: AVIKNRVAPVSLGPIDIGRLQRTNPKMPLTSDNQNLNNSETLGHQGSHVVTLQLRVDGMHCQSCVLNIEENIGQLPGVQNVQVSLENRTAQVQYD  284
H: AAIKSKVAPLSLGPIDIERLQSTNPKRPLSSANQNFNNSETLGHQGSHVVTLQLRIDGMHCKSCVLNIEENIGQLLGVQSIQVSLENKTAQVKYD  302
   *.**.:***:******* *** **** **:* ***:*******************:*****:************* ***.******:****:***
                                                                  Cu3
C: PSCVTAGALQRAIEALPPGNFKVSLPAAAAGSETGNRFSACAAPAPAPRTPAPGRCDTVMLAIVGMTCASCVQSIEGLISQREGVQQISVSLAEG  379
H: PSCTSPVALQRAIEALPPGNFKVSLPDGAEGSGTDHRSSSSHSPGSPPRNQVQGTCSTTLIAIAGMTCASCVHSIEGMISQLEGVQQISVSLAEG  397
   **.:. ******************* .* ** *.:* *:. :*...**. . * *.*.::**.********:****:*** ************
                                                                         Cu4
C: TAVVLYDPSIIGPEELRAAVEEMGFETSVLSENGYSNHVGNHSAGNSSAHTTAGVPVSVQEGAPHTEGLPGNHSPGRPSRSPPASTSVTAQKCFL  474
H: TATVLYNPSVISPEELRAAIEDMGFEASVVSESCSTNPLGNHSAGNSMVQTTDGTPTSVQEVAPHTGRLPANHAPDILAKSPQSTRAVAPQKCFL  492
   **.***:**:*.*******:*:****:**:**.  :* :******** .:** *.*.**** ****  **.**:*.  ::** :: :*:.*****

C: QITGMTCASCVSNIERKLQKEAGVVSVLVALMAGKAEVKYHPDVIQPLEIAQLIQDLGFEATVLEDYAGSEGDLELIITGMTCASCVHNIESKLT  569
H: QIKGMTCASCVSNIERNLQKEAGVLSVLVALMAGKAEIKYDPEVIQPLEIAQFIQDLGFEAAVMEDYAGSDGNIELTITGMTCASCVHNIESKLT  587
   **.************:*******:************:**.*:*********:********:*:******:*::** *****************
      Cu5                                                                      Cu6
C: RMAGITYASVALATSKAHVKFDPEIIGPRDIVKVIEEIGFHASPAQRNPSAHHLDHKVEIKQWKKSFLCSLVFGIPVMGLMIYMLVPSSTPHESM  664
H: RTNGITYASVALATSKALVKFDPEIIGPRDIIKIIEEIGFHASLAQRNPNAHHLDHKMEIKQWKKSFLCSLVFGIPVMALMIYMLIPSNEPHQSM  682
   *  ************** *************:*:********* *****.*******:********************.******:**. **:**
                                                                        Tm1
C: VLDHNVIPGLSILNLIFFILCTFVQLLGGWYFYVQAYRSLRHRAANMDVLIVLATSIAYTYSLVILVVAVAERAERSPVTFFDTPPMLFVFIALG  759
H: VLDHNIIPGLSILNLIFFILCTFVQLLGGWYFYVQAYKSLRHRSANMDVLIVLATSIAYVYSLVILVVAVAEKAERSPVTFFDTPPMLFVFIALG  777
   *****:*******************************:*****:****************.***********:*********************
                  Tm2                          Tm3                                     Tm4
C: RWLEHIAKSKTSEALAKLMSLQATEATVVTLGEDNLILREEQVPMELVQRGDVIKVVPGGKFPVDGKVLEGNTMADESLITGEAMPVTKKPGSTV  854
H: RWLEHLAKSKTSEALAKLMSLQATEATVVTLGEDNLIIREEQVPMELVQRGDIVKVVPGGKFPVDGKVLEGNTMADESLITGEAMPVTKKPGSTV  872
   *****:*******************************:**************::*****************************************
                                                                   td
C: IAGSMNAHGSVLVTATHVGNDTTLAQIVKLVEEAQMSKAPIQQLADRFSGYFVPFIIIISTLTLVVWIIIGFIDFGVVQKYFPTPNKHISEAEVI  949
H: IAGSINAHGSVLIKATHVGNDTTLAQIVKLVEEAQMSKAPIQQLADRFSGYFVPFIIIMSTLTLVVWIVIGFIDFGVVQRYFPNPNKHISQTEVI  967
   ****:*******:.*******************************************:*********:**********:***.******::***
                                                            Tm5
C: IRFAFQTSITVLCIACPCSLGLATPTAVMVGTGVAAQNGILIKGGKPLEMAHKIKTVMFDKTGTITHGVPKVMRVLLLVDVATLPLRKVLAVVGT 1044
H: IRFAFQTSITVLCIACPCSLGLATPTAVMVGTGVAAQNGILIKGGKPLEMAHKIKTVMFDKTGTITHGVPRVMRVLLLGDVATLPLRKVLAVVGT 1062
   **********************************************************************:******* ****************
                Tm6                                          Ph
C: AEASSEHPLGVAVTKYCKEELGTETLGYCTDFQAVPGCGIGCKVSSVEGILAPGERQRSKQAAPPGTVGGVPEETDETPQTFSVLIGNREWMRRN 1139
H: AEASSEHPLGVAVTKYCKEELGTETLGYCTDFQAVPGCGIGCKVSNVEGILAHSERPLSAPASHLNEAGSLPAEKDAVPQTFSVLIGNREWLRRN 1157
   *********************************************.****** .**  *  *:  . .*.:* *.* .*************:***

C: GLTISSDISDAMADHEMKGQTAILVAIDGVLCGMIAIADAVKQEAALAVHTLKSMGVDVVLITGDNRKTARAIATQVGINKVFAEVLPSHKVAKV 1234
H: GLTISSDVSDAMTDHEMKGQTAILVAIDGVLCGMIAIADAVKQEAALAVHTLQSMGVDVVLITGDNRKTARAIATQVGINKVFAEVLPSHKVAKV 1252
   *******:****:***************************************:******************************************

C: QELQNEGKKVAMVGDGVNDSPALARADVGIAIGTGTDVAIEAADVVLIRNDLLDVVASIHLSKRTVWRIRLNLVLALIYNLVGIPIAAGVFMPIG 1329
H: QELQNKGKKVAMVGDGVNDSPALAQADMGVAIGTGTDVAIEAADVVLIRNDLLDVVASIHLSKRTVRRIRINLVLALIYNLVGIPIAAGVFMPIG 1347
   *****:******************:**:*:*************************************** ***:************************
                 hinge                                                             Tm7
C: VVLQPWMGSAAMAASSVSVVLSSLQLKCYKKPDLERYEAQAQGRMKPLTASQVSVHIGMDDRRWDSPRATPWDQVSRVSQVSLSSLKSDKLSRHS 1424
H: IVLQPWMGSAAMAASSVSVVLSSLQLKCYKKPDLERYEAQAHGHMKPLTASQVSVHIGMDDRWRDSPRATPWDQVSYVSQVSLSSLTSDKPSRHS 1442
   :****************************************:*:*****************  ************ *********.*** ****
       Tm8
C: AAADDGGDTWSLLLNDRDEEQCI 1447
H: AAADDDGDKWSLLLNGRDEEQYI 1465
   *****.**.******.***** *
```

Figure 5-2. Canine predicted *ATP7B* protein compared to human protein. (H) Human (NP_000044.2) shown exon 2 to 21, numbering includes 17 amino acids encoded by exon 1. (C) Canine numbering begins at the first amino acid encoded by exon 2. Only two repeats in exon 2 are shown (underlined) as observed in the Bedlington terrier, Maltese, and Doberman. Otherwise, the putative protein was determined using the boxer genomic sequence. Conserved domains are shaded: copper-binding (Cu1-6), transmembrane (Tm1-8), transduction (td), phosphorylation (Ph), ATP-hinge. Symbols denote degree of conservation between amino acids: identical (*), conserved (:), semi-conservated (.), as determined by Clustal W (1.83).

A

```
hmm773           MELSYTFLEMQVMLPRTSLSSLGCFAPPAPAPELQERPLLSVPEGECHPPCPEAGSWERT 60
Ensembl          ------------------------------------------------------------
XM_534107        ------------MEAGSFLTEHAADKKPAPAPELQERPLLSVPEGECHPPCPEAGSWERT 48
                             *     *        *********************************

hmm773           WPKGDRAGLQRRRCLRAGSCTRRPGWGPSPLRARVGPCAEVLGAECSVMSERVPIGWKHG 120
Ensembl          ------------------------------------------------------------
XM_534107        WPKGDRAGLQRRRCLRAGSCTRRPGWGPSPLRARVGPCAEVLGAECSVMSERVPIGWKHV 108
                 ************************************************************

hmm773           ------------------------------------------------------------
Ensembl          ------------------------------------------------------------
XM_534107        GKQGQVRMQRVQPPGLAPSRGESAAAGGRKPRTGGAPCSWGHLYSVASHLPRQPGARELL 168

hmm773           -----ARDAVMEKGGGKPSFLATLGDPQVTLVSVHKRWSFRRPP-----------GARGS 164
Ensembl          -------------GGGKPSFLATLGDPQVTLVSVHKRWSFRRP------------GARGS 35
XM_534107        ALCQGARDAVMEKGGGKPSFLATLGDPQVTLVSVHKRWSFRRPPWGPGLHQASARGGGGG 228
                      ***************************************           *  *

hmm773           TRPVPE------------------EEEEEGELSQKGLNGAWGVG----GDQ 193
Ensembl          TRPVPE------------------EEEEEGELSQKGLNGAWGVG----GDQ 64
XM_534107        GRVVTEGFEWSVGRRWRSGQCAADTAEPRGPWTACTAPGRFSPGTRGPGDQ 279
                  * * *                    *  *        *    *    ***
```

B

```
hmm773           MELSYTFLEMQVMLPRTSLSSLGCFAPPAPAPELQERPLLSVPEGECHPPCPEAGSWERT 60

hmm773           WPKGDRAGLQRRRCLRAGSCTRRPGWGPSPLRARVGPCAEVLGAECSVMSERVPIGWKHG 120
alt sheep        -----------------------------------------------------------M 1

mouse            -------------------MDPRKNLASVGT---------MPEQERQVTAKE-------- 24
rat              ----------------------------------------MPEQERKVTAKE-------- 12
human            ----------------------------------------MPEQERQITAREG------- 13
sheep            ------------------------------M---------KPEEERPIIDREK------- 14
Ensembl          --------GGGKPSFLATLGDPQVTLVSVHKRWSFRRP-GARGSTRPVPEEEE-----EE 46
hmm773           ARDAVMEKGGGKPSFLATLGDPQVTLVSVHKRWSFRRPPGARGSTRPVPEEEE-----EE 175
alt sheep        ERAGDQAPGNPEPSSLATLGDPQVTLLTVHKRWSFKRSPGTGGSSRPVISEEECPPPSEE 61
                  *      *   ** ***********  ******* * **  ** **           **

mouse            --------------ASRK 28
rat              --------------ASRK 16
human            --------------ASRK 17
sheep            --------------ASRR 18
Ensembl          GELSQKGLNGAWGVGGDQ 64
hmm773           GELSQKGLNGAWGVGGDQ 193
alt sheep        GEFSQKVLNGSEEISSKQ 79
                 ** *** ***
```

Figure 5-3. Comparison of the putative N-terminus of predicted canine *ATP7B* transcripts and other species. (A) Alignment of N-terminal canine ATP7B predictions upstream of exon 2. **(B)** Alignment of N-ternimal canine ATP7B predictions upstream of exon 2 with 5' protein sequence from other species. Canine predictions: hmm773 (NCBI Gnomon hidden Markov model) Ensembl (ENSCAFP00000006351), XM_534107 (NCBI Genscan prediction). Mouse (NP_036643.1), rat (NP_036643.1), human (NP_000044.2), sheep (AF032881), sheep alternatively spliced transcript product (AF118225). Asterix (*) denotes identical amino acid.

III. ATP7B SEQUENCE ANALYSIS

In total, 11 polymorphisms were identified in the Bedlington *ATP7B* gene compared with the public genomic sequence of the boxer (Table 5-4). Polymorphisms were named according to nomenclature recommendations [298] listed on the Human Genome Variation Society website (http://www.hgvs.org/mutnomen/). It should be noted that with the lack of exon 1, nucleotide 1 of exon 2 was assigned as nucleotide 1. The first of the polymorphisms occurs in exon 2 in a small repeat region. In the public genome sequence this region consists of three repeats, GCC(GCCCCC)$_3$GCC, while only two repeats could be identified in the Bedlington terriers sequenced. Towards the end of exon 2, a single base pair change was identified in three dogs: father and daughter, IV:v and V:v respectively, and IV:vii. This polymorphism was present in a heterozygous state in all three dogs and did not lead to any amino acid change. Just after exon 2, in the 5' donor site, a thymine to cytosine transition was identified in the same three dogs. This change occurs in the splice site sequence TG/GTA(T/C)GT, in the plus four position. This position is typically occupied by an adenine in the consensus sequence AG/GTRAGT, and C and T both appear in this position 9% of the time [287]. Two polymorphisms occur within exon 3, but do not result in any amino acid change. These changes were observed in the same three dogs mentioned and exist in a heterozygous state. Also observed in a heterozygous state, were two polymorphisms in exon 11 and one polymorphism in intron 11. Neither of the two coding changes altered amino acid sequence and the intronic single base deletion did not create a new exon splicing consensus sequence. Once again, all three changes were observed in the same three dogs. In intron 16, a thymine to cytosine transition was observed in all dogs. Where the boxer sequence is homozygous C/C, the Bedlington terriers sequenced here were homozygous

Table 5-4. Summary of single nucleotide polymorphisms (SNPs) identified in Bedlington ATP7B compared with the boxer genome sequence.
The location and nomenclature of the polymorphism are listed, as well as the amino acid affect by the change. Changes were found to be in phase when placed on dog pedigrees and the two *ATP7B* allele combinations were given numerical values (Haplotype 1 or 2).

Location	**Nomenclature**	**Amino Acid**	**Haplotype 1**	**Haplotype 2**
Exon 2	c.991_996delGCCCCC	A(AP)$_{3\rightarrow 2}$	delGCCCCC	delGCCCCC
Exon 2	c.1083C>T	Ile361Ile	C	T
Intron 2	IVS2+4T>C	N/A	T	C
Exon 3	c.1275A>G	Ala425Ala	A	G
Exon 3	c.1302T>C	Ala434Ala	T	C
Exon 11	c.2646G>A	Gln882Gln	G	A
Exon 11	c.2673G>A	Gln891Gln	G	A
Intron 11	IVS11+42delT	N/A	T	delT
Intron 16	IVS16+8C>T	N/A	T	C
Intron 16	IVS16-4G>A	N/A	G	A
Exon 21	c.4196G>A	Arg1399Gln	A	A

NOTE: The sequence variation designation and amino acid affected are numbered according to the public boxer genome sequence. The Bedlington terrier sequence varies from the boxer in exon 2, having one less repeat, and as a consequence the protein is two amino acids shorter, an all the numbering shifts by two. Also note that for nomenclature purposes, nucleotide 1 is the first nucleotide of exon 2.

T/T, apart from the aforementioned three dogs that were heterozygous T/C. The same three dogs are also heterozygous for a base change in the 3' acceptor sequence before exon 17. This change occurs in the minus 4 position of the splice site, CT(G/A)CAG/G, which corresponds to the N position in the consensus sequence KNYAG/G [287] where each base has a 25% chance of being in that position. Therefore, we do not expect this change to lead to exon skipping of exon 17. Finally, in exon 21, a single base change observed in all Bedlington terriers sequenced in homozygous form, an adenine to guanine base substitution, results in an Arg1399Gln amino acid change compared with the public genome sequence. This substitution was not seen in the Doberman BAC or Maltese sample.

IV. DISCUSSION

Analysis of the canine *ATP7B* gene identified a pseudogene lacking exon 12, but was unable to identify exon 1 in the functional copy of the gene. Sequence analysis of the Bedlington terrier *ATP7B* identified 11 polymorphisms when compared with the boxer public database genomic sequence, however pedigree analysis suggests that *ATP7B* is not a modifier of *MURR1* in our Bedlington kindred, given that not one of these polymorphisms followed the expected pattern in affected and unaffected dogs.

In our canine *ATP7B* cDNA, we were unable to identify sequence upstream of exon 2 with similarity to human exon 1. An additional transcript for canine *ATP7B*, DQ016628, recently submitted to the NCBI transcript database, also lacks exon 1. However, exons upstream of exon 2 are predicted in the original Ensembl and NCBI predicted transcripts, ENSCAFT00000006859 and XM_534107. An NCBI model transcript (hmm773) was also recently predicted with coding sequence upstream of exon 2. Comparison of the putative amino-termini of these predicted canine transcripts shows that XM_534107 has several segments that do not align with the other two transcripts (Fig 5-3A). Omitting this predicted cDNA and comparing the 5' end of the remaining transcripts with those from other species, allows identification of an alignment with the alternative liver transcript identified in the sheep (Fig 5-3B). All breeds of sheep are susceptible to copper accumulation [299,300], and it has been suggested that the alternative *ATP7B* transcript found in the sheep might be involved in this susceptibility [301]. If the dog does in fact have an *ATP7B* gene with a 5' end similar to the sheep alternative transcript, it may explain why copper toxicosis has been observed in so many breeds of dog.

We examined the possibility that the Bedlington terrier may have a specific *ATP7B* polymorphism allowing dogs without a homozygous *MURR1* deletion to develop CT. In total 11 polymorphisms were identified in the Bedlington terrier versus the public boxer genomic sequence (NCBI). In our extended pedigree, these polymorphisms appeared to be in phase with one another without any observed recombination. Therefore, the entire haplotype for *ATP7B* could be given a single numerical value (haplotype 1 or 2, Table 5-4). When the *ATP7B* haplotypes are placed on our pedigree (Fig 5-1), there appears to be no correlation with copper toxicosis and any three or four haplotype combinations between *MURR1* and *ATP7B*. Therefore, it appears that *ATP7B* is not a modifier of *MURR1*. However, expression studies should be done to confirm that *MURR1* deletions do not affect ATP7B at the protein level.

Of the 11 polymorphisms identified, only two affect the predicted protein. The first of these is the shortening of the protein by two amino acids due to the loss of one repeat in exon 2 (Table 5-4). This change is not restricted to the Bedlington breed, as subsequent analysis of the Doberman BAC containing *ATP7B* (57N9) and Maltese genomic DNA gave the same result, suggesting that the extra repeat is either unique to the boxer breed which was used for sequencing the dog genome, or an error in the boxer DNA sequence. The predicted transcripts from Ensembl (ENSCAFT00000006859) and NCBI (XM_534107) do not include this sequence, but rather consider it part of a small intron. However, the DQ016628 transcript also predicts a putative protein with one less repeat in exon 2, but the breed used for isolation of the cDNA is not stated.

The second sequence change appears to be specific to the Bedlington terrier and results in an arginine to glutamine substitution in exon 21. This particular arginine corresponds to Arg1415 in the human ATP7B protein. The arginine to glutamine substitution has yet to be associated with Wilson disease in humans and Arg1415 is highly conserved in sheep, rat, and mouse. The Bedlington terrier substitution causes a positively charged basic residue to be replaced by an uncharged polar amino acid and *SIFT* (Sorting Intolerant From Tolerant) [302] gives this substitution a score of 0.02. The *SIFT* program presumes that important amino acids are conserved in a protein family and uses homology between species to predict whether a given amino acid substitution will affect protein function. A substitution with a *SIFT* score less than 0.05 is predicted to be deleterious to protein function. Given a *SIFT* score of 0.02, the conservation of this amino acid across species, and that this change is only seen in our Bedlington terriers, we suggest that this change could be disadvantageous, perhaps allowing for the susceptibility for copper accumulation seen in this breed.

When CT in the Bedlington was linked to C04107, there was poor marker coverage and little sequence information available for the dog. The linkage study [248] evaluated 213 microsatellites, and C04107 was the only microsatellite to give a significant LOD score. The linkage was strong, and all affected dogs were identified as 2-2 for C04107. The current 1Mb canine radiation hybrid map [303] consists of 3270 markers, and a minimal screening set for genome scans composed of 325 microsatellites. With the identification of more 1-2 or 1-1 affected dogs, future studies could include a full genome scan study to find potential loci associated with CT in these particular pedigrees. Taking a candidate approach, there are several other genes that could be looked at as potential modifiers. Such genes include those identified in the copper transport pathway and genes identified in general metal homeostasis. Of these, *XIAP*, the X-linked inhibitor of apoptosis [304], is an interesting candidate, particularly since all our affected 1-2 or 1-1 dogs are female. XIAP has been shown to interact with MURR1 [305]. More importantly, this interaction does not appear to affect apoptosis, but rather elicits an effect on copper levels. When XIAP protein levels are purposefully reduced by RNA interference, MURR1 protein levels increase and copper concentrations decrease [305]. Inversely, XIAP overexpression leads to a decrease in MURR1 protein, and copper concentrations increase. This novel role for *XIAP* in copper homeostasis only reinforces the fact that there are still many players to be identified in copper pathways. We believe that the Bedlington terrier will continue to be a useful animal model of copper storage leading to the elucidation of additional proteins important for copper homeostasis in mammals.

CHAPTER 6 : *COMMD1* (*MURR1*) As A Candidate In Patients With Copper Storage Disease Of Undefined Etiology

Veronica A. Coronado[1], Jennifer A. Bonneville[1], Hisham Nazer[2],
Eve A. Roberts[3] and Diane W. Cox[1].
[1]Department of Medical Genetics, University of Alberta, Edmonton, AB, Canada.
[2]King Faisal Specialist Hospital and Research Centre, Riyadh, Saudi Arabia.
[3]Department of Pediatrics, The Hospital for Sick Children, Toronto, ON, Canada.

Clinical Genetics (2005) **68**: 548-551

For this publication JAB assisted with first round genotyping with microsatellites. HN and EAR provided samples and pedigree information.

I. INTRODUCTION

Wilson disease (WND) is an autosomal recessive disorder of copper transport due to mutations in *ATP7B*, a gene encoding a copper transporting P-type ATPase expressed predominantly in the liver [61,62]. Defects in the ATP7B protein lead to inefficient copper excretion, resulting in hepatic copper accumulation and subsequent deposition in the brain and kidney. As a result, symptomatic presentations of WND include liver disease and/or neurological dysfunction, often associated with kidney damage. Early diagnosis is essential, as treatment can prevent tissue damage.

Copper overload is also a feature of Indian childhood cirrhosis (ICC) [213], endemic Tyrolean infantile cirrhosis (ETIC) [214], and idiopathic copper toxicosis (ICT) [208]. However, the involvement of *ATP7B* in ICC, ETIC, and some cases of ICT was excluded [222]. *COMMD1* [306], previously known as *MURR1*, was recently proposed as the gene mutated in Bedlington terriers affected with copper toxicosis [251], although exceptions have been reported in some pedigrees [295,296]. A recent screen of 23 children with non-Wilsonian copper toxicosis identified no mutations and no polymorphisms in the exonic sequences or intron-exon boundaries of *COMMD1* [223]. A second study, looking at *COMMD1* as a modifier of WND identified six polymorphisms in the *COMMD1* gene [307].

In WND, pre-symptomatic diagnosis of sibs is based on haplotype analysis and assumes the involvement of only *ATP7B*. Therefore, it is extremely important to determine the potential role of any other gene in producing similar clinical phenotypes, which could interfere in pre-symptomatic sib diagnosis. Here we present sequence and microsatellite data on 26 selected patients with evidence of copper storage not confirmed as WND by mutation analysis.

II. PATIENTS

Since we cannot assume that clinical or biochemical manifestations in patients with human COMMD1 deficiency will be exactly as found in WND, we included a wide range of patients that fell into three general categories, selected from more than 260 patients undergoing mutation analysis for *ATP7B* (see Table 6-1 for selection criteria). Sequencing of specific exons based on patient ethnicity provides a high probability of identifying a mutation of *ATP7B* [308]. *ATP7B* sequencing in Group 1 provided an 85-99% chance of mutation detection based on frequencies. No mutation has yet been identified. Group 2 patients include a wide range of age of onset, clinical features, and racial and ethnic origins. *ATP7B* sequencing provided an 80-91% chance of detecting *ATP7B* mutations. However, no mutation was found. In Group 3, biochemical parameters suggested WND, but haplotype analysis at 13q14.3 made WND unlikely: in two families, affected sibs did not share common 13q14.3 haplotypes, in the other family, a predicted patient has consistently tested biochemically and clinically normal. Later onset WND is of course a possibility in this third patient. 25 normal unrelated individuals (2 Chinese, 2 Middle Eastern, 21 Caucasian Canadians of European descent) were also included. Our study was approved by the local Research Ethics Board and conducted with informed consent.

Table 6-1. COMMD1 sequencing results in 26 clinically affected patients with copper storage of unknown etiology.

Phenotype	Proband (UA #)	Ethnic origin	Onset (years)	Disease Type[a]	*COMMD1* analysis[b]		
					exon 1	exon 2	exon 3
Group 1: Typical WND							
• diagnosed as WND by experienced clinicians	1357	British	15	N	n	n	n
• sent to laboratory for mutation analysis	1611	British	12	H	n	n/G	n
• all on treatment except UA#2811	1630	British	10	H	n	n/G	n
• clinical/biochemical features supportive of WND:	1908	British	24	N/Psy	n	n	n
- increased urinary copper (>0.6μM per 24 hrs)	1923	Saudi Arabian	5	H-olt	n	n	n
- and/or low serum ceruloplasmin (<200mg/L)	2047	Saudi Arabian	11	H	n	n/G	n
- and/or increased hepatic copper (>50μg/g dry weight)	2084	British	26	N	n	G/G	n
- and/or Kayser-Fleischer rings (all British patients)	2303	Saudi Arabian	10	N	n	n	n/C
• no mutations in *ATP7B* (85-99% coverage)	2811	British	9	H-fhf	n	n	n
Group 2: Possible WND							
• sent to laboratory as query WND patients	1704	British/Polish	7	N	n	n/G	n/C
• characteristic clinical WND symptoms	1950	Saudi Arabian	2.5	H	n	G/G	n
• some biochemical evidence of copper storage	1992	Seph Jew/French	3	H	n	n/G	n
• either increased urinary or hepatic copper	2049	Saudi Arabian	14	H	n	n	n
• no mutations in *ATP7B* (80-91% coverage)	2060	French	9	H	n	n/G	n
	2177	Saudi Arabian	3.5	H	n	n	n
	2202	1st Nation	10	H	n	n	n
	2206	Saudi Arabian	6	H/N	n	n/G	n
	2261	1st Nation	12	H	n	n	n
	2277	Chinese	38	H	n	n	n
	2333	Italian/German	28	H	n	n	n
	2543	European	13	H/Psy	n	n	n
	2825	British	2	H	n	n	n
	2964	German/Irish	64	H	n	n/G	n
Group 3: Not WND by Haplotype							
• familial copper storage and abnormal biochemical parameters	**1926**	Saudi Arabian	6	H	n	n	n
• haplotye analysis at 13q14.3 made WND unlikely	**1934**	Saudi Arabian	13	H	n	n	n
	2275	Irish	15	N	n	n	n/C

Probands in bold have affected sibs and were included in *COMMD1* haplotype analysis (Fig 6-1). [a]Type of disease presentation: N, neurological; H, hepatic; fhf, fulminant hepatic failure; otl, orthologous liver transplant; Psy, psychiatric. [b]Sequence analysis including exon-intron boundaries; n, common normal sequence, n/ : heterozygote for common sequence and indicated polymorphism.

III. RESULTS AND DISCUSSION

1. *COMMD1* MUTATION AND HAPLOTYPE ANALYSIS

No mutations in the *COMMD1* coding region or exon-intron boundaries were identified in the 26 patients tested (Table 6-1). This included approx. 90 bp of each of the 5' and 3' UTRs and 90-180 bp of intronic sequence flanking each of the three exons of *COMMD1*. Two common polymorphisms, previously identified by Stuehler et al. [307], were also observed in our patient set. The first lies in intron 2, c.471+63c>g, in the sequence ttgt(**c/g**)tatt. The guanine substitution, not predicted to create a new consensus splice sequence, was observed in 12 out of 52 patient chromosomes (23%, eight European, four Saudi Arabian chromosomes) and 14 out of 50 normal chromosomes sequenced (28%, one out of four Middle Eastern, 13 out of 42 European descent). The second sequence change, c.501T>C, occurs in exon 3 within the codon GAT, which codes for Asp164 of the COMMD1 protein. The change from a thymine to a cytosine is silent and leads to no amino acid substitution. This sequence change was observed in three out of 52 patient chromosomes (5.8%, two British, one Saudi Arabian) and six out of 50 normal chromosomes sequenced (12%, six out of 42 European descent) at the *COMMD1* locus.

In two families (Fig 6-1), marker analysis at the WND locus in affected sibs did not support the involvement of *ATP7B* in their disease. Family UA52, includes three affected sibs, but sib II:ii did not share identical WND haplotypes with the proband (II:i). Similarly in family UA53, markers at the WND locus were not shared by any of the three affected sibs. *COMMD1* spans approximately 190 kb and its open reading frame only comprises 573 bp. Therefore, although no mutations were found in the *COMMD1* coding region of the probands in these two families, mutations far into the introns or the

Family UA52

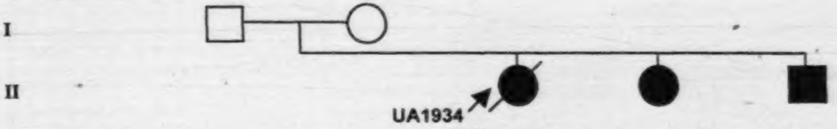

D13S314	1 6	7 7	6 7	1 7	6 7
D13S301	4 4	5 5	4 5	4 5	4 5
ATP7B	N W?	N W?	W? W?	**N** W?	W? N/W?
D13S133	26 4	5 6	4 6	26 6	4 5
D13S316	7 5	5 5	5 5	7 5	5 5
D13S297	2 13	13 13	13 13	2 13	13 13
D2S337	4 9	4 5	9 5	9 5	4 5
D2S2165/*COMMD1*	4/N 4/D?	4/N 5/D?	4/D? 5/D?	4/D? 5/D?	4/**N** 5/D?
D2S2206	4 5	3 7	5 7	5 7	4 7

Family UA53

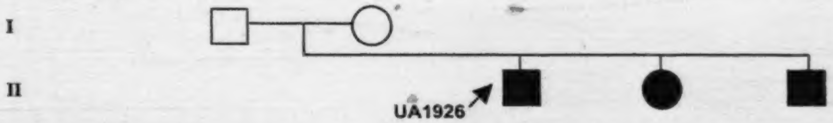

D13S314	3 10	1 6	10 6	3 1	3 6
D13S301	6 6	3 3	6 3	6 3	6 3
ATP7B	N W?	N W?	W? W?	**N** **N**	**N** W?
D13S133		4 28	8 28	26 4	26 28
D13S316	7 4	4 7	4 7	7 4	7 7
D13S297					
D2S337	8 9	4 9	9 9	9 4	8 9
D2S2165/*COMMD1*	4/N 4/D?	1/N 4/D?	4/D? 4/D?	4/D? 1/**N**	4/**N** 4/D?
D2S2206	9 9	13 4	9 4	9 13	9 4

Figure 6-1. Haplotype analysis at the Wilson disease (WND) and *COMMD1* loci. Proband is indicated by arrow, number indicates proband designation from Table 6-1. Filling indicates individuals affected by copper storage. Beginning with the proband and parents to establish phase, sibs were genotyped and assigned alleles as follows; N: assumed normal *ATP7B* or *COMMD1*, W?: assumed mutated *ATP7B*, D?: assumed *COMMD1* disease copy. Bold N, W?, or D? indicates disagreement between copper storage and a possible mutation at that particular locus. Family UA52: proband (UA#1934, II:i) presented with onset of hepatic disease with a cholestatic component at the age of 13, with increased urinary copper, sib (II:ii) had progressive liver disease onset also at 13 years, younger sib (II:iii) had clinical liver disease onset at four months, seven unaffected sibs (not shown). Family UA53: proband (UA#1926, II:i) showed hepatic presentation at the age of six with high urinary and hepatic copper, liver transplant at age 13, sib (II:ii) had clinical liver disease onset 13 years, younger sib (II:iii) had abnormal liver function tests at 11 months, seven unaffected sibs (not shown). All patients had normal serum ceruloplasmin. This was uninformative for diagnosis, as ceruloplasmin levels are normal in a significant number of patients with hepatic presentation of WND [309].

uncharacterized promoter would not be identified by direct sequencing methods. In order to identify the presence of potential mutations in these regions, we used three microsatellite markers around *COMMD1* for haplotype analysis in these two selected families. D2S2165 lies within intron 1 of *COMMD1*, D2S337 lies 514 Kb upstream (telomeric), and D2S2206 lies 334 Kb downstream (centromeric). Like WND, copper toxicosis in the Bedlington terrier is a recessive disorder [246] and one would also expect to find two mutant copies in its human counterpart. Analysis of the haplotypes flanking *COMMD1* (Fig 6-1) also failed to identify co-segregation, indicating no association between the *COMMD1* locus and copper storage in these families.

Taken together with previously published results [223], the data presented here suggest that *COMMD1* is not a significant contributor to Wilson-like copper storage disorders in humans, although very rare occurrences of *COMMD1* mutations cannot be excluded. Alternatively, the COMMD1 phenotype could be clinically and biochemically distinct from WND. Our data support the continued use of WND markers for reliable genetic diagnosis of pre-symptomatic sibs of firmly diagnosed patients.

CHAPTER 7 : Preliminary Studies for the Functional Characterization of human MURR1 (COMMD1)

Veronica A. Coronado and Diane Wilson Cox

Department of Medical Genetics, University of Alberta, Edmonton, Alberta, Canada

Unpublished

I. INTRODUCTION

MURR1 (COMMD1) has been suggested as the gene defective in copper toxicosis in the Bedlington terrier [251] and the protein has since been shown to be multifunctional participating in many diverse biological pathways. In the NF-κB signaling pathway, MURR1 has been shown to associate with IκB-α [310] and NF-κB subunits directly [306], inhibiting κB-responsive transcription. In this pathway, MURR1 has the ability to inhibit HIV-1 replication in resting $CD4^+$ lymphocytes [310]. Yeast-two hybrid studies have also identified two other proteins that interact with MURR1, the human delta epithelial sodium channel subunit (δENaC)[311] and the X-linked inhibitor of apoptosis (XIAP) [305]. With MURR1 being implicated in so many different pathways, it is interesting that the only shared phenotype expressed by all CT-affected Bedlington terriers is copper accumulation in the liver, leading to hepatic damage [237].

Two recent studies considered the role of *MURR1* as a candidate gene in human patients with copper storage of undefined etiology [223,312]. However, neither of these studies identified any disease causing mutations in *MURR1*. Despite the apparent absence of disease causing mutations in *MURR1* in patients with copper storage, data connecting *MURR1* to copper homeostasis in humans is mounting. Stuehler et al. [307] analyzed the potential of *MURR1* as a modifier of Wilson disease (WD). WD is an autosomal recessive disorder of copper transport, leading to copper accumulation in the liver and caused by mutations in the *ATP7B* gene [61,62]. The authors suggest that a silent polymorphism in *MURR1* is associated with earlier onset of WD. However, a recent modifier study conducted in 218 Chinese WD patients found no correlation between *MURR1* and WD [313]. MURR1 has however, been shown to directly interact with the

N-terminus of endogenous human ATP7B from *HepG2* lysates in GST pull-down assays expressing recombinant protein [297]. In addition, copper homeostasis is disrupted in human embryonic kidney (*HEK*) *293* cells when they are subjected to *MURR1*-targeted RNA-interference [305]. Although decreasing MURR1 expression in *HEK293* cells led to a moderate increase (1.6-fold) in copper levels, these studies have yet to be carried out in hepatocytes, which are the main cell type affected in copper toxicosis.

The human hepatoma cell line, *HepG2* expresses endogenous *ATP7B* and *MURR1* [297]. ATP7B localizes to the *trans*-Golgi network [69,78] and trafficks to cytosolic vesicles and the apical (canalicular) membrane under increased copper conditions in polarized *HepG2* cells [80]. A current theory is that MURR1 is essential for biliary copper excretion downstream of ATP7B and that its ubiquitous expression and cytosolic localization are consistent with a probable function in cell-specific vesicular transport [251,297]. I propose to evaluate copper resistance and sensitivity in *HepG2*, after overexpression and knockdown of *MURR1*, respectively, and to determine the effect of *MURR1*-RNA interference (RNAi) on copper-induced ATP7B movement by comparing normal *HepG2* cells with *HepG2* cells subjected to *MURR1*-RNAi. In this system, it could also be determined whether ATP7B and MURR1 colocalize to the same vesicular compartments during copper-induced trafficking.

Before these studies can be undertaken, several pre-requisites have to be accomplished. This chapter describes the generation of *MURR1* expression constructs, determination of cell specific copper toxicity, recombinant-MURR1 purification and antibody production, and preliminary optimization of conditions for RNAi in *HepG2* cells.

II. METHODS AND MATERIALS

I. CONSTRUCTION OF *MURR1* EXPRESSION VECTORS

Total RNA was extracted from human blood collected in PAXgene blood RNA tubes as per manufacturer's instructions (PAXgene blood RNA kit, PreAnalytiX, Qiagen). First-strand cDNA was synthesized from 1μg total RNA using Superscript II (Invitrogen) and an oligo(dT) primer. Using 2 μl of the cDNA reaction, the complete coding region of MURR1 was amplified using the following primers: forward primer: 5' CTCGAGCCTTCGCAGA GCAT 3' and reverse primer: 5' ACCAATGCGGGCACAAGAAT 3'. This product was electrophoresed and gel extracted (QIAquick gel extraction kit, Qiagen) prior to cloning into the TA-cloning vector, pGEM-T (Promega). Using M13 primers, this construct was directly sequenced on a 3130xl Genetic Analyzer (Applied Biosystems) to confirm the correct full-length sequence before subcloning into pcDNA1/Amp (Invitrogen) and pET-28b (Novagen). For mammalian overexpression studies, a *XhoI/NsiI* pGEM-T+*MURR1* fragment was cloned into pcDNA1 cut by the same restriction endonucleases. A *XhoI/NotI* pGEM-T+*MURR1* fragment was subcloned into pET-28b cut with *SalI/NotI* to express a fusion protein of human MURR1 with 5' His- and T7-tags. Subcloned constructs were directly sequenced using a T7 primer, to confirm proper reading frame.

II. EXPRESSION AND PURIFICATION OF RECOMBINANT-*MURR1*

The pET-28b+*MURR1* construct was used to transform BL21(DE3)pLysS cells (Invitrogen) and BL21(DE3) cells (Invitrogen). Expression of recombinant-MURR1 protein was induced according to the pET-expression system manual (Novagen). In brief, overnight cultures were diluted 10-fold and incubated at 37°C until reaching an OD_{600} between 0.8 and 1.0. At this point, isopropylthiogalatosidase (IPTG) was added to a final concentration of 1mM and cultures were incubated for another 3 hours. Cells were harvested by centrifugation, washed in one-quarter-volume 20 mM Tris-HCl pH 8.0, centrifuged again and the pellet frozen at -80°C. Cell pellets were allowed to thaw at room temperature then lysed in lysis buffer (300 mM NaCl, 50 mM sodium phosphate buffer, 10 mM imidazole, pH 8.0) with protease inhibitor cocktail (Sigma), PMSF, and DNaseI (Roche). Transformed BL21(DE3)pLysS cells produced soluble protein, which was purified on nickel charged nitriloacetic acid (Ni-NTA) agarose (Qiagen) under non-denaturing conditions according to instructions provided by the Ni-NTA His-bind resins manual (Novagen).

Recombinant protein from BL21(DE3) transformed cells was insoluble and purified on the Ni-NTA resin under denaturing conditions in 8 M urea buffers with increasing concentrations of imidazole as previously described [314]. Initial protein identity was verified by Western analysis using 1:10,000 dilution of mouse monoclonal T7-tag antibody (Novagen) and 1:10,000 goat-anti-mouse secondary antibody (Pierce) conjugated with horseradish peroxidase. Bands were visualized with SuperSignal West Dura Extended duration substrate (Pierce). T7-tag positive control extract (31.1 kDa) was purchased from Novagen.

Purified protein was electrophoresed on a 12% SDS-polyacrylamide preparative gel and stained with Coomassie Brilliant Blue. Bands of interest were cut out and placed into SnakeSkin dialysis tubing (Pierce) with elution buffer (200 mM Tris-Ac, 1% SDS, 10 mM DTT) and electroeluted in running buffer (50 mM Tris-Ac, 0.1% SDS) at 50 V overnight at 4°C. The next morning, buffer was changed and electroelution continued for 3 hours at 100 V, followed by another buffer exchange and 1 hour electroelution. For the final hour of electroelution, the buffer was exchanged once last time omitting SDS. Clear gel pieces were removed from the tubing and the protein solution concentrated on Amicon Ultra 10K centrifugal filter devices (Millipore). MURR1 protein purity was validated by SDS-PAGE followed by Coomassie brilliant blue staining and Mass-spectrometry analysis (Institute for Biomolecular Design Mass-Spectrometry Facility, University of Alberta).

III. GENERATION AND EVALUATION OF ANTISERUM

Antiserum to MURR1 was obtained by serial immunizations of two female Hartley-outbred guinea pigs (Charles River) with purified recombinant His-T7-MURR1 protein. The primary injection included complete Freund's adjuvant, followed by booster injections of protein with incomplete Freund's adjuvant. Each injection contained 150 μg protein. Blood, pre- and post-immunization, was left at 4°C overnight and centrifuged at 2,500 RPM for 20 minutes to isolate clear serum for testing. BSA protein (Pierce) was used as a negative control. *HepG2* cell lysate was used as a positive endogenous control for MURR1. In competition assays, 1 μl antiserum was incubated with 9.65 μg purified protein, or 38.6 μg BSA, overnight at 4°C. Goat-anti-guinea pig secondary antibody (Sigma-Aldrich) conjugated with peroxidase was used for Western blotting.

IV. CELL CULTURE

Chinese hamster ovary (*CHO*) and human hepatocellular carcinoma (*HepG2*) cells were purchased from the American Type Culture Collection resource and cultured in Dulbecco's modified Eagle's medium (Gibco) supplemented with 10% fetal bovine serum (Gibco). For determination of cellular copper toxicity, cells were seeded in 6-well plates to reach 80-90% confluency next day, at which time copper chloride solution was added to a final concentration of 0-800 μM. Following an overnight incubation, cells were trypsinized (Gibco) and stained with 0.4% trypan blue solution (Sigma) and live cells were counted. Counts were done in duplicate. The mean number of cells in 0 μM copper was taken as 100% survival, and the survival at each copper concentration assayed was represented as a percentage of that number.

V. MURR1-RNA INTERFERENCE

Using the siRNA target finder available online from Ambion (www.ambion.com/techlib/misc/siRNA_finder.html), oligonucleotides were chosen based on BLAST (www.ncbi.nih.gov/BLAST) results with hits to the target gene only. Two targets were chosen for *ATP7B*. DNA templates had the following sequence: target 1: 5' AACAACCGATGGCACATATCCTGTCTC 3' (sense), 5' AAATATGTGCCATCGGTTCTGCCTGTCTC 3' (antisense); target 2: 5' AATATCCCGTGGACCGATAATCCTGTCTC 3' (sense), 5' AAATTATCGGTCCACGGGATACCTGTCTC 3' (antisense). Negative scrambled controls were generated by the same program. For *MURR1*, the target finder identified a sequence previously targeted by Burstein et al. [305], who successfully demonstrated *MURR1*-RNAi in *HEK293* cells. Therefore, the same sense and antisense oligonucleotides were synthesized for siRNA construction.

siRNAs were constructed using the *Silencer* siRNA construction kit (Ambion) according to the manufacturer's protocol. *GAPDH* control Cy3-labelled siRNA (Ambion) was used as a transfection control. For transfection, four different buffers were tested: siPORT *NeoFX* (Ambion), siPORT *Amine* (Ambion), siPORT *Lipid* (Ambion), and X-tremeGENE (Roche). *HepG2* cells were seeded (1×10^5 cells/well) onto glass coverslips in 6-well plates for approximately 50% confluency the next day. Cells were transfected with a final concentration of 30 nM Cy3-*GAPDH* siRNA with the recommended volumes of transfection reagent according to each manufacturer's individual protocols. Media was removed 24 hrs after transfection and coverslips mounted onto slides with Vectashield mounting media plus DAPI (Vector Laboratories, Inc.). The remaining cells were trypsinized, resuspended in phosphate buffered saline (PBS), and a sample also mounted on slides. From a second transfection well, cells were harvested 48 hrs after transfection for RNA extraction. RNA was extracted using QIAshredder columns (Qiagen) and the RNeasy mini kit protocol (Qiagen). Total cDNA was synthesized as described above. Multiplex semi-quantitative PCR was performed to test *GAPDH* knockdown at the mRNA level using *β-actin* as a control. PCR was performed with an annealing temperature of 62°C and 25 cycles with 2 mM magnesium. *GAPDH* primers were: forward: 5' GCTCAGACACCATGGGGAAG 3', reverse: 5' GGCCATCCACAGTCTTCTGG 3'. *β-actin* primers have been previously published [315].

III. RESULTS

I. EXPRESSION AND PURIFICATION OF RECOMBINANT-MURR1

Initial expression in BL21(DE3)pLysS cells produced low levels of protein, which could be purified with increasing concentrations of imidazole. Once high protein expression was achieved in BL21(DE3) cells, the recombinant protein began to aggregate into insoluble protein pellets, which had to be solubilized in denaturants (Fig 7-1A). The recombinant His-T7-MURR1 protein migrated at approximately 27 kDa (Fig 7-1B), compared with the reported migration of endogenous MURR1 of 23 kDa [316]. Using imidazole for non-denaturing purification, His-T7-MURR1 was consistently associated with a lower molecular weight contaminant (Fig 7-1C, left panel), identified as bacterial FKBP-type peptidyl propyl cis-trans isomerase by mass-spectrometry. Denaturing purification caused the elimination of the FKBP-type protein co-purification (Fig 7-1C, right panel).

II. ANTISERUM CHARACTERIZATION

Immunoblots were performed to investigate whether the immunized guinea pigs produced antibodies towards the recombinant MURR1 protein. In contrast to pre-immune serum, antiserum of immunized guinea pigs contained antibodies that bound purified recombinant MURR1 protein and gave the expected sized band for endogenous MURR1 in *HepG2* lysates (Fig 7-2). The association appeared to be specific to MURR1, as tested by competition assays using BSA as a negative control (Fig 7-2). Sensitivity of the antiserum was established by serial dilutions of protein on blots and antiserum in washes (not shown). At a 1:3,000 dilution, the antiserum allowed the detection of

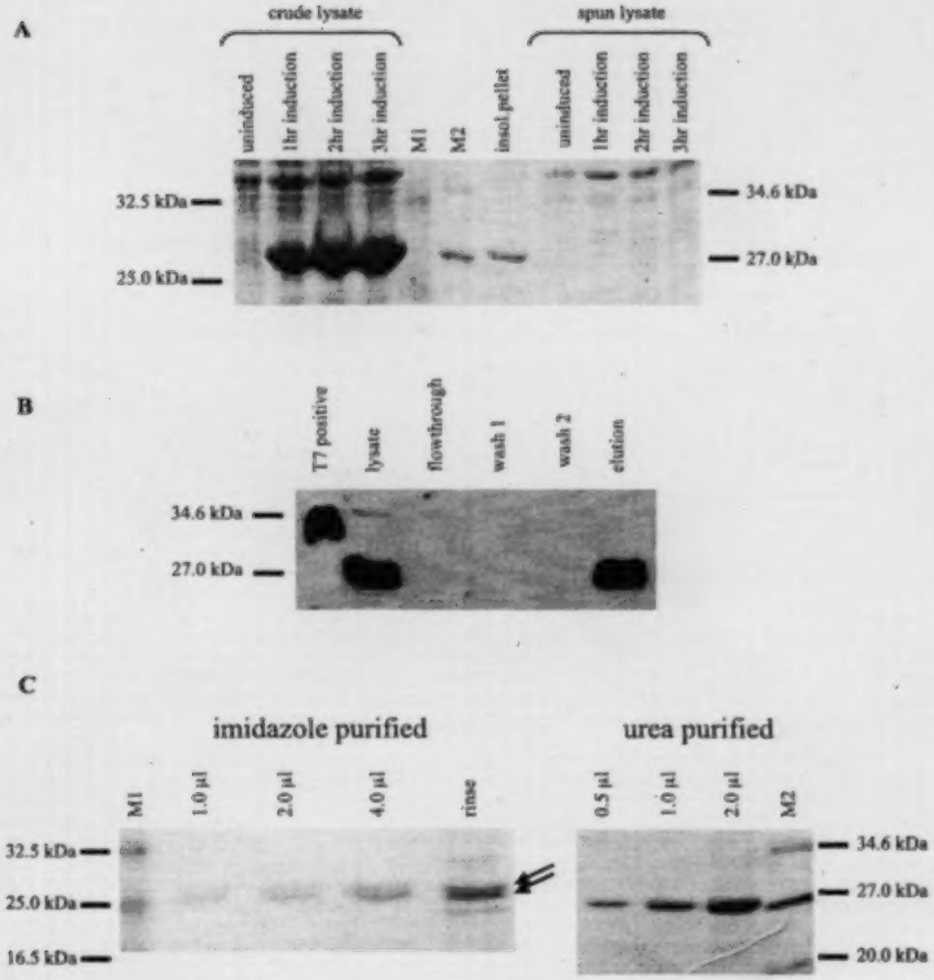
A
crude lysate
spun lysate
uninduced
1hr induction
2hr induction
3hr induction
M1
M2
insol pellet
uninduced
1hr induction
2hr induction
3hr induction
32.5 kDa
25.0 kDa
34.6 kDa
27.0 kDa
B
T7 positive
lysate
flowthrough
wash 1
wash 2
elution
34.6 kDa
27.0 kDa
C
imidazole purified
urea purified
M1
1.0 µl
2.0 µl
4.0 µl
rinse
0.5 µl
1.0 µl
2.0 µl
M2
32.5 kDa
25.0 kDa
16.5 kDa
34.6 kDa
27.0 kDa
20.0 kDa

Figure 7-1. Expression and purification of recombinant-MURR1. (A) Lysates from BL21(DE3)+MURR1, pre- and post-induction, crude and spun. Insoluble pellet was dissolved in 3.9 M guanidine-HCl. **(B)** Western analysis of purification fractions. Primary antibody, 1:10,000 anti-T7-tag. Secondary antibody, 1:10,000 goat-anti-mouse peroxidase conjugate. Lanes: 80 ng T7-tag control, and 16 µl each: spun BL21(DE3)pLysS+MURR1 lysate, bind flowthrough, wash flowthrough (1 and 2), imidazole elution. **(C)** Recombinant-MURR1 purified on Ni-NTA resin, either using imidazole or urea. Rinse: post-purification column rinse to dislodge all remaining bound proteins. **(A)** and **(C)** 12% SDS-PAGE stained with Coomassie brilliant blue. Molecular weight markers: M1: P7708S and M2: P7702S (New England Biolabs).

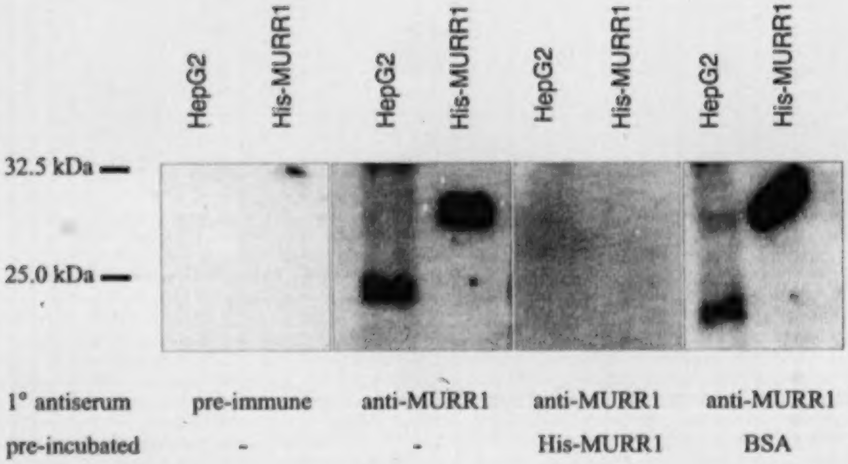
HepG2
His-MURR1
HepG2
His-MURR1
HepG2
His-MURR1
HepG2
His-MURR1
32.5 kDa
25.0 kDa
1° antiserum
pre-immune
anti-MURR1
anti-MURR1
anti-MURR1
pre-incubated
-
-
His-MURR1
BSA

Figure 7-2. Characterization of antiserum to recombinant-MURR1. Competition assay strips. Recombinant-MURR1 migrates at 27 kDa. Endogenous MURR1 migrates at approximately 23 kDa. Lanes: 5 µl *HepG2* liver cell lysate, 0.13 ng recombinant-MURR1. Strips were pre-incubated overnight with primary (1°) antiserum (1:3,000 dilution) and buffer alone, or recombinant-MURR1 or BSA. Secondary antibody: goat-anti-guinea pig peroxidase conjugate (1:10,000 dilution).

endogenous MURR1 in 5 μg *HepG2* liver cell lysate and as little as 0.13 ng recombinant protein (Fig 7-2).

III. CELL SPECIFIC COPPER TOXICITY

Copper concentrations tested for *CHO* were based on previously published studies [71,317]. These same concentrations were initially used for *HepG2* copper toxicity, but no significant changes in survival were observed (not shown). *CHO* cells were reduced to approximately 50% survival at 100 μM copper, while *HepG2* did not reach this level until 600 μM copper (Fig 7-3).

IV. MURR1-RNAI OPTIMIZATION

HepG2 is a difficult cell type to transfect because cells do not grow in a monolayer, but have a tendency to grow on top of each other in clumps. For this reason, we tried siPORT *NeoFX* transfection reagent to transfect cells in suspension prior to seeding (neofection). By this method, the transfection reagent and siRNAs have an opportunity to equally bathe all cells. siPORT *NeoFX* has also been optimized in *HepG2* by the manufacturer and 90% target knockdown has been demonstrated. siPORT *Amine/Lipid* may also work effectively in *HepG2* [318], but detailed conditions are not available. Lastly, 60-70% knockdown in *HepG2* has been observed using X-tremeGENE according to the manufacturer, but conditions are not published. Starting with the recommended volumes and concentrations for 6-well plate transfections for each individual reagent, *HepG2* cells were transfected with Cy3-*GAPDH* siRNA and fluorescence visualized under microscope with a tetramethyl rhodamine (TRITC) filter. Transfection efficiency was measured as the percentage of nuclei associated with Cy3-signal compared to total

A

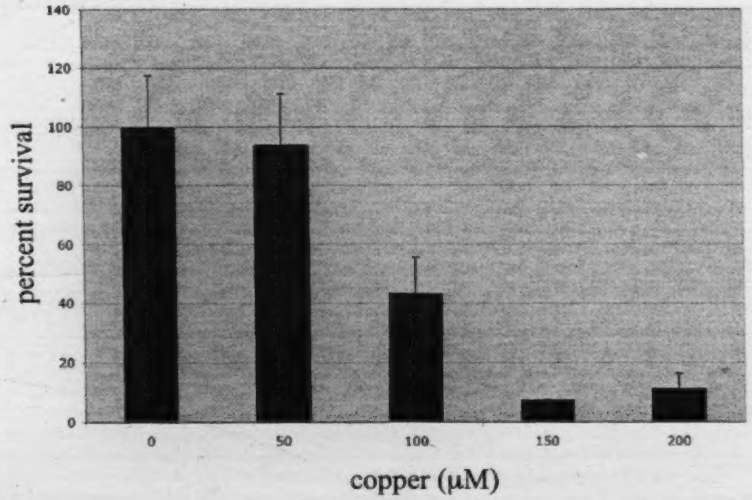

B

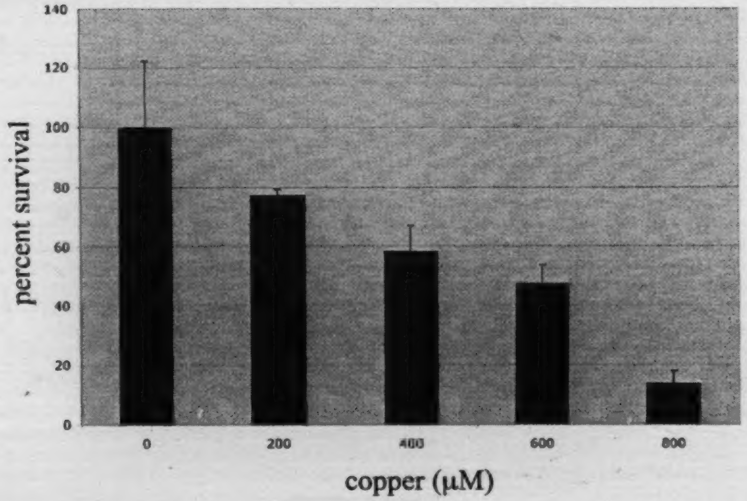

Figure 7-3. Cell specific copper toxicity. (A) *CHO* cells grown overnight in 0-200 μM $CuCl_2$. **(B)** *HepG2* cells grown overnight in 0-800 μM $CuCl_2$. Survival at each copper concentration is represented as a percentage of the mean number of cells at 0 μM $CuCl_2$, which is taken to be 100%. Bars represent standard deviation.

nuclei. Four fields of view were counted for each transfection. Among the four buffers being compared, siPORT *Amine* gave the highest transfection efficiency of 46%, followed by X-tremeGENE at 39% (Fig 7-4). Neofection was not as effective as we expected, with only 29% transfection efficiency. Lastly, siPORT *Lipid* gave only 17% transfection and also contributed to background signal during fluorescent microscopy. These levels of transfection however, did not translate into decreased levels of *GAPDH* mRNA as measured by multiplex semi-quantitative PCR (not shown). Further optimization is required before proceeding with *MURR1* or *ATP7B* siRNAs.

IV. DISCUSSION

II. MURR1 IS A UBIQUITOUS PROTEIN WITH MULTIPLE FUNCTIONS

MURR1 mRNA is ubiquitously expressed in human tissues, with highest level of expression in the liver and heart, and moderate expression in the kidney, brain, and skeletal muscle [295,319]. Significant levels are also observed in the thymus, lung, prostate, uterus, testis, ovary, skin, thyroid, pancreas, spleen, and intestine [295,306,319], but only low levels are detected in leukocytes [295,319]. In the mouse, *MURR1* mRNA is preferentially expressed from the maternal allele in all tissues, but predominantly in the adult brain [320]. Conversely, human *MURR1* is expressed biallelically in adult and fetal brains, and other tissues [319]. Imprinting of the murine gene is thought to result from retrotransposition of a paternally expressed gene, *U2af1-rs1*, into intron 1 of *MURR1* [320], which in humans is present on a separate chromosome [282]. Paternal expression of murine *U2af1-rs1* is predicted to interfere with expression of *MURR1* from the same chromosome causing a reduction in expression of the paternal *MURR1* allele. In this model the absence of *U2af1-rs1* in human *MURR1* would allow for unhindered

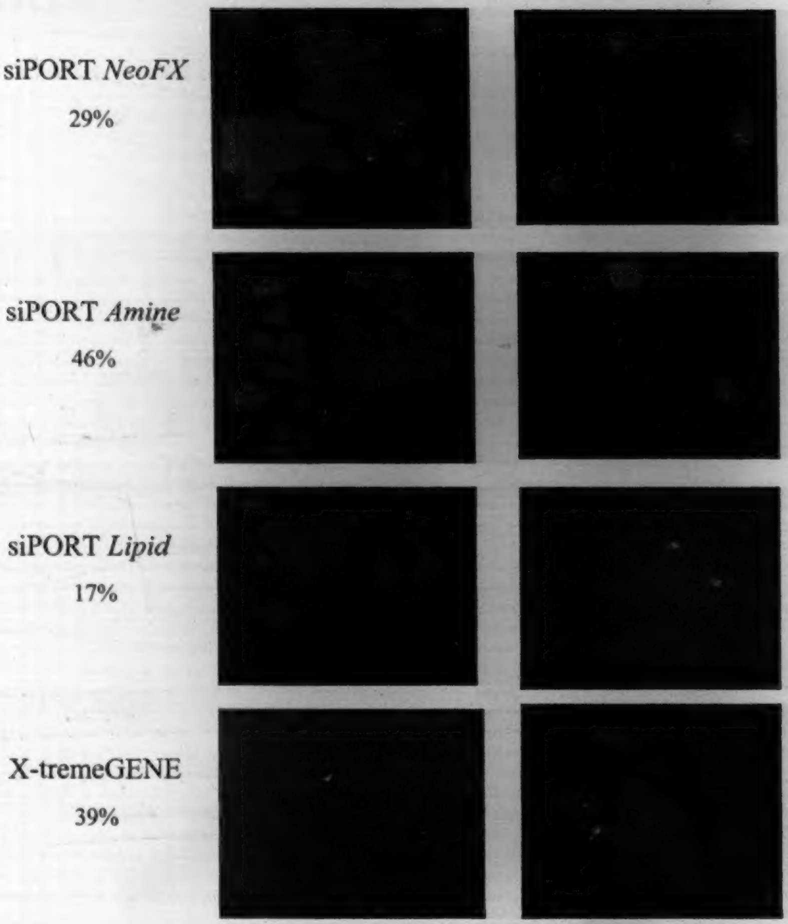
siPORT *NeoFX*
29%
siPORT *Amine*
46%
siPORT *Lipid*
17%
X-tremeGENE
39%

Figure 7-4. Transfection reagent testing. *HepG2* cells transfected with 30 nM Cy3-*GAPDH* siRNA and the transfection reagent shown, either: siPORT *NeoFX* (Ambion), siPORT *Amine* (Ambion), siPORT *Lipid* (Ambion), or X-tremeGENE (Roche), transfection efficiencies listed as percentage of dual signal nuclei. Coverslips mounted with Vectashield with DAPI. Left view shows cells grown on coverslip, 20X magnification. Right view shows cells resuspended in PBS 40-100X magnification. Blue: nuclei. Red: siRNA.

expression from both paternal and maternal alleles, and no imprinting. A novel antisense transcript (*U2mu*), derived from portions of *U2af1-rs1* and *MURR1*, is also expressed in the mouse as a result of *U2af1-rs1* retrotransposition [321].

Endogenous MURR1 protein expression has been confirmed in the hepatocellular carcinoma cell lines *HepG2*, *Hep3B*, and *PLC/PRF/5*, the colon carcinoma cell lines *Caco2* and *HT29*, the lung carcinoma cell lines *A549* and *H441*, the cervical carcinoma cell line *Hela*, and the embryonic kidney carcinoma cell line *HEK293* [316], as well as the prostate carcinoma cell line *DU145* [306] and primary $CD4^+$ and $CD8^+$ T-lymphocytes [310].

Among the many binding partners of MURR1 identified, some were found to share homology with MURR1 in their carboxy-termini [306]. This shared motif is called the copper metabolism gene *MURR1* domain (COMMD) and has led to the discovery of a family of COMMD containing proteins in humans with structural and functional homology to MURR1 (COMMD1). The COMM domain is leucine-rich and consists of approximately 70-85 amino acids predicted to form a β-sheet [306]. In addition to MURR1, there are another nine COMMD proteins in humans (COMMD2-10), of which only four have been previously characterized. Microarray analysis reveals that all the COMMD proteins are ubiquitously expressed to varying levels in different tissues [306]. GST-pulldown assays demonstrate the ability of all the COMMD proteins to form complexes with MURR1, including MURR1 itself [306]. The composition of the complexes is most likely tissue specific given the different ratios of COMMD proteins in different tissues. Endogenous complexes of MURR1 with COMMD6 have been immunoprecipitated from *HEK293* cells [322], but *in vivo* confirmation of the other complexes is still lacking.

Yeast-two hybrid and co-immunoprecipitation studies have also identified other binding partners of MURR1 not belonging to the COMMD family [297,305,310,311], implicating this protein in a variety of cellular processes, including copper excretion, sodium uptake, NFκB transcription, and apoptosis.

a. MURR1 and the Copper Pathway

The identification of *MURR1* deletions in Bedlington terriers affected with CT automatically implicated the MURR1 protein in the copper transport pathway. Supporting a role for MURR1 in copper homeostasis, transient knockdown of MURR1 in *HEK293* cells leads to a 1.6-fold increase in cellular copper concentration [305]. Additional support comes from the demonstration that the WD protein, ATP7B, directly interacts with MURR1 [297]. Unlike many WD patients, Bedlington terriers with CT exhibit normal to increased levels of ceruloplasmin, which is synthesized in the *trans*-Golgi network (TGN). In the affected Bedlington terrier, similarly to WD patients, copper accumulates in lysosomes, and biliary excretion of copper is severely reduced. These features of WD and CT, in addition to the interaction between ATP7B and MURR1, suggest a possible role for MURR1 downstream of the TGN, either facilitating ATP7B-mediated vesicular copper transport or lysosome degranulation at the bile canalicular membrane [323]. This proposed role of MURR1 is said to be consistent with the observation that MURR1 localizes to a vesicular compartment showing partial overlap with endosomal and lysosomal markers [316]. However, this vesicular staining pattern was observed in carcinoma cell lines of the cervix (*Hela*), lung (*A549* and *H441*), and kidney (*HEK293*), but could not be detected in hepatocellular (*HepG2*, *Hep3B*, or *PLC/PRF/5*) or colon carcinoma cell lines (*Caco2* or *HT29*) [316].

b. MURR1 and the Sodium Pathway

The human epithelial sodium channel (ENaC) is a multimeric complex responsible for non-voltage-sensitive ion movement across the plasma membrane. Four human subunits have been identified, α, β, δ, and γ, and the biophysical properties of ENaC depend upon the subunit composition of the channel. The α, β, and γ subunits are highly expressed in epithelial tissues, such as kidney, lung, and colon, while the δ subunit is expressed predominantly in the brain, testis, ovary, and pancreas, although transcripts are detected in all tissues [324-326]. The carboxy-termini of the α, β, and γ subunits contain a conserved PPPXY motif, which mediates binding of a Nedd4 ubiquitin ligase [327]. However, this motif is not conserved in the δ subunit, suggesting different regulatory mechanisms and different binding motifs [326].

A yeast-two hybrid screen of a human brain cDNA library, using the carboxy-terminus of the δ subunit, identified a possible interaction with MURR1 [311]. Subsequent experiments confirmed this interaction *in vitro*, as well as interactions between MURR1 and the β, and γ subunits, but not the α subunit. Functional characterization of these interactions, showed that coexpression of MURR1 with αβγENaC or δβγENaC in *Xenopus* oocytes resulted in inhibition of the sodium current in a dose-dependent manner. The inhibition was significantly lower upon deletion of the δ subunit carboxy-terminus, but not deletion of the β or γ subunit carboxy-termini, suggesting that the contribution of the β and γ subunits to MURR1 inhibition is minimal. The exact mechanism of MURR1 inhibition has yet to be determined, but the authors propose three possibilities: either MURR1 alters trafficking of the subunits to or from the plasma membrane, consistent with its proposed function in copper excretion and vesicular trafficking of ATP7B, or MURR1 may directly affect channel gating, or MURR1 may act as an adapter molecule linking the channel to other regulatory proteins.

c. MURR1 and the Apoptotic Pathway

The X-linked inhibitor of apoptosis (XIAP) comprises three amino-terminal BIR domains and a carboxy-terminal RING domain with E3 ubiquitin ligase activity. Apoptosis is facilitated by a family of cysteine proteases known as caspases. XIAP inhibits mitochondrial and receptor (Fas)-mediated apoptotic pathways, by directly binding to and inhibiting initiator and effector caspases, specifically caspase-3, -7, and –9 [304]. Binding and inhibition of caspases by XIAP occurs via the BIR domains. By virtue of its RING domain, XIAP has also been implicated in proteosome-mediated degradation of target proteins by its ability to function as an E3 ubiquitin ligase [328,329].

Using full-length XIAP as bait in a yeast-two-hybrid screen of a human liver cDNA library, MURR1 was identified as a XIAP binding protein [305]. This interaction was confirmed *in vivo* with endogenous protein in *HEK293* cells and was shown to be dependent on BIR3, but the mechanism of binding appears to be distinct from that used to bind caspases, as demonstrated by point mutations. MURR1 did not appear to modulate the anti-apoptotic properties of XIAP, but expression of XIAP was able to affect copper levels by increasing MURR1 ubiquitination and leading to subsequent MURR1 degradation. Overexpression of XIAP in *HEK293* cells led to decreased levels of MURR1 and an increase in intracellular copper levels comparable to those achieved by RNA interference of MURR1 in these same cells [305]. Conversely, in tissues from XIAP null mice, MURR1 levels are modestly increased and copper levels are reduced 1.2 to 3-fold. However, this interaction is not specific to XIAP, as other BIR-containing proteins were also able to immunoprecipitate MURR1. The functional significance of these interactions remains to be investigated, but suggests that MURR1 may be a general downstream target of other anti-apoptotic proteins.

In models of copper storage, XIAP levels are greatly reduced [330]. Copper binding produces a conformational change in XIAP that shifts XIAP mobility of SDS-PAGE, and accelerates XIAP degradation, as well as decreasing its ability to inhibit caspase-3 leading to apoptosis. The copper-dependent mobility-shift and decrease in XIAP levels were observed in liver samples from WD patients, Bedlington terriers affected by CT, the *tx*^{J} mouse, and a cocker spaniel with secondary copper accumulation due to cholestasis, and was recapitulated in *HEK293* cells in 50 μM copper [330].

d. MURR1 and the NF-κB Pathway

Nuclear factor-κB (NF-κB) regulates transcription of many gene products involved in a number of biological processes including immune and inflammatory responses, apoptosis, cell survival and proliferation, and carcinogenesis. NF-κB is a dimeric complex formed by members of the Rel protein family comprised of c-Rel (Rel), RelA (p65), RelB, p50 (NF-κB1), and p52 (NF-κB2) [331]. NF-κB is activated by a variety of signals including proinflammatory cytokines, lipopolysaccharides, viruses, and cellular stress. XIAP is another potent activator of NF-κB [332]. Given the interaction between XIAP and MURR1, it was postulated that MURR1 could affect NF-κB activation [310].

NF-κB dependent HIV-replication and expression of endogenous NF-κB regulated genes in T-cells and *HEK293* cells is inhibited by *MURR1* overexpression [310,333]. In the classic NF-κB pathway, NF-κB complexes are retained in the cytoplasm by binding to inhibitor of κB (IκB) proteins. Activation of the NF-κB pathway by external signals leads to IκB phosphorylation by IκB kinases (IKK), which targets IκB proteins for ubiquitination by the Skp1-Cul1-β-TrCP1 complex and degradation by the 26S proteosome, releasing NF-κB [331]. MURR1 inhibition of the NF-κB pathway was determined to occur downstream of IκB phosphorylation and an interaction between tagged-MURR1 and endogenous NF-κB and IκB-α was detected by immunoprecipitation, suggesting tertiary complex association [310]. An interaction between MURR1 and Cul1 was also identified and the investig[illegible]rs conclude that MURR1 may block NF-κB activation by interacting with the ubiquitin ligase complex and inhibiting degradation of IκB-α. Further analysis of NF-κB inhibition by MURR1 revealed that NF-κB translocation to the nucleus is unaffected [306]. This is not unexpected, as IκB-α is only able to mask one nuclear localization signal in the NF-κB dimer [334], but also suggests additional mechanisms of inhibition by MURR1. MURR1 is observed both in the cytosolic and nuclear fractions of *HEK293* cells [306]. Chromatin immunoprecipitation (ChIP) showed MURR1 recruitment to a κB responsive promoter upon NF-κB activation, limiting the association of NF-κB with chromatin.

All other COMMD proteins are also able to inhibit NF-κB activated transcription in a κB-responsive reporter assay, although COMMD3 and COMMD8 do so only weakly [306]. The other COMMD family members are also able to precipitate NF-κB complexes, with different affinities for the various NF-κB subunits. Some COMMD proteins associate broadly with NF-κB subunits, others favor RelB- and p150-containing complexes, while some preferentially interact with RelA-containing complexes [306]. MURR1 is the only COMMD family member able to precipitate c-Rel, which coincidently maps to the same chromosomal region as MURR1, and MURR1 is also the only COMMD protein known to interact with IκB. Given the varying levels of expression of COMMD proteins in different tissues and the differential patterns of precipitated NF-κB complexes, this family of proteins may provide a novel mechanism able to regulate the NF-κB pathway in a cell specific manner.

e. MURR1 and Vesicular Trafficking

The methods and results presented in this chapter were necessary steps to carry out future studies on the characterization of MURR1 and its proposed function in the copper transport pathway, specifically its effect on ATP7B copper-induced vesicular trafficking. The proposed studies involve overexpression and knockdown of MURR1 in a human liver cell line that expresses both ATP7B and MURR1, such as *HepG2*. Several cell lines have been used for mammalian studies of copper transport, including *HepG2* [80,335], but copper toxicity levels in this cell line for experimental use have not been reported. *CHO* cells have been used extensively for copper analysis because they do not express endogenous *ATP7B* and are sensitive to copper. However, transfecting *CHO* cells with *ATP7B* can increase cell survival [317]. Choosing *CHO* as a control, copper toxicity levels were determined for *HepG2*. Consistent with previous studies [71,317], *CHO* could not tolerate very high levels of copper, with less than 20% survival at 150 to 200 μM copper. In *HepG2*, 100 μM copper sulfate has been reported to be a pathological concentration of copper [336]. This concentration is two-fold physiologic copper concentrations and induces a chronic copper stress response mimicking hepatocytes at the early stages of WD [336]. Although, this concentration may cause internal change within the cell, such as up-regulation of oxidative-stress response genes, significant cell death was not detectable up until 600 μM copper (Fig 7-3). Additionally, this apparent contradiction may be related to the copper solution being applied since in our experiments we used copper chloride and not copper sulfate. It remains to be seen whether overexpression of MURR1 can increase this resistance to copper or if knockdown of MURR1 expression by RNAi can lead to copper sensitivity, in this cell line.

As a control for the MURR1-RNAi induced copper sensitivity, I propose to use siRNAs targeted toward ATP7B, a proven copper transporter [71]. By the same method that transfecting *CHO* cells with *ATP7B* increases copper resistance of the cell, knockdown of ATP7B in *HepG2* should lead to copper sensitivity. Copper resistance and sensitivity would be determined as a measure of cell survival in increasing concentrations of copper. This experimental approach has been successfully demonstrated by Radyuk et al. [337], who used overexpression and RNAi for two thioredoxin peroxidases to test cell survival in H_2O_2, paraquat, cadmium, and copper-induced oxidizing conditions.

To confirm overexpression and knockdown of MURR1 at the protein level, we first had to purify MURR1 and produce an antibody against it. Endogenous human MURR1 protein, predicted to be 21 kDa, has an apparent molecular weight of 23 kDa on a 12-12.5 % SDS-polyacrylamide gel (Fig 7-2) [316]. Recombinant protein was detected at 27 kDa (Fig 7-1). High recombinant protein levels were achieved by inducing protein expression in BL21(DE3) cells transformed with pET-28b+MURR1 (Fig 7-1A). However, this led to protein aggregation and formation of insoluble protein pellets. This is common in expression systems and was also not unexpected, since MURR1 has been shown to interact with itself [306].

What was unexpected was the co-purification of a bacterial FKBP-type protein under non-denaturing conditions. FKBP immunophilins, FK506-binding proteins, belong to a large family of peptidyl-prolyl *cis-trans* isomerases (PPIases), known to be involved in cell signaling, protein trafficking, and transcription [338]. One of the large molecular weight FKBPs, FKBP52, is inducible by heat and chemical stress [339], and can function as a molecular chaperone *in vitro* suppressing protein aggregation [340]. Although the possibility exists that the putative association with the bacterial FKBP-type protein, observed during purification of recombinant-MURR1, was in the capacity of a folding-chaperone to prevent aggregation, the co-purification was observed under conditions of low expression, where the inducible band was not even visible after Coomassie brilliant blue staining (not shown). Support for the concept that this interaction is not an artifact is a recent paper identifying a novel role for FKBP52 in copper transport [341]. Overexpression of FKBP52 in *HEK293* cells was shown to increase copper efflux and in the presence of copper, FKBP52 was shown to interact with ATOX1 [341], a metallochaperone that interacts with and delivers copper to ATP7B in the secretory pathway [51,52,57]. FKBP52 localizes to microtubules and also interacts with the dynein-associated dynactin complex, responsible for the movement of vesicles along microtubules [342-344]. Recently, an interaction between ATP7B and the dynactin p62-subunit has also been demonstrated [345]. Immunophilins, such as FKBP52, appear to be involved in cargo recognition, either directly or through additional protein interactions, linking proteins to the dynein-dynactin complex for cellular trafficking [343,346]. Based on the potential circle of interactions between FKBP52, ATOX1, ATP7B, dynactin, and MURR1, the putative interaction between MURR1 and an FKBP-type protein should be investigated further.

CHAPTER 8 : General Discussion and Conclusions

I. THE JACKSON TOXIC MILK MOUSE

The toxic milk mouse is a WD model with a mutation in *Atp7b*. The Jackson toxic milk mouse (*tx*^{J}) is the third naturally occurring animal model of WD. Currently this animal model is the most accessible virus-free toxic milk strain available being used in studies of neurological and metabolic diseases where copper accumulation plays an active role in pathology. Since its appearance in the animal resources colony at the Jackson Laboratory in Bar Harbor, Maine in 1987, the mutation has been maintained on a C3HeB/FeJ background, but the mutation had not been identified.

I. THE JACKSON TX MOUSE MUTATION

The *tx*^{J} mouse mutation arose independently and was shown to be allelic to the original *tx* mouse mutation [259]. I cloned and sequenced the *tx*^{J} mouse *Atp7b* cDNA and identified a guanine to adenine sequence variation in exon 8 [chapter 2]. This causes an aspartic acid residue to substitute for glycine712 in the second putative transmembrane domain, which is highly conserved across species. This sequence change was concluded to be the causative mutation in the *tx*^{J} mouse based on the species conservation and the nature of the substitution. Glycine is a small aliphatic amino acid, while aspartate is an acidic negatively charged residue. In a transmembrane domain, which contributes to channel formation, such a substitution would be expected to alter both structure and function. This hypothesis is supported by *SIFT* (Sorting Intolerant From Tolerant) [302] analysis, which gives a Gly712Asp substitution in Atp7b a score of 0.03. *SIFT* presumes that important amino acids are conserved in a protein family and uses homology between species to predict whether a given substitution will affect protein function. A substitution with a *SIFT* score less than 0.05 is predicted to be deleterious to protein function.

By characterizing the *Atp7b* mutation responsible for copper storage in the tx^J mouse, I have identified a fundamentally important region of the Atp7b protein. Gly712 in mouse Atp7b corresponds to Gly710 in human ATP7B. The specific tx^J mutation has not been observed in humans, but different mutations of Gly710 have been described. In addition to the three human mutations described in chapter 2 (Gly710Ala/Ser/Arg), a fourth Gly710 mutation was identified in our laboratory leading to substitution of glycine by valine [347]. This particular change is not as dramatic as the tx^J mouse substitution and receives a *SIFT* score of 0.21. This is not predicted to be deleterious to ATP7B function, but this change was not observed in 79 control chromosomes. Functional studies in yeast are currently underway for this patient variant, to assess its disease causing potential.

II. THE JACKSON TX MOUSE AS A MODEL OF COPPER STORAGE

Identification of the mutation in the tx^J mouse has been essential to the use of this animal model in recent studies of neurological diseases, such as Alzheimer disease, in which copper accumulation plays an active role in pathology [252]. Phinney et al. [348] observed reduced numbers of amyloid plaques and amyloid-β (Aβ) peptide plasma levels in mice transgenic for the tx^J mutation and an amyloid precursor protein variant (APP$_{695}$) that results in robust Aβ-deposition. Alone, the APP$_{695}$ transgene is associated with postnatal lethality [349], however in combination with tx^J homozygosity, survival of young animals increased, suggesting that the tx^J mutation, in association with increased intracellular copper, may have a protective effect in the brain. This finding has recently been supported by a second study, which concludes that bioavailable copper is beneficial in Alzheimer model mice [350].

As an animal model of copper storage, the tx^J mutant mouse has also been used to study the effects of copper accumulation on the modification and degradation of XIAP [330], the X-linked inhibitor of apoptosis [304]. Immunoblot analysis of tx^J tissues shows decreased XIAP levels in liver, but not brain. The authors conclude that these changes are the direct result of copper accumulation, given that a mutation in the murine *Atp7b* results in massive copper accumulation in the liver with only limited changes in brain copper levels. Although these results were confirmed in other species, this comment on murine *Atp7b* mutants is a generalization and not specific to the tx^J mutant. The authors used tx^J mutant tissues in their study, but refer to the *Atp7b* null mutant when generalizing about brain copper levels. Copper levels in the brain of *Atp7b* null mice are said to increase slightly, but specific values are not given [206]. In the original *tx* mouse, copper levels are significantly higher in different areas of the brain compared with controls [197,199,351]. Similarly, by six months of age, copper levels in the tx^J mutant brain are 3-fold higher than in isogenic controls [348]. Although these changes are minimal when compared with copper levels in the tx^J mutant liver (over 50-fold higher than controls), the authors may not have considered that levels of residual Atp7b function are mutation dependent and may be modified by differences in genetic backgrounds existing between these mutants.

III. FUTURE DIRECTIONS

Functional analyses of the original *tx* mutant Atp7b, have shown it to be defective in copper-translocating activity [71] and copper-induced trafficking [317]. These studies have yet to be done with the tx^J mutant Atp7b protein to see how much residual activity is retained. Functional analysis of this mutant and human substitutions at the corresponding amino acid would provide information on the essentiality of glycine in this position of the protein.

WD is a highly variable disease and modifiers have been suggested to account for the observed phenotypic variability. However, human modifier studies require a large number of patients with the same mutation in order to reach significance. In a mouse model, mutations can be easily transferred to defined genetic backgrounds in order to explore the effect of modifier genes [205]. There are several examples where mouse modifier genes have led to the identification of modifier genes in humans [352].

Providing information on the pathogenesis and treatment of WD remains of major importance for animal models. Recent studies in the *tx* mouse have tested the potential of tetrathiomolybdate, bone marrow stem cell transplantation, and embryonic hepatocyte intrasplenic transplantation to correct liver dysfunction and reduce copper accumulation [353-356]. Just as phenotypes vary in WD, so do patient responses to treatment. WD treatment studies have not yet been tested on the tx^J mouse, but again the potential exists to compare treatment responses with those in the original *tx* mouse and to transfer these mutations onto different backgrounds to identify possible modifiers involved in modulating treatment responses.

II. COPPER TOXICOSIS: THE ROLE OF *MURR1*

Copper toxicosis (CT) is an autosomal recessive disorder of copper storage observed at high frequency in Bedlington terriers. The Bedlington terrier originated in Northern

England and is one of the oldest terrier breeds. The specific breeds involved in the development of the Bedlington terrier are unknown. Based on feature similarities, the Bedlington terrier is believed to have been bred from a combination of local terriers, such as the Dandie Dinmont and Kerry Blue, with an outcross to Whippets. The first dog to be called a Bedlington terrier was Piper, whelped in 1825 by Joseph Ainsley who lived in the town of Bedlington in Northumberland County.

I. IDENTIFICATION OF THE CT GENE

ATP6H encodes a vacuolar-ATPase subunit and was suggested as a candidate for CT because it mapped to a human chromosomal region showing conserved synteny with the CT locus in the dog [250] and yeast defective in vacuolar-ATPase display abnormal metal homeostasis [269]. We cloned and sequenced the canine *ATP6H* cDNA to assess its role in CT in the Bedlington terrier [chapter 3]. Our analysis did not identify any sequence differences between affected and unaffected dogs from a North American pedigree and we excluded *ATP6H* as the causative gene of CT. Further analysis of the CT locus led to the exclusion of other known genes in the candidate region and expressed sequence tags, and the identification of an exon 2 deletion in the *MURR1* gene of most affected dogs [chapter 4, [251]].

From these studies, breeders hoped to obtain a reliable molecular test for the diagnosis of CT and identification of CT-carriers. The deletion in the Bedlington terrier removes exon 2 completely [chapter 4, [251]]. Southern blot analysis of the deletion is time consuming and requires the use of radioisotopes and large amounts of DNA. MURR1 protein is undetectable in the liver of affected dogs homozygous for the deletion [316]. However, protein analysis is not feasible because it requires tissue samples for protein extraction and Western analysis. Homozygotes can easily identified by polymerase chain reaction (PCR) analysis, which is negative for exon 2, but distinguishing heterozygotes is not as straight forward using this process. Dogs heterozygous for the deletion can be determined by cDNA analysis because they produce both the full length and truncated transcripts [251], but cDNA analysis is also not feasible due to the instability of RNA. Two other methods have been optimized to detect dogs heterozygous for the deletion: quantitative-PCR (Q-PCR) and multiplex-PCR. Both of these methods use DNA as the starting material and only small amounts are required. Q-PCR analysis of the *MURR1* deletion detects the number of copies of exon 2 present in a DNA sample compared to a two-copy control gene and an internal *MURR1* control [357]. Multiplex-PCR analysis required the identification of the deletion breakpoints and involves PCR amplification across the deletion multiplexed with PCR amplification of fragments inside and outside the deletion [358]. However, although the deletion has been characterized and molecular tests for this deletion are now available, our group and others have identified copper accumulation in dogs without the homozygous deletion casting doubt as to the causative nature of *MURR1* in CT [chapter 4, [296]]. This suggests that the ultimate test for CT diagnosis is still unavailable and a negative result for a *MURR1* deletion should not be interpreted as a clear status.

II. NOT ALL DOGS ARE CREATED EQUAL

The Bedlington terrier is a highly pure inbred dog. As a result of decades of inbreeding, it was assumed that all CT affected Bedlington terriers would be homozygous for the identical recessive mutation inherited from a common ancestor. However, I discovered that not all affected dogs in our cohort (consisting of North American and Finnish pedigrees) carried the *MURR1* homozygous deletion previously identified in C04107 2-2 dogs [chapter 4]. Sequence analysis of all exons and exon-intron boundaries of *MURR1* did not identify any *de novo* mutations, but did identify a novel splice site polymorphism. The splice site polymorphism does not appear to alter mRNA processing and did not correlate with disease status. Due to their large size, the introns of *MURR1* could not be fully sequenced, but marker analysis was undertaken to identify possible regions of homozygosity in the gene. Haplotype analysis, using two previously identified microsatellites [248,281] and a newly identified splice site polymorphism [chapter 4], did not identify any regions of shared homozygosity between all affected dogs, but did indicate that the Bedlington breed is not as homogeneous as originally predicted. Pedigree analysis reveals the existence of five haplotypes of the *MURR1* gene [chapter 4 and 5, [296,359]].

These results led us to the hypothesis that in some Bedlington terriers, CT may result from *MURR1* haploinsufficiency in combination with a modifier gene or from an independent gene defect. Confirmation of our results has also come from haplotype studies in an Australian Bedlington terrier pedigree [296]. We looked at the possibility that *ATP7B* was modifying the expression of the disease in Bedlington terriers and conducted sequence analysis to identify polymorphisms that may contribute to CT in Bedlington terriers lacking the homozygous *MURR1* deletion [chapter 5]. Although we identified several polymorphisms in *ATP7B*, they were observed in all Bedlington terriers analyzed and did not specifically segregate with the disease. We did, however, identify a specific polymorphism (Arg1399Gln) in Bedlington terriers that was not observed in the boxer, Doberman pinscher, or Maltese, that may contribute to the breed's susceptibility to copper accumulation.

In general, dogs have a disadvantage when it comes to copper homeostasis. Dogs have approximately 10-fold higher hepatic copper concentrations than humans [244]. Copper homeostasis in dogs is different than in humans. Canine albumin lacks histidine in its copper-binding domain, which lessens its affinity for copper [360]. As a result, dog plasma shows a decreased retention of copper. This could lead to more rapid passage of copper to the liver and may explain the substantial levels of MT observed in livers of normal dogs [94]. Dog food also contains high levels of copper. An average 10 kg dog ingests about 5 mg of copper per day and absorbs around 1 mg per day [244]. In comparison, an average human adult, that ingests about 2 mg of copper per day, absorbs approximately 0.6 to 1.6 mg per day. Bedlington terriers appear to have an extra disadvantage with respect to copper metabolism and as a result exhibit a high frequency of CT. We hypothesize that this breed susceptibility is due to a 3' polymorphism identified in ATP7B of the Bedlington terrier [chapter 5].

III. HUMAN MURR1 ANALYSIS

With concerns regarding the precise role of *MURR1* in CT, we looked for evidence of MURR1 involvement in copper storage disease in humans. The human *MURR1* gene is located on chromosome 2 and spans over 200 kb with an open reading frame of 573 bp. It consists of three exons and the promoter has not been identified. The predicted human protein shares 87% identity with canine MURR1, including conservation of the predicted phosphorylation and N-myristoylation sites [251]. I sequenced the coding region and splice junctions of *MURR1* in 26 patients with copper storage not specifically identified as WD by mutational analysis of *ATP7B* [chapter 6]. A subset of two patients was selected for haplotype analysis at the *MURR1* locus in affected sibs to compare *MURR1* non-coding and surrounding sequence. No disease causing mutations were identified and haplotype analysis also failed to establish segregation between non-Wilsonian copper toxicosis and a mutation in *MURR1* in selected patients. A similar study did not identify any mutations in *MURR1* upon sequence analysis of 12 patients with ICC, one patient with ETIC, and 10 patients with ICT [223]. A third study, trying to assess the contribution of *MURR1* in human copper toxicosis, specifically focused on WD patients with ceruloplasmin levels in the normal range, which is more comparable to CT in the Bedlington terrier [361]. Patients were excluded if two mutations in *ATP7B* had already been identified. No phenotype-genotype correlation could be found, but the sample size was small (n=14) and a larger scale study was proposed.

A recent study has suggested that a *MURR1* sequence variation is associated with early onset of WD [307]. However, a subsequent study in 218 Chinese patients was unable to find any correlation between polymorphisms in *MURR1* and WD [313]. Seven polymorphisms have been identified in *MURR1* [307,313]. Of these, only one is found in the coding region (c.501T>C), resulting in a synonymous change for Asp164 [chapter 6, not Asn164 as published by [307] or propagated by [313,361]]. In the first modifier study, the average age of onset for neurological symptoms in five patients heterozygous for this polymorphism was 17 years compared with about 30 years for 14 patients homozygous T-T [307]. In five patients homozygous for the His1069Gln mutation in *ATP7B*, this earlier presentation of *MURR1* heterozygotes was even more pronounced: 13

years earlier onset of neurologic symptoms (three patients) and eight years earlier hepatic presentation (two patients). Although statistical significance was reached ($P<0.05$) in all three examples, the sample sizes were small and larger scale studies are required. This polymorphism has not been observed in Chinese patients [313], which may explain the inability of the second modifier study to reproduce these results.

Taken together, these studies suggest that *MURR1* does not play a major role in human copper toxicosis. Perhaps MURR1 in humans is too essential for survival, precluding the observance of *MURR1* mutations in humans. Alternatively, MURR1 in humans may have a different functional role than in the dog or share redundant functions with other proteins, such as its COMMD family members.

IV. MAKING SENSE OF MURR1

An important goal is discover the precise function of MURR1 in the cell. For our laboratory, our goal is to discover further supporting evidence of the involvement of MURR1 in copper homeostasis, both for humans and the Bedlington terrier, which still presents a problem with respect to CT inheritance.

MURR1 has been proposed as the causative gene in CT and shown to interact with ATP7B, implicating it in copper homeostasis. In addition, MURR1 has also been shown to interact with IκB, NF-κB, ENaC, and XIAP. By virtue of its interactions, MURR1 has been implicated in many seemingly distinct pathways. In addition to these multiple pathways being connected through MURR1 interactions, connections at other points in these pathways have also been made (Fig 8-1). The copper connection to MURR1 was

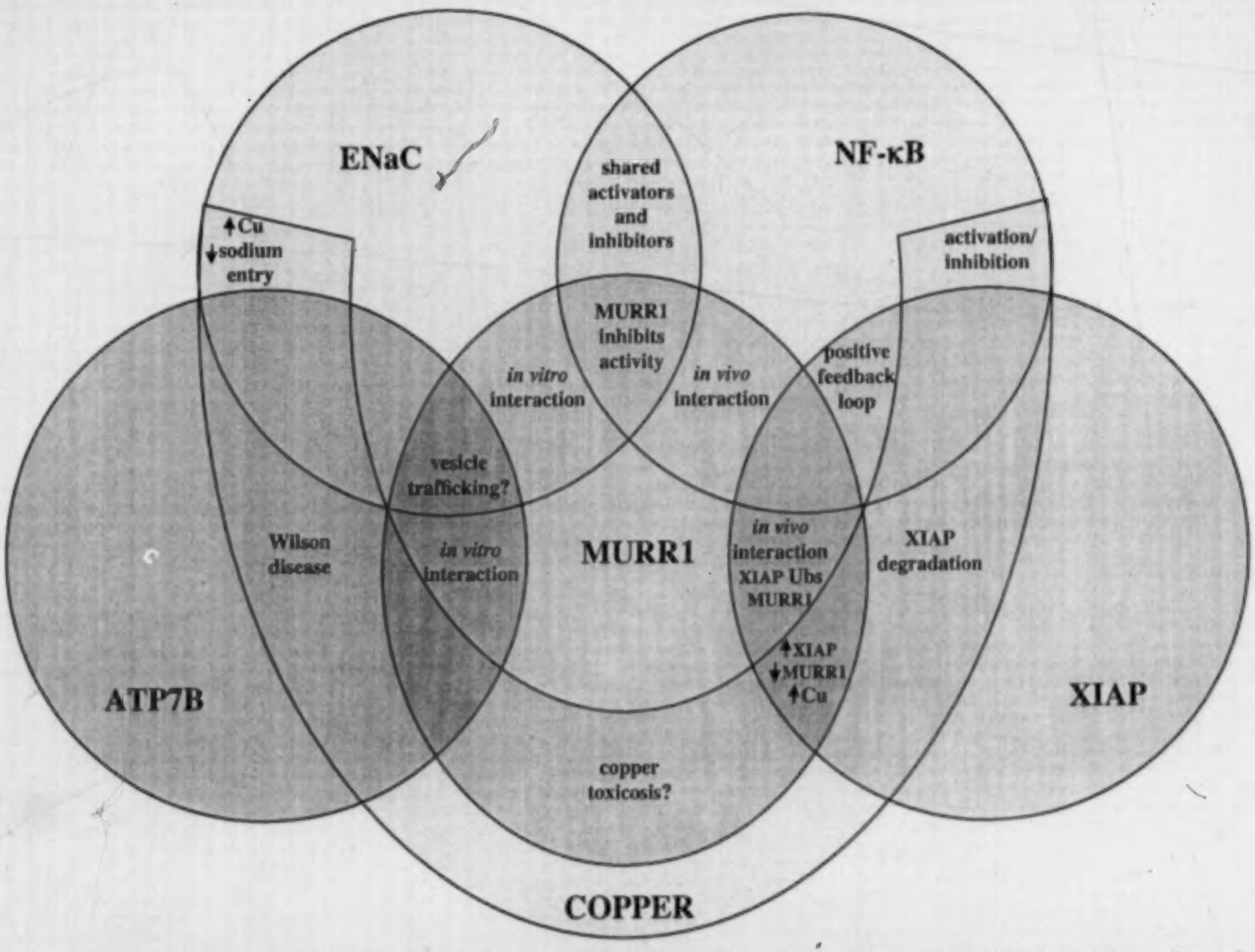
ENaC
shared activators and inhibitors
NF-κB
↑Cu ↓sodium entry
activation/ inhibition
MURR1 inhibits activity
in vitro interaction
in vivo interaction
positive feedback loop
vesicle trafficking?
Wilson disease
in vitro interaction
MURR1
in vivo interaction XIAP Ubs MURR1
XIAP degradation
↑XIAP ↓MURR1 ↑Cu
ATP7B
XIAP
copper toxicosis?
COPPER

Figure 8-1. Diagram of interactions with MURR1 and overlapping pathways. Epithelial sodium channel (ENaC), nuclear factor-κB (NF-κB), x-linked inhibitor of apoptosis (XIAP), copper (Cu), ubiquitinates (Ubs).

first made by the identification of homozygous MURR1 deletions in Bedlington terriers affected by CT [chapter 4, [251]]. This was further supported by an interaction with ATP7B [297], a known copper transporter defective in the phenotypically similar WD, although this interaction has yet to be confirmed *in vivo*. A connection between copper efflux and sodium uptake has been demonstrated in fish gills, frog skin, and vertebrate epithelia from the intestine and kidney [reviewed in [362]]. In general, addition of copper slows sodium entry into mucosal cells, while removal of sodium slows copper entry. A relationship between ENaC activity and NF-κB also exists. Several activators of ENaC appear to up-regulate NF-κB and down-regulators of ENaC activity can also inhibit NF-κB, such activators include the cystic fibrosis transmembrane-conductance regulator (CFTR), IKKβ, and tumour necrosis factor (TNF)-α, as well as MURR1 [363,364]. Copper and NF-κB also appear to have a relationship in which copper can either inhibit or activate NF-κB signaling depending upon the levels and oxidative state of copper and the cell type under investigation [365,366]. XIAP is also linked to NF-κB through a positive feedback loop in which NF-κB-dependent transcription of XIAP leads to augmentation of NF-κB activity [332]. Copper binding to XIAP results in a conformational change, which shortens the half-life of XIAP [330]. Similarly, XIAP ubiquitinates MURR1 leading to its degradation and an increase in copper levels [305].

MURR1 is a highly conserved gene that appears to be restricted to vertebrate species. The significance of this has yet to be determined, but may reflect the ability of vertebrates to produce bile. This would be consistent with its proposed role in copper excretion and ATP7B vesicular trafficking. However, it has yet to be firmly established whether or not MURR1 is the initial defect that leads to copper accumulation in Bedlington terriers.

Alternatively, MURR1 may play a role in copper sensing and controlling various cellular events in response to copper excess. Although, MURR1 is ubiquitously expressed, one can speculate that the phenotype of CT is restricted to the liver because the liver is the major site of copper excretion. Copper accumulation is known to produce reactive oxygen species, which are known to activate NF-κB [367]. Deregulation of NF-κB due to a lack of inhibition, as a result of a recessive deletion in *MURR1*, could result in the observed liver pathology of CT. Copper loading in rats has been shown to induce early histological changes in the liver and increase NF-κB DNA binding [366]. NF-κB can subsequently induce expression of TNF-α [367], a key cytokine involved in inflammation, proliferation, and cell death signaling [368]. In the LEC rat, TNF-α expression is increased in the liver and increased apoptosis correlates with TNF-α expression, suggesting that TNF-α plays a major role in the pathogenesis of liver disease [369]. Under excess copper conditions, the anti-apoptotic effect of XIAP would not be realized due to copper binding, which shortens the half-life of XIAP and decreases its ability to inhibit caspase-3 [330]. No defect in sodium homeostasis has been reported in affected Bedlington terriers, although sodium uptake may play a role in hepatic swelling due to a lack of ENaC inhibition by virtue of the absence of MURR1.

V. FUTURE DIRECTIONS

The Arg1399Gln polymorphism identified in the carboxy-terminus of ATP7B of the Bedlington terrier [chapter 5] is predicted to alter the function of the protein. Arginine in this position is conserved across species, and a glutamine substitution causes a positively charged basic residue to be replaced by an uncharged polar amino acid. A *SIFT* score of 0.02 also predicts that this variant has a high probability of being deleterious [302].

Functional studies testing the ability of this variant to transport copper in a yeast complementation assay are currently underway in the laboratory. Future studies could also analyze the ability of the variant to traffick under high-copper conditions.

Future studies are also necessary to identify additional genes and/or modifying factors of CT in the Bedlington terrier, which may account for affected non-*MURR1*-deletion dogs. Currently, two parallel studies are under way using whole genome scan to identify possible loci associated with copper accumulation in the Bedlington terrier, one of which is being conducted by our laboratory. Availability of canine sequence and SNP chip analysis has made such studies possible [370]. In addition, we are continuing to analyze candidate modifiers, including XIAP. XIAP has been implicated in the copper pathway due to its apparent ability to control MURR1 degradation and subsequently alter copper concentrations in the cell [305]. Apoptosis has also been suggested to play a role in the pathogenesis of CT in the Bedlington terrier [240]. A protective XIAP allele may inhibit apoptosis to a higher degree and may explain why some of our affected dogs accumulate copper but do not exhibit any histological changes characteristic of CT. Alternatively, a XIAP polymorphism leading to enhanced degradation of MURR1 may create a phenocopy of CT in dogs with no MURR1 deletion. Further studies identifying factors influencing CT in the Bedlington terrier may lead to the subsequent identification of genes modifying WD or candidate genes for ICT.

MURR1 is a relatively newly discovered gene and many questions about its function and regulation remain to be answered. Regulation of *MURR1* at the transcriptional level has not been adequately investigated, and the *MURR1* promoter remains to be identified. In

Hela, *A549*, *H441*, and *Caco2* cells cultured in 0, 100, or 150 μM copper, MURR1 levels remain constant [316], arguing against copper-induced transcription or translation of *MURR1*. Other cell lines from tissues more intimately involved in copper excretion, including kidney and liver, have yet to be investigated. Copper regulation of MURR1 degradation may be provided *via* XIAP, which appears to target MURR1 for proteosomal degradation [305]. XIAP is post-translationally modified by copper [330], providing a mechanism of copper-regulated MURR1 degradation. However, although copper binding to XIAP accelerates its degradation and decreases its ability to inhibit caspase-3, MURR1 does not appear to be significantly or consistently increased in the tissues analyzed [330]. Further investigations are required to resolve this issue.

Function is closely associated with protein structure. Other than the COMMD domain, analysis of primary protein structure reveals no other known functional domains in MURR1. Secondary structure analysis predicts that MURR1 folds in a cytokine-folding pattern, consisting of four amphipathic α-helical regions [371]. This folding pattern may be associated with the function of MURR1 in the NF-κB signaling pathway, which can be activated by several cytokines [331]. A three-dimensional structural analysis of MURR1 is lacking and could identify other structural components essential for its function.

The exact function of MURR1 in each of its implicated pathways remains to be fully elucidated. Given our interest in copper metabolism, we have begun to address one particular question: is MURR1 required for proper ATP7B trafficking? To this end, we have designed an RNA interference (RNAi) experiment targeted against MURR1 to analyze copper-induced ATP7B trafficking in polarized *HepG2* cells [chapter 7]. Although still in the preliminary stages, this study should yield functionally relevant information as to the role of MURR1 in vesicular trafficking and copper accumulation. Initial results, suggesting a possible interaction between MURR1 and an FKBP-type protein [chapter 7], support a role for MURR1 in vesicular trafficking. FKPB proteins appear to be involved in cargo recognition, linking proteins to the dynein-dynactin complex for cellular trafficking [343,346]. A large FKBP protein, FKBP52, has recently been shown to influence copper efflux and interact with ATOX1 [341], an ATP7B-interacting copper chaperone, and ATP7B has been shown to interact with a dynactin subunit [345]. The putative interaction between MURR1 and an FKBP-type protein should be investigated further. Endogenous confirmation of the MURR1 interaction with ATP7B, as well as with ENaC subunits, is also still lacking. These interactions have been demonstrated in systems of co-transfection and overexpression, and endogenous cell lysates on GST-MURR1 columns. However, the consequences of these interactions *in vivo* remain to be elucidated.

In addition to cellular RNAi knockdown, MURR1 knockout organisms could be useful to dissect the function of MURR1. Currently a mouse knockout model is being developed [372], however the mouse presents unique problems: an imprinted gene within the *MURR1* intron [282], an antisense transcript transcribed from portions of *MURR1* [321], and imprinting of the *MURR1* locus in the adult mouse [320].

IV. CONCLUDING REMARKS

This thesis underscores the importance of animal models in studying human disease, and particularly their importance in the study of copper transport. Animal models are easily manipulated, can be created on defined genetic backgrounds, and can produce significant sample sizes. The *tx^J* mouse has already proven useful in several studies and will continue to be a useful model of copper storage. While my research has identified a correlation between CT and *MURR1* deletions in specific dogs, it also makes one question whether *MURR1* is the sole contributor to the disorder, indicating that there is still an unidentified gene(s) involved in the copper transport pathway in the Bedlington terrier. Identification of human orthologues of this gene(s) brings the continued promise of a deeper understanding of copper homeostasis and identification of the causes of copper storage disorders of undefined etiology.

REFERENCES

1. CRICHTON, R.R. and PIERRE, J.L. (2001) Old iron, young copper: from Mars to Venus. *Biometals* **14**: 99-112

2. HALLIWELL, B. and GUTTERIDGE, J.M. (1984) Oxygen toxicity, oxygen radicals, transition metals and disease. *Biochem J* **219**: 1-14

3. HART, E.B., STEENBOCK, H., WADELL, J. and ELVEHJEM, C.A. (1928) Iron Nutrition VII. Copper is a supplement to iron for hemoglobin building in the rat. *J Biol Chem* **77**: 797-812

4. UAUY, R., OLIVARES, M. and GONZALEZ, M. (1998) Essentiality of copper in humans. *Am J Clin Nutr* **67**: 952S-959S

5. TAPIERO, H., TOWNSEND, D.M. and TEW, K.D. (2003) Trace elements in human physiology and pathology. Copper. *Biomed Pharmacother* **57**: 386-398

6. HALLIWELL, B. and GUTTERIDGE, J.M. (1990) Role of free radicals and catalytic metal ions in human disease: an overview. *Methods Enzymol* **186**: 1-85

7. PREDKI, P.F. and SARKAR, B. (1992) Effect of replacement of "zinc finger" zinc on estrogen receptor DNA interactions. *J Biol Chem* **267**: 5842-5846

8. LINDER, M.C. and HAZEGH-AZAM, M. (1996) Copper biochemistry and molecular biology. *Am J Clin Nutr* **63**: 797S-811S

9. TURNLUND, J.R. (1998) Human whole-body copper metabolism. *Am J Clin Nutr* **67**: 960S-964S

10. LINDER, M.C. (1991) *The Biochemistry of Copper*. New York: Plenum.

11. WELSH, M.J. and SMITH, A.E. (1993) Molecular mechanisms of CFTR chloride channel dysfunction in cystic fibrosis. *Cell* **73**: 1251-1254

12. SARKAR, B. and WIGFIELD, Y. (1968) Evidence for albumin-Cu(II)-amino acid ternary complex. *Can J Biochem* **46**: 601-607

13. LAU, S.J. and SARKAR, B. (1971) Ternary coordination complex between human serum albumin, copper (II), and L-histidine. *J Biol Chem* **246**: 5938-5943

14. LINDER, M.C., WOOTEN, L., CERVEZA, P., COTTON, S., SHULZE, R. and LOMELI, N. (1998) Copper transport. *Am J Clin Nutr* **67**: 965S-971S

15. ZHOU, B. and GITSCHIER, J. (1997) hCTR1: a human gene for copper uptake identified by complementation in yeast. *Proc Natl Acad Sci USA* **94**: 7481-7486

16. LEE, J., PENA, M.M., NOSE, Y. and THIELE, D.J. (2002) Biochemical characterization of the human copper transporter Ctrl. *J Biol Chem* **277**: 4380-4387

17. KUO, Y.M., ZHOU, B., COSCO, D. and GITSCHIER, J. (2001) The copper transporter CTR1 provides an essential function in mammalian embryonic development. *Proc Natl Acad Sci USA* **98**: 6836-6841

18. BAUERLY, K.A., KELLEHER, S.L. and LONNERDAL, B. (2004) Functional and molecular responses of suckling rat pups and human intestinal Caco-2 cells to copper treatment. *J Nutr Biochem* **15**: 155-162

19. PETRIS, M.J., SMITH, K., LEE, J. and THIELE, D.J. (2003) Copper-stimulated endocytosis and degradation of the human copper transporter, hCtr1. *J Biol Chem* **278**: 9639-9646

20. ALLER, S.G. and UNGER, V.M. (2006) Projection structure of the human copper transporter CTR1 at 6-Å resolution reveals a compact trimer with a novel channel-like architecture. *Proc Natl Acad Sci USA* **103**: 3627-3632

21. KLOMP, A.E., JUIJN, J.A., VAN DER GUN, L.T., VAN DEN BERG, I.E., BERGER, R. and KLOMP, L.W. (2003) The N-terminus of the human copper transporter 1 (hCTR1) is localized extracellularly, and interacts with itself. *Biochem J* **370**: 881-889

22. GUNSHIN, H., MACKENZIE, B., BERGER, U.V., et al. (1997) Cloning and characterization of a mammalian proton-coupled metal-ion transporter. *Nature* **388**: 482-488

23. TANDY, S., WILLIAMS, M., LEGGETT, A., et al. (2000) Nramp2 expression is associated with pH-dependent iron uptake across the apical membrane of human intestinal Caco-2 cells. *J Biol Chem* **275**: 1023-1029

24. ARREDONDO, M., MUNOZ, P., MURA, C.V. and NUNEZ, M.T. (2001) HFE inhibits apical iron uptake by intestinal epithelial (Caco-2) cells. *FASEB J* **15**: 1276-1278

25. ARREDONDO, M., MUNOZ, P., MURA, C.V. and NUNEZ, M.T. (2003) DMT1, a physiologically relevant apical Cu1+ transporter of intestinal cells. *Am J Physiol Cell Physiol* **284**: C1525-C1530

26. LINDER, M.C., ZEROUNIAN, N.R., MORIYA, M. and MALPE, R. (2003) Iron and copper homeostasis and intestinal absorption using the Caco2 cell model. *Biometals* **16**: 145-160

27. RAE, T.D., SCHMIDT, P.J., PUFAHL, R.A., CULOTTA, V.C. and O'HALLORAN, T.V. (1999) Undetectable intracellular free copper: the requirement of a copper chaperone for superoxide dismutase. *Science* **284**: 805-808

28. HUFFMAN, D.L. and O'HALLORAN, T.V. (2000) Energetics of copper trafficking between the Atx1 metallochaperone and the intracellular copper transporter, Ccc2. *J Biol Chem* **275**: 18611-18614

29. HARRISON, M.D., JONES, C.E. and DAMERON, C.T. (1999) Copper chaperones: function, structure and copper-binding properties. *J Biol Inorg Chem* **4**: 145-153

30. ARNESANO, F., BANCI, L., BERTINI, I. and BONVIN, A.M. (2004) A docking approach to the study of copper trafficking proteins; interaction between metallochaperones and soluble domains of copper ATPases. *Struct* **12**: 669-676

31. ARNESANO, F., BANCI, L., BERTINI, I., et al. (2002) Metallochaperones and metal-transporting ATPases: a comparative analysis of sequences and structures. *Genome Research* **12**: 255-271

32. ROSENZWEIG, A.C. (2002) Metallochaperones: bind and deliver. *Chem Biol* **9**: 673-677

33. FIELD, L.S., LUK, E. and CULOTTA, V.C. (2002) Copper chaperones: personal escorts for metal ions. *J Bioenerg Biomembr* **34**: 373-379

34. PROHASKA, J.R. and GYBINA, A.A. (2004) Intracellular copper transport in mammals. *J Nutr* **134**: 1003-1006

35. CULOTTA, V.C., KLOMP, L.W., STRAIN, J., CASARENO, R.L., KREMS, B. and GITLIN, J.D. (1997) The copper chaperone for superoxide dismutase. *J Biol Chem* **272**: 23469-23472

36. SCHMIDT, P.J., RAE, T.D., PUFAHL, R.A., et al. (1999) Multiple protein domains contribute to the action of the copper chaperone for superoxide dismutase. *J Biol Chem* **274**: 23719-23725

37. HARRIS, E.D. (2003) Basic and clinical aspects of copper. *Crit Rev Clin Lab Sci* **40**: 547-586

38. CARUANO-YZERMANS, A.L., BARTNIKAS, T.B. and GITLIN, J.D. (2006) Mechanisms of the copper-dependent turnover of the copper chaperone for superoxide dismutase. *J Biol Chem* **281**: 13581-13587

39. AMARAVADI, R., GLERUM, D.M. and TZAGOLOFF, A. (1997) Isolation of a cDNA encoding the human homolog of *COX17*, a yeast gene essential for mitochondrial copper recruitment. *Hum Genet* **99**: 329-333

40. SRINIVASAN, C., POSEWITZ, M.C., GEORGE, G.N. and WINGE, D.R. (1998) Characterization of the copper chaperone Cox17 of Saccharomyces cerevisiae. *Biochem* **37**: 7572-7577

41. BEERS, J., GLERUM, D.M. and TZAGOLOFF, A. (1997) Purification, characterization, and localization of yeast Cox17p, a mitochondrial copper shuttle. *J Biol Chem* **272**: 33191-33196

42. GLERUM, D.M., SHTANKO, A. and TZAGOLOFF, A. (1996) Characterization of *COX17*, a yeast gene involved in copper metabolism and assembly of cytochrome oxidase. *J Biol Chem* **271**: 14504-14509

43. CARR, H.S. and WINGE, D.R. (2003) Assembly of cytochrome c oxidase within the mitochondrion. *Acc Chem Res* **36**: 309-316

44. HORNG, Y.C., COBINE, P.A., MAXFIELD, A.B., CARR, H.S. and WINGE, D.R. (2004) Specific copper transfer from the Cox17 metallochaperone to both Sco1 and Cox11 in the assembly of yeast cytochrome C oxidase. *J Biol Chem* **279**: 35334-35340

45. HORNG, Y.C., LEARY, S.C., COBINE, P.A., et al (2005) Human Sco1 and Sco2 function as copper-binding proteins. *J Biol Chem* **280**: 34113-34122

46. COBINE, P.A., OJEDA, L.D., RIGBY, K.M. and WINGE, D.R. (2004) Yeast contain a non-proteinaceous pool of copper in the mitochondrial matrix. *J Biol Chem* **279**: 14447-14455

47. KLOMP, L.W., LIN, S.J., YUAN, D.S., KLAUSNER, R.D., CULOTTA, V.C. and GITLIN, J.D. (1997) Identification and functional expression of *HAH1*, a novel human gene involved in copper homeostasis. *J Biol Chem* **272**: 9221-9226

48. ROSENZWEIG, A.C., HUFFMAN, D.L., HOU, M.Y., WERNIMONT, A.K., PUFAHL, R.A. and O'HALLORAN, T.V. (1999) Crystal structure of the Atx1 metallochaperon protein at 1.02 A resolution. *Structure Fold Des* **7**: 605-617

49. LIN, S.J. and CULOTTA, V.C. (1995) The *ATX1* gene of *Saccharomyces cerevisiae* encodes a small metal homeostasis factor that protects cells against reactive oxygen toxicity. *Proc Natl Acad Sci USA* **92**: 3784-3788

50. PORTNOY, M.E., ROSENZWEIG, A.C., RAE, T., HUFFMAN, D.L., O'HALLORAN, T.V. and CULOTTA, V.C. (1999) Structure-function analyses of the ATX1 metallochaperone. *J Biol Chem* **274**: 15041-15045

51. HAMZA, I., SCHAEFER, M., KLOMP, L.W. and GITLIN, J.D. (1999) Interaction of the copper chaperone HAH1 with the Wilson disease protein is essential for copper homeostasis. *Proc Natl Acad Sci USA* **96**: 13363-13368

52. LARIN, D., MEKIOS, C., DAS, K., ROSS, B., YANG, A.S. and GILLIAM, T.C. (1999) Characterization of the interaction between the Wilson and Menkes disease proteins and the cytoplasmic copper chaperone, HAH1p. *J Biol Chem* **274**: 28497-28504

53. TERADA, K., NAKAKO, T., YANG, X.L., et al. (1998) Restoration of holoceruloplasmin synthesis in LEC rat after infusion of recombinant adenovirus bearing WND[illegible]A. *J Biol Chem* **273**: 1815-1820

54. PETRIS, M.J., STRAUSAK, D. and MERCER, J.F. (2000) The Menkes copper transporter is required for the activation of tyrosinase. *Hum Mol Genet* **9**: 2845-2851

55. EL MESKINI, R., CULOTTA, V.C., MAINS, R.E. and EIPPER, B.A. (2003) Supplying copper to the cuproenzyme peptidylglycine alpha-amidating monooxygenase. *J Biol Chem* **278**: 12278-12284

56. GITSCHIER, J., MOFFAT, B., REILLY, D., WOOD, W.I. and FAIRBROTHER, W.J. (1998) Solution structure of the fourth metal-binding domain from the Menkes copper-transporting ATPase. *Nat Struct Biol* **5**: 47-54

57. WERNIMONT, A.K., HUFFMAN, D.L., LAMB, A.L., O'HALLORAN, T.V. and ROSENZWEIG, A.C. (2000) Structural basis for copper transfer by the metallochaperone for the Menkes/Wilson disease proteins. *Nat Struct Biol* **7**: 766-771

58. MURATA, Y., KODAMA, H., ABE, T., et al (1997) Mutation analysis and expression of the mottled gene in the macular mouse model of Menkes disease. *Pediatr Res* **42**: 436-442

59. MERCER, J.F.B., LIVINGSTONE, J., HALL, B., et al. (1993) Isolation of a partial candidate gene for Menkes disease by positional cloning. *Nat Genet* **3**: 20-25

60. VULPE, C., LEVINSON, B., WHITNEY, S., PACKMAN, S. and GITSCHIER, J. (1993) Isolation of a candidate gene for Menkes disease and evidence that it encodes a copper-transporting ATPase [erratum in Nat Genet 3:273]. *Nat Genet* **3**: 7-13

61. BULL, P.C., THOMAS, G.R., ROMMENS, J.M., FORBES, J.R. and COX, D.W. (1993) The Wilson disease gene is a putative copper transporting P-type ATPase similar to the Menkes gene [erratum in Nat Genet 6:214]. *Nat Genet* **5**: 327-337

62. TANZI, R.E., PETRUKHIN, K.E., CHERNOV, I., et al. (1993) The Wilson disease gene is a copper transporting ATPase with homology to the Menkes disease gene. *Nat Genet* **5**: 344-350

63. BULL, P.C. and COX, D.W. (1994) Wilson disease and Menkes disease: new handles on heavy-metal transport. *Trends Genet* **10**: 246-252

64. SOLIOZ, M. and VULPE, C. (1996) CPx-type ATPases: a class of P-type ATPases that pump heavy metals. *Trends Biochem Sci* **21**: 237-241

65. PAYNE, A.S. and GITLIN, J.D. (1998) Functional expression of the Menkes disease protein reveals common biochemical mechanisms among the copper-transporting P-type ATPases. *J Biol Chem* **273**: 3765-3770

66. FORBES, J.R. and COX, D.W. (1998) Functional characterization of missense mutations in *ATP7B*: Wilson disease mutation or normal variant? *Am J Hum Genet* **63**: 1663-1674

67. VOSKOBOINIK, I., BROOKS, H., SMITH, S., SHEN, P. and CAMAKARIS, J. (1998) ATP-dependent copper transport by the Menkes protein in membrane vesicles isolated from cultured Chinese hamster ovary cells. *FEBS Lett* **435**: 178-182

68. LA FONTAINE, S.L., FIRTH, S.D., CAMAKARIS, J., et al. (1998) Correction of the copper transport defect of Menkes patient fibroblasts by expression of the Menkes and Wilson ATPases. *J Biol Chem* **273**: 31375-31380

69. HUNG, I.H., SUZUKI, M., YAMAGUCHI, Y., YUAN, D.S., KLAUSNER, R.D. and GITLIN, J.D. (1997) Biochemical characterization of the Wilson disease protein and functional expression in the yeast *Saccharomyces cerevisiae*. *J Biol Chem* **272**: 21461-21466

70. PAYNE, A.S., KELLY, E.J. and GITLIN, J.D. (1998) Functional expression of the Wilson disease protein reveals mislocalization and impaired copper-dependent trafficking of the common H1069Q mutation. *Proc Natl Acad Sci USA* **95**: 10854-10859

71. VOSKOBOINIK, I., GREENOUGH, M., LA FONTAINE, S., MERCER, J.F. and CAMAKARIS, J. (2001) Functional studies on the Wilson copper P-type ATPase and toxic milk mouse mutant. *Biochem Biophys Res Commun* **281**: 966-970

72. LUTSENKO, S., EFREMOV, R.G., TSIVKOVSKII, R. and WALKER, J.M. (2002) Human copper-transporting ATPase ATP7B (the Wilson's disease protein): biochemical properties and regulation. *J Bioenerg Biomembr* **34**: 351-362

73. TAO, T.Y. and GITLIN, J.D. (2003) Hepatic copper metabolism: insights from genetic disease. *Hepatology* **37**: 1241-1247

74. MYARI, A., HADJILIADIS, N., FATEMI, N. and SARKAR, B. (2004) Copper(I) interaction with model peptides of WD6 and TM6 domains of Wilson ATPase: regulatory and mechanistic implications. *J Inorg Biochem* **98**: 1483-1494

75. YAMAGUCHI, Y., HEINY, M.E., SUZUKI, M. and GITLIN, J.D. (1996) Biochemical characterization and intracellular localization of the Menkes disease protein. *Proc Natl Acad Sci USA* **93**: 14030-14035

76. DIERICK, H.A., ADAM, A.N., ESCARA-WILKE, J.F. and GLOVER, T.W. (1997) Immunocytochemical localization of the Menkes copper transport protein (ATP7A) to the *trans*-Golgi network. *Hum Mol Genet* **6**: 409-416

77. SCHAEFER, M., ROELOFSEN, H., WOLTERS, H., et al (1999) Localization of the Wilson's disease protein in human liver. *Gastroenterology* **117**: 1380-1385

78. SCHAEFER, M., HOPKINS, R.G., FAILLA, M.L. and GITLIN, J.D. (1999) Hepatocyte-specific localization and copper-dependent trafficking of the Wilson's disease protein in the liver. *Am J Physiol* **276**: G639-G646

79. PETRIS, M.J., MERCER, J.F., CULVENOR, J.G., LOCKHART, P., GLEESON, P.A. and CAMAKARIS, J. (1996) Ligand-regulated transport of the Menkes copper P-type ATPase efflux pump from the Golgi apparatus to the plasma membrane: a novel mechanism of regulated trafficking. *EMBO J* **15**: 6084-6095

80. ROELOFSEN, H., WOLTERS, H., VAN LUYN, M.J., MIURA, N., KUIPERS, F. and VONK, R.J. (2000) Copper-induced apical trafficking of ATP7B in polarized hepatoma cells provides a mechanism for biliary copper excretion. *Gastroenterology* **119**: 782-793

81. PETRIS, M.J. and MERCER, J.F. (1999) The Menkes protein (ATP7A; MNK) cycles via the plasma membrane both in basal and elevated extracellular copper using a C-terminal di-leucine endocytic signal. *Hum Mol Genet* **8**: 2107-2115

82. MONTY, J.F., LLANOS, R.M., MERCER, J.F. and KRAMER, D.R. (2005) Copper exposure induces trafficking of the Menkes protein in intestinal epithelium of ATP7A transgenic mice. *J Nutr* **135**: 2762-2766

83. FERENCI, P., ZOLLNER, G. and TRAUNER, M. (2002) Hepatic transport systems. *J Gastroenterol Hepatol* **17**: S105-S112

84. FANNI, D., PILLONI, L., ORRU, S., et al. (2005) Expression of ATP7B in normal human liver. *Eur J Histochem* **49**: 371-378

85. WALKER, J.M., TSIVKOVSKII, R. and LUTSENKO, S. (2002) Metallochaperone Atox1 transfers copper to the NH2-terminal domain of the Wilson's disease protein and regulates its catalytic activity. *J Biol Chem* **277**: 27953-27959

86. HAMZA, I., PROHASKA, J. and GITLIN, J.D. (2003) Essential role for Atox1 in the copper-mediated intracellular trafficking of the Menkes ATPase. *Proc Natl Acad Sci USA* **100**: 1215-1220

87. COUSINS, R.J. (1985) Absorption, transport, and hepatic metabolism of copper and zinc: Special reference to metallothionein and ceruloplasmin. *Physiol Rev* **65**: 238-308

88. WANG, W. and BALLATORI, N. (1998) Endogenous glutathione conjugates: occurrence and biological functions. *Pharmacol Rev* **50**: 335-356

89. STEINEBACH, O.M. and WOLTERBEEK, H.T. (1994) Role of cytosolic copper, metallothionein and glutathione in copper toxicity in rat hepatoma tissue culture cells. *Toxicology* **92**: 75-90

90. FREEDMAN, J.H., CIRIOLO, M.R. and PEISACH, J. (1989) The role of glutathione in copper metabolism and toxicity. *J Biol Chem* **264**: 5598-5605

91. STEINKUHLER, C., SAPORA, O., CARRI, M.T., et al. (1991) Increase of Cu,Zn-superoxide dismutase activity during differentiation of human K562 cells involves activation by copper of a constantly expressed copper-deficient protein. *J Biol Chem* **266**: 24580-24587

92. MUSCI, G., DI MARCO, S., BELLENCHI, G.C. and CALABRESE, L. (1996) Reconstitution of ceruloplasmin by the Cu(I)-glutathione complex. Evidence for a role of Mg2+ and ATP. *J Biol Chem* **271**: 1972-1978

93. NAKAMURA, S., KAWATA, T., NAKAYAMA, A., KUBO, K., MINAMI, T. and SAKURAI, H. (2004) Implication of the differential roles of metallothionein 1 and 2 isoforms in the liver of rats as determined by polyacrylamide-coated capillary zone electrophoresis. *Biochem Biophys Res Commun* **320**: 1193-1198

94. HUNT, D.M., WAKE, S.A., MERCER, J.F. and DANKS, D.M. (1986) A study of the role of metallothionein in the inherited copper toxicosis of dogs. *Biochem J* **236**: 409-415

95. TAPIA, L., GONZALEZ-AGUERO, M., CISTERNAS, M.F., et al. (2004) Metallothionein is crucial for safe intracellular copper storage and cell survival at normal and supra-physiological exposure levels. *Biochem J* **378**: 617-624

96. LIU, S.X., FABISIAK, J.P., TYURIN, V.A., et al (2000) Reconstitution of apo-superoxide dismutase by nitric oxide-induced copper transfer from metallothioneins. *Chem Res Toxicol* **13**: 922-931

97. KANG, Y.J. (1999) The antioxidant function of metallothionein in the heart. *Proc Soc Exp Biol Med* **222**: 263-273

98. MALARKEY, D.E., JOHNSON, K., RYAN, L., BOORMAN, G. and MARONPOT, R.R. (2005) New insights into functional aspects of liver morphology. *Toxicol Pathol* **33**: 27-34

99. BEATH, S.V. (2003) Hepatic function and physiology in the newborn. *Semin Neonatol* **8**: 337-346

100. SCHILSKY, M.L., IRANI, A.N., GORLA, G.R., VOLENBERG, I. and GUPTA, S. (2000) Biliary copper excretion capacity in intact animals: correlation between ATP7B function, hepatic mass, and biliary copper excretion. *J Biochem Mol Toxicol* **14**: 210-214

101. DIJKSTRA, M., KUIPERS, F., VAN DEN BERG, G.J., HAVINGA, R. and VONK, R.J. (1997) Differences in hepatic processing of dietary and intravenously administered copper in rats. *Hepatology* **26**: 962-966

102. GROSS, J.B., MYERS, B.M., KOST, L.J., KUNTZ, S.M. and LARUSSO, N.F. (1989) Biliary copper excretion by hepatocyte lysosomes in the rat. *J Clin Invest* **83**: 30-39

103. HARADA, M., SAKISAKA, S., YOSHITAKE, M., et al (1993) Biliary copper excretion in acutely and chronically copper-loaded rats. *Hepatology* **17**: 111-117

104. HOUWEN, R., DIJKSTRA, M., KUIPERS, I., SMIT, E.P., HAVINGA, R. and VONK, R.J. (1990) Two pathways for biliary copper excretion in the rat. The role of glutathione. *Biomed Pharm* **39**: 1039-1044

105. DIJKSTRA, M., IN T'VELD, G., VAN DEN BERG, G.J., MULLER, M., KUIPERS, F. and VONK, R.J. (1995) Adenosine triphosphate-dependent copper transport in isolated rat liver plasma membranes. *J Clin Invest* **95**: 412-416

106. DIJKSTRA, M., VAN DEN BERG, G.J., WOLTERS, H., et al. (1996) Adenosine triphosphate-dependent copper transport in human liver. *J Hepatol* **25**: 37-42

107. SUGAWARA, N., SATO, M., YUASA, M. and SUGAWARA, C. (1995) Biliary excretion of copper, metallothionein, and glutathione into Long- Evans Cinnamon rats: a convincing animal model for Wilson disease. *Biochem Mol Med* **55**: 38-42

108. TERADA, K., AIBA, N., YANG, X.L., et al. (1999) Biliary excretion of copper in LEC rat after introduction of copper transporting P-type ATPase, ATP7B. *FEBS Lett* **448**: 53-56

109. MENG, Y., MIYOSHI, I., HIRABAYASHI, M., et al. (2004) Restoration of copper metabolism and rescue of hepatic abnormalities in LEC rats, an animal model of Wilson disease, by expression of human ATP7B gene. *Biochim Biophys Acta* **1690**: 208-219

110. IYENGAR, V., BREWER, G.J., DICK, R.D. and CHUNG, O.Y. (1988) Studies of cholecystokinin-stimulated biliary secretions reveal a high molecular weight copper-binding substance in normal subjects that is absent in patients with Wilson's disease. *J Lab Clin Med* **111**: 267-274

111. CHOWRIMOOTOO, G.F., AHMED, H.A. and SEYMOUR, C.A. (1996) New insights into the pathogenesis of copper toxicosis in Wilson's disease: evidence for copper incorporation and defective canalicular transport of caeruloplasmin. *Biochem J* **315**: 851-855

112. MENKES, J.H., ALTER, M., STEIGLEDER, G., WEAKLEY, D.R. and SUNG, J.H. (1962) A sex-linked recessive disorder with retardation of growth, peculiar hair, and focal cerebral and cerebellar degeneration. *Pediatrics* **29**: 764-779

113. WILSON, S.A.K. (1912) Progressive lenticular degeneration: a familial nervous disease associated with cirrhosis of the liver. *Brain* **34**: 295-509

114. DANKS, D.M. (1995) Disorders of copper transport. In: *The Molecular and Metabolic Basis of Inherited Disease*, 7th Edition. Scriver, C.R., Beaudet, A.L., Sly, W.S. and Valle, D. Eds. McGraw-Hill, New York: pp. 4125-4158.

115. VOSKOBOINIK, I. and CAMAKARIS, J. (2002) Menkes copper-translocating P-type ATPase (ATP7A): biochemical and cell biology properties, and role in Menkes disease. *J Bioenerg Biomembr* **34**: 363-371

116. FLEISCHER, B. (1912) Uber eine der "pseudosclerose" nahestehende bisher unbekannte Krankheit. *Dtsch Z Nervenheilk* **44**: 179-201

117. CUMINGS, JN. (1948) Copper and iron content of brain and liver in normal and in hepatolenticular degeneration. *Brain* **71**: 410-415

118. GOLLAN, J.L. and GOLLAN, T.J. (1998) Wilson disease in 1998: genetic, diagnostic and therapeutic aspects. *J Hepatol* **28**: 28S-36S

119. COX, D.W. and ROBERTS, E.A (2006) Wilson Disease. In: *GeneReviews at GeneTests: Medical Genetics Information Resource (www.genetests.org)*, University of Washington, Seattle.

120. RIORDAN, S.M. and WILLIAMS, R. (2001) The Wilson's disease gene and phenotypic diversity. *J Hepatol* **34**: 165-171

121. KAYSER, B. (1902) Ueber einen Fall von angeborener grunlicher Verfarbung der Kornea. *Klin Mbl Augenheilk* **40**: 22-25

122. FLEISCHER, B. (1903) Zwei weitere Falle von grunliche Verfarbung der Kornea. *Klin Mbl Augenheilk* **41**: 489-491

123. STEINDL, P., FERENCI, P., DIENES, H.P., et al (1997) Wilson's disease in patients presenting with liver disease: a diagnostic challenge. *Gastroenterology* **113**: 212-218

124. LANGNER, C. and DENK, H. (2004) Wilson disease. *Virchows Arch* **445**: 111-118

125. LOUDIANOS, G. and GITLIN, J.D. (2000) Wilson's disease. *Semin Liver Dis* **20**: 353-364

126. GU, M., COOPER, J.M., BUTLER, P., et al. (2000) Oxidative-phosphorylation defects in liver of patients with Wilson's disease. *Lancet* **356**: 469-474

127. KITZBERGER, R., MADL, C. and FERENCI, P. (2005) Wilson disease. *Metab Brain Dis* **20**: 295-302

128. ALANEN, A., KOMU, M., PENTTINEN, M. and LEINO, R. (1999) Magnetic resonance imaging and proton MR spectroscopy in Wilson's disease. *Br J Radiol* **72**: 749-756

129. SCHIEFERMEIER, M., KOLLEGGER, H., MADL, C., et al. (2000) The impact of apolipoprotein E genotypes on age at onset of symptoms and phenotypic expression in Wilson's disease. *Brain* **123**: 585-590

130. GRUBENBECHER, S., STUVE, O., HEFTER, H. and KORTH, C. (2006) Prion protein gene codon 129 modulates clinical course of neurological Wilson disease. *Neuroreport* **17**: 549-552

131. POLIO, J., ENRIQUEZ, R.E., CHOW, A., WOOD, W.M. and ATTERBURY, C.E. (1989) Hepatocellular carcinoma in Wilson's disease. Case report and review of the literature. *J Clin Gastroenterol* **11**: 220-224

132. FERENCI, P., CACA, K., LOUDIANOS, G., et al. (2003) Diagnosis and phenotypic classification of Wilson disease. *Liver Int* **23**: 139-142

133. SCHEINBERG, I.H. and GITLIN, D. (1952) Deficiency of ceruloplasmin in patients with hepatolenticular degeneration (Wilson's disease). *Science* **116**: 484-485

134. ROBERTS, E.A. and SCHILSKY, M.L. (2003) A practice guideline on Wilson disease. *Hepatology* **37**: 1475-1492

135. BREWER, G.J. and ASKARI, F.K. (2005) Wilson's disease: clinical management and therapy. *J Hepatol* **42**: S13-S21

136. WALSHE, J.M. (1956) Penicillamine. A new oral therapy for Wilson's disease. *Am J Med* **21**: 487-495

137. WALSHE, J.M. (1970) Triethylene tetramine. *Lancet* **2**: 154.

138. FERENCI, P. (2004) Diagnosis and current therapy of Wilson's disease. *Aliment Pharmacol Ther* **19**: 157-165

139. SCHEINBERG, I.H., JAFFE, M.E. and STERNLIEB, I. (1987) The use of trientine in preventing the effects of interrupting penicillamine therapy in Wilson's disease. *New Eng J Med* **317**: 209-213

140. BREWER, G.J., HEDERA, P., KLUIN, K.J., et al. (2003) Treatment of Wilson disease with ammonium tetrathiomolybdate: III. Initial therapy in a total of 55 neurologically affected patients and follow-up with zinc therapy. *Arch Neurol* **60**: 379-385

141. LEE, D.Y., BREWER, G.J. and WANG, Y.X. (1989) Treatment of Wilson's disease with zinc. VII. Protection of the liver from copper toxicity by zinc-induced metallothionein in a rat model. *J Lab Clin Med* **114**: 639-645

142. CZLONKOWSKA, A., GAJDA, J. and RODO, M. (1996) Effects of long-term treatment in Wilson's disease with D-penicillamine and zinc sulphate. *J Neurol* **243**: 269-273

143. BEARN, A.G. (1960) A genetical analysis of 30 families with Wilson's disease (hepatolenticular degeneration). *Ann Hum Genet* **24**: 33-43

144. FRYDMAN, M., BONNE-TAMIR, B., FARRER, L.A., et al. (1985) Assignment of the gene for Wilson disease to chromosome 13: linkage to the esterase D locus. *Proc Natl Acad Sci USA* **82**: 1819-1821

145. BOWCOCK, A.M., FARRER, L.A., HEBERT, J.M., et al. (1988) Eight closely linked loci place the Wilson disease locus within 13q14-q21. *Am J Hum Genet* **43**: 664-674

146. PETRUKHIN, K., LUTSENKO, S., CHERNOV, I., ROSS, B.M., KAPLAN, J.H. and GILLIAM, T.C. (1994) Characterization of the Wilson disease gene encoding a P-type copper transporting ATPase: genomic organization, alternative splicing, and structure/function predictions. *Hum Mol Genet* **3**: 1647-1656

147. THOMAS, G.R., FORBES, J.R., ROBERTS, E.A., WALSHE, J.M. and COX, D.W. (1995) The Wilson disease gene: spectrum of mutations and their consequences. *Nat Genet* **9**: 210-217

148. OH, W.J., KIM, E.K., PARK, K.D., HAHN, S.H. and YOO, O.J. (1999) Cloning and characterization of the promoter region of the Wilson disease gene. *Biochem Biophys Res Commun* **259**: 206-211

149. OH, W.J., KIM, E.K., KO, J.H., YOO, S.H., HAHN, S.H. and YOO, O.J. (2002) Nuclear proteins that bind to metal response element a (MREa) in the Wilson disease gene promoter are Ku autoantigens and the Ku-80 subunit is necessary for basal transcription of the WD gene. *Eur J Biochem* **269**: 2151-2161

150. BORJIGIN, J., PAYNE, A.S., DENG, J., et al. (1999) A novel pineal night-specific ATPase encoded by the Wilson disease gene. *J Neurosci* **19**: 1018-1026

151. COX, D.W. and MOORE, S.D. (2002) Copper transporting P-type ATPases and human disease. *J Bioenerg Biomembr* **34**: 333-338

152. MOLLER, L.B., OTT, P., LUND, C. and HORN, N. (2005) Homozygosity for a gross partial gene deletion of the C-terminal end of ATP7B in a Wilson patient with hepatic and no neurological manifestations. *Am J Med Genet A* **138**: 340-343

153. THOMAS, G.R., ROBERTS, E.A., WALSHE, J.M. and COX, D.W. (1995) Haplotypes and mutations in Wilson disease. *Am J Hum Genet* **56**: 1315-1319

154. CHUANG, L.M., WU, H.P., JANG, M.H., et al. (1996) High frequency of two mutations in codon 778 in exon 8 of the *ATP7B* gene in Taiwanese families with Wilson disease. *J Med Genet* **33**: 521-523

155. NANJI, M.S., NGUYEN, V.T., KAWASOE, J.H., et al. (1997) Haplotype and mutation analysis in Japanese patients with Wilson disease. *Am J Hum Genet* **60**: 1423-1429

156. GITLIN, J.D. (2003) Wilson disease. *Gastroenterology* **125**: 1868-1877

157. GUPTA, A., AIKATH, D., NEOGI, R., et al. (2005) Molecular pathogenesis of Wilson disease: haplotype analysis, detection of prevalent mutations and genotype-phenotype correlation in Indian patients. *Hum Genet* **118**: 49-57

158. DIDONATO, M., HSU, H.F., NARINDRASORASAK, S., QUE, L.J. and SARKAR, B. (2000) Copper-induced conformational changes in the N-terminal domain of the Wilson disease copper-transporting ATPase. *Biochem* **39**: 1890-1896

159. RALLE, M., LUTSENKO, S. and BLACKBURN, N.J. (2004) Copper transfer to the N-terminal domain of the Wilson disease protein (ATP7B): X-ray absorption spectroscopy of reconstituted and chaperone-loaded metal binding domains and their interaction with exogenous ligands. *J Inorg Biochem* **98**: 765-774

160. WALKER, J.M., HUSTER, D., RALLE, M., MORGAN, C.T., BLACKBURN, N.J. and LUTSENKO, S. (2004) The N-terminal metal-binding site 2 of the Wilson's Disease Protein plays a key role in the transfer of copper from Atox1. *J Biol Chem* **279**: 15376-15384

161. FATEMI, N. and SARKAR, B. (2002) Insights into the mechanism of copper transport by the Wilson and Menkes disease copper-transporting ATPases. *Inorganica Chim Acta* **339**: 179-187

162. TSIVKOVSKII, R., EFREMOV, R.G. and LUTSENKO, S. (2003) The role of the invariant His-1069 in folding and function of the Wilson's disease protein, the human copper-transporting ATPase ATP7B. *J Biol Chem* **278**: 13302-13308

163. MORGAN, C.T., TSIVKOVSKII, R., KOSINSKY, Y.A., EFREMOV, R.G. and LUTSENKO, S. (2004) The distinct functional properties of the nucleotide-binding domain of ATP7B, the human copper-transporting ATPase: analysis of the Wilson disease mutations E1064A, H1069Q, R1151H, and C1104F. *J Biol Chem* **279**: 36363-36371

164. EFREMOV, R.G., KOSINSKY, Y.A., NOLDE, D.E., TSIVKOVSKII, R., ARSENIEV, A.S. and LUTSENKO, S. (2004) Molecular modelling of the nucleotide-binding domain of Wilson's disease protein: location of the ATP-binding site, domain dynamics and potential effects of the major disease mutations. *Biochem J* **382**: 293-305

165. DMITRIEV, O., TSIVKOVSKII, R., ABILDGAARD, F., MORGAN, C.T., MARKLEY, J.L. and LUTSENKO, S. (2006) Solution structure of the N-domain of Wilson disease protein: Distinct nucleotide-binding environment and effects of disease mutations. *Proc Natl Acad Sci USA* **103**: 5302-5307

166. ACHILA, D., BANCI, L., BERTINI, I., BUNCE, J., CIOFI-BAFFONI, S. and HUFFMAN, D.L. (2006) Structure of human Wilson protein domains 5 and 6 and their interplay with domain 4 and the copper chaperone HAH1 in copper uptake. *Proc Natl Acad Sci USA* **103**: 5729-5734

167. HELLMAN, N.E., KONO, S., MANCINI, G.M., HOOGEBOOM, A.J., DE JONG, G.J. and GITLIN, J.D. (2002) Mechanisms of copper incorporation into human ceruloplasmin. *J Biol Chem* **277**: 46632-46638

168. HARRIS, Z.L., TAKAHASHI, Y., MIYAJIMA, H., SERIZAWA, M., MACGILLIVRAY, R.T. and GITLIN, J.D. (1995) Aceruloplasminemia: molecular characterization of this disorder of iron metabolism. *Proc Natl Acad Sci USA* **92**: 2539-2543

169. WANG, T. and WEINMAN, S.A. (2004) Involvement of chloride channels in hepatic copper metabolism: ClC-4 promotes copper incorporation into ceruloplasmin. *Gastroenterology* **126**: 1157-1166

170. HUSTER, D., FINEGOLD, M.J., MORGAN, C.T., et al. (2006) Consequences of copper accumulation in the livers of the *Atp7b-/-* (Wilson disease gene) knockout mice. *Am J Pathol* **168**: 423-434

171. CATER, M.A., LA FONTAINE, S., SHIELD, K., DEAL, Y. and MERCER, J.F. (2006) ATP7B mediates vesicular sequestration of copper: insight into biliary copper excretion. *Gastroenterology* **130**: 493-506

172. GUO, Y., NYASAE, L., BRAITERMAN, L.T. and HUBBARD, A.L. (2005) NH2-terminal signals in ATP7B Cu-ATPase mediate its Cu-dependent anterograde traffic in polarized hepatic cells. *Am J Physiol Gastrointest Liver Physiol* **289**: G904-G916

173. NAGANO, K., NAKAMURA, K., URAKAMI, K.I., et al. (1998) Intracellular distribution of the Wilson's disease gene product (ATPase7B) after in vitro and in vivo exogenous expression in hepatocytes from the LEC rat, an animal model of Wilson's disease. *Hepatol* **27**: 799-807

174. HARADA, M., SAKISAKA, S., TERADA, K., et al. (2000) Role of ATP7B in biliary copper excretion in a human hepatoma cell line and normal rat hepatocytes. *Gastroenterology* **118**: 921-928

175. HARADA, M., KUMEMURA, H., SAKISAKA, S., et al. (2003) Wilson disease protein ATP7B is localized in the late endosomes in a polarized human hepatocyte cell line. *Int J Mol Med* **11**: 293-298

176. HARADA, M., KAWAGUCHI, T., KUMEMURA, H., et al. (2005) The Wilson disease protein ATP7B resides in the late endosomes with Rab7 and the Niemann-Pick C1 protein. *Am J Pathol* **166**: 499-510

177. HARADA, M., SAKISAKA, S., KAWAGUCHI, T., et al. (2000) Copper does not alter the intracellular distribution of ATP7B, a copper-transporting ATPase. *Biochem Biophys Res Commun* **275**: 871-876

178. KASAI, N., OSANAI, T., MIYOSHI, I., KAMIMURA, E., YOSHIDA, M.C. and DEMPO, K. (1990) Clinico-pathological studies of LEC rats with hereditary hepatitis and hepatoma in the acute phase of hepatitis. *Lab Anim Sci* **40**: 502-505

179. LI, Y., TOGASHI, Y., SATO, S., et al. (1991) Spontaneous hepatic copper accumulation in Long-Evans Cinnamon rats with hereditary hepatitis. *J Clin Invest* **87**: 1858-1861

180. YAMADA, T., AGUI, T., SUZUKI, Y., SATO, M. and MATSUMOTO, K. (1993) Inhibition of the copper incorporation into ceruloplasmin leads to the deficiency in serum ceruloplasmin activity in Long-Evans cinnamon mutant rat. *J Biol Chem* **268**: 8965-8971

181. MURATA, Y., YAMAKAWA, E., IIZUKA, T., et al. (1995) Failure of copper incorporation into ceruloplasmin in the Golgi apparatus of LEC rat hepatocytes [published erratum appears in *Biochem Biophys Res Commun* 211:348]. *Biochem Biophys Res Commun* **209**: 349-355

182. HAYASHI, M., KUGE, T., ENDOH, D., et al. (2000) Hepatic copper accumulation induces DNA strand breaks in the liver cells of Long-Evans Cinnamon strain rats. *Biochem Biophys Res Commun* **276**: 174-178

183. YOSHIDA, M., MASUDA, C.R., SASAKI, M., et al. (1987) New mutation causing hereditary hepatitis in the laboratory rat. *J Hered* **78**: 361-365

184. KATO, J., KOHGO, Y., SUGAWARA, N., et al. (1993) Abnormal hepatic iron accumulation in LEC rats. *Jpn J Cancer Res* **84**: 219-222

185. FUENTEALBA, I.C. and ABURTO, E.M. (2003) Animal models of copper-associated liver disease. *Comp Hepatol* **2**: 5-12

186. MASUDA, R., YOSHIDA, M.C., SASAKI, M., DEMPO, K. and MORI, M. (1988) Hereditary hepatitis of LEC rats is controlled by a single autosomal recessive gene. *Lab Animal* **22**: 166-169

187. MASUDA, R., YOSHIDA, M.C., SASAKI, M., DEMPO, K. and MORI, M. (1988) High susceptibility to hepatocellular carcinoma development in LEC rats with hereditary hepatitis. *Jpn J Cancer Res* **79**: 828-835

188. SUGAWARA, N., LI, D., SUGAWARA, C. and MIYAKE, H. (1993) Decrease in biliary excretion of copper in Long-Evans cinnamon (LEC) rats causing spontaneous hepatitis due to a gross accumulation of hepatic copper. *Res Commun Chem Pathol Pharmacol* **81**: 45-52

189. SCHILSKY, M.L., STOCKERT, R.J. and STERNLIEB, I. (1994) Pleiotropic effect of LEC mutation: a rodent model of Wilson's disease. *Am J Physiol* **266**: G907-G913

190. FUJII, Y., SHIMIZU, K., SATOH, M., et al. (1993) Histochemical demonstration of copper in LEC rat liver. *Histochemistry* **100**: 249-256

191. MORI, M., HATTORI, A., SAWAKI, M., et al. (1994) The LEC rat: a model for human hepatitis, liver cancer, and much more. *Am J Pathol* **144**: 200-204

192. ONO, T., TAKADA, S. and YOSHIDA, M.C. (1994) The *WD* gene for Wilson's disease links to the hepatitis of LEC rats. *Jpn J Cancer Res* **85**: 771-774

193. SASAKI, N., HAYASHIZAKI, Y., MURAMATSU, M., et al. (1994) The gene responsible for LEC hepatitis, located on rat chromosome 16, is the homolog to the human Wilson disease gene. *Biochem Biophys Res Commun* **202**: 512-518

194. WU, J., FORBES, J.R., CHEN, H.S. and COX, D.W. (1994) The LEC rat has a deletion in the copper transporting ATPase gene homologous to the Wilson disease gene. *Nat Genet* **7**: 541-545

195. WU, J., FORBES, J.R. and COX, D.W. (1997) Further Characterization of the *Atp7b* Gene in LEC rats. *J Trace Elements Exp Med* **10**: 147-152

196. HUANG, Z., DENG, J. and BORJIGIN, J. (2005) A novel H28Y mutation in LEC rats leads to decreased NAT protein stability *in vivo* and *in vitro*. *J Pineal Res* **39**: 84-90

197. RAUCH, H. (1983) Toxic milk, a new mutation affecting copper metabolism in the mouse. *J Hered* **74**: 141-144

198. BIEMPICA, L., RAUCH, H., QUINTANA, N. and STERNLIEB, I. (1988) Morphological and chemical studies on a murine mutation (toxic milk) resulting in hepatic copper toxicosis. *Lab Invest* **59**: 500-508

199. HOWELL, J.M. and MERCER, J.F.B. (1994) The pathology and trace element status of the toxoic milk mutant mouse. *J Comp Path* **110**: 37-47

200. MERCER, J.F., GRIMES, A., DANKS, D.M. and RAUCH, H. (1991) Hepatic ceruloplasmin gene expression is unaltered in the toxic milk mouse. *J Nutr* **121**: 894-899

201. MERCER, J.F., GRIMES, A. and RAUCH, H. (1992) Hepatic metallothionein gene expression in toxic milk mice. *J Nutr* **122**: 1254-1259

202. MERCER, J.F., PAYNTER, J.A. and GRIMES, A. (1994) The toxic milk mouse does have elevated hepatic metallothionein mRNA. *Biochem J* **304**: 317-318

203. REED, V., WILLIAMSON, P., BULL, P.C., COX, D.W. and BOYD, Y. (1995) Mapping of the mouse homologue of the Wilson disease gene to mouse chromosome 8. *Genomics* **28**: 573-575

204. RAUCH, H. and WELLS, A.J. (1995) The toxic milk mutation, *tx*, which results in a condition resembling Wilson disease in humans, is linked to mouse chromosome 8. *Genomics* **29**: 551-552

205. THEOPHILOS, M.B., COX, D.W. and MERCER, J.F. (1996) The toxic milk mouse is a murine model of Wilson disease. *Hum Mol Genet* **5**: 1619-1624

206. BUIAKOVA, O.I., XU, J., LUTSENKO, S., et al. (1999) Null mutation of the murine ATP7B (Wilson disease) gene results in intracellular copper accumulation and late-onset hepatic nodular transformation. *Hum Mol Genet* **8**: 1665-1671

207. YANO, M., SAKAMOTO, N., TAKIKAWA, T. and HAYASHI, H. (1993) Intrahepatocellular localization of copper in Wilson's disease. *Nagoya J Med Sci* **55**: 131-137

208. SCHEINBERG, I.H. and STERNLIEB, I. (1996) Wilson disease and idiopathic copper toxicosis. *Am J Clin Nutr* **63**: 842S-845S

209. MULLER, T., MULLER, W. and FEICHTINGER, H. (1998) Idiopathic copper toxicosis. *Am J Clin Nutr* **67**: 1082S-1086S

210. NAYAK, N.C. and RAMILINGASWANI, V. (1975) Indian childhood cirrhosis. *Clin Gastroenterol* **4**: 333-349

211. PORTMAN, B., TANNER, M.S., MOWAT, A.P. and WILLIAMS, R. (1979) Orcein positive liver deposits in Indian childhood cirrhosis. *Lancet* **1**: 1203-1205

212. GOLDFISCHER, S., POPPER, H. and STERNLIEB, I. (1980) The significance of variations in the distribution of copper in liver disease. *Am J Pathol* **99**: 715-730

213. TANNER, M.S. (1998) Role of copper in Indian childhood cirrhosis. *Am J Clin Nutr* **67**: 1074S-1081S

214. MULLER, T., FEICHTINGER, H., BERGER, H. and MULLER, W. (1996) Endemic Tyrolean infantile cirrhosis: an ecogenetic disorder. *Lancet* **347**: 877-880

215. MULLER, T., SCHAFER, H., RODECK, B., et al. (1999) Familial clustering of infantile cirrhosis in Northern Germany: A clue to the etiology of idiopathic copper toxicosis. *J Pediatr* **135**: 189-196

216. TANNER, M.S., KANTARJIAN, A.H., BHAVE, S.A. and PANDIT, A.N. (1983) Early introduction of copper-contaminated animal milk feeds as a possible cause of Indian childhood cirrhosis. *Lancet* **2**: 992-995

217. CHAUDHURI, A. and CHAUDHURI, K.C. (1965) The kareotype in infantile cirrhosis of the liver (Sen's syndrome). *Indian J Pediat* **32**: 209-218

218. PRASAD, R., KAUR, G., NATH, R. and WALIA, B.N. (1996) Molecular basis of pathophysiology of Indian childhood cirrhosis: role of nuclear copper accumulation in liver. *Mol Cell Biochem* **156**: 25-30

219. GAHL, W., ADAMSON, M., GOODMAN, Z., et al. (1988) Hepatic copper storage resembling Indian childhood cirrhosis (ICC) in a non-Indian boy: a genetic disease. *Am J Hum Genet* **43**: A7

220. BHAVE, S.A., PANDIT, A.N. and TANNER, M.S. (1987) Comparison of feeding history of children with Indian childhood cirrhosis and paired controls. *J Pediatr Gastroenterol Nutr* **6**: 562-567

221. AGARWAL, S.S., LAHORI, U.C., MEHTA, S.K., SMITH, D.G. and BAJPAI, P.C. (1979) Inheritance of Indian childhood cirrhosis. *Hum Hered* **29**: 82-89

222. WIJMENGA, C., MULLER, T., MURLI, I.S., et al. (1998) Endemic Tyrolean infantile cirrhosis is not an allelic variant of Wilson's disease. *Eur J Hum Genet* **6**: 624-628

223. MULLER, T., VAN DE SLUIS, B., ZHERNAKOVA, A., et al. (2003) The canine copper toxicosis gene *MURR1* does not cause non-Wilsonian hepatic copper toxicosis. *J Hepatol* **38**: 164-168

224. MACLACHLAN, G.K. and JOHNSTON, W.S. (1982) Copper poisoning in sheep from North Ronaldsay maintained on a diet of terrestrial herbage. *Vet Rec* **111**: 299-301

225. HAYWOOD, S., MULLER, T., MULLER, W., HEINZ-ERIAN, P., TANNER, M.S. and ROSS, G. (2001) Copper-associated liver disease in North Ronaldsay sheep: a possible animal model for non-Wilsonian hepatic copper toxicosis of infancy and childhood. *J Pathol* **195**: 264-269

226. ISHMAEL, J., GOPINATH, C. and HOWELL, J.M. (1971) Experimental chronic copper toxicity in sheep. Histological and histochemical changes during the development of the lesions in the liver. *Res Vet Sci* **12**: 358-366

227. KUMARATILAKE, J.S. and HOWELL, J.M. (1987) Histochemical study of the accumulation of copper in the liver of sheep. *Res Vet Sci* **42**: 73-81

228. HAYWOOD, S., MULLER, T., MACKENZIE, A.M., et al. (2004) Copper-induced hepatotoxicosis with hepatic stellate cell activation and severe fibrosis in North Ronaldsay lambs: a model for non-Wilsonian hepatic copper toxicosis of infants. *J Comp Pathol* **130**: 266-277

229. HARDY, R.M., STEVENS, J.B. and STOWE, C.M. (1975) Chronic progressive hepatitis in Bedlington terriers associated with elevated liver copper concentrations. *Minn Vet* **15**: 13-24

230. SU, L.C., RAVANSHAD, S., OWEN, C.A.Jr., MCCALL, J.T., ZOLLMAN, P.E. and HARDY, R.M. (1982) A comparison of copper-loading disease in Inherited copper toxisis in Bedlington terriers: Wilson's disease (hepatolenticular degeneration). *Am J Physiol* **243**: 226-230

231. OWEN, C.A.Jr., BOWIE, E.J., MCCALL, J.T. and ZOLLMAN, P.E. (1980) Hemostasis in the copper-laden Bedlington terrier: a possible model of Wilson's disease. *Haemostasis* **9**: 160-16

232. HULTGREN, B.D., MENKEN, B.Z. and CSALLANY, A.S. (1986) Copper inhibition of the thiobarbituric acid reaction in Bedlington terriers. *Am J Vet Res* **47**: 818-89.

233. TWEDT, D.C., STERNLIEB, I. and GILBERTSON, S.R. (1979) Clinical, morphologic, and chemical studies on copper toxicosis of Bedlington Terriers. *J Am Vet Med Assoc* **175**: 269-275

234. LUDWIG, J., OWEN, C.A.J., BARHAM, S.S., MCCALL, J.T. and HARDY, R.M. (1980) The liver in the inherited copper disease of Bedlington terriers. *Lab Invest* **43**: 82-7.

235. OWEN, C.A. Jr. and LUDWIG, J. (1982) Inherited copper toxicosis in bedlington terriers: Wilson's disease (hepatolenticular degeneration). *Am J Pathol* **106**: 432-434

236. ERIKSSON, J. (1983) Copper toxicosis in Bedlington Terriers. *Acta Vet Scand* **24**: 148-52.

237. HERRTAGE, M.E. (1987) Inherited copper toxicosis in the dog. *Pedigree Digest* **14**: 6-7

238. JOHNSON, G.F., MORELL, A.G., STOCKERT, R.J. and STERNLEIB, I. (1981) Hepatic lysosomal copper protein in dogs with an inherited copper toxicosis. *Hepatology* **1**: 243-248

239. LERCH, K., JOHNSON, G.F, GRUSHOFF, P.S. and STERNLEIB, I. (1985) Canine hepatic lysosomal copper protein: identification as metallothionein. *Arch Biochem Biophys* **243**: 108-114

240. HAYWOOD, S., FUENTEALBA, I.C., FOSTER, J. and ROSS, G. (1996) Pathobiology of copper-induced injury in Bedlington terriers: ultrastructural and microanalytical studies. *Anal Cell Pathol* **10**: 229-41

241. HYUN, C. and FILIPPICH, L.J. (2004) Inherited canine copper toxicosis in Australian Bedlington Terriers. *J Vet Sci* **5**: 19-28

242. LEHTO, J. (1987) Bedlingtonterrierin kuparitoksikoosi-yhteenvetoa maksabiopsiatutkisista [Copper toxicosis in Bedlington terriers: review of the liver biopsy studies]. *Suomen Elainlaakarilehti* **93**: 207-210

243. KAWAMURA, M., TAKAHASHI, I. and KANEKO, J.J. (2002) Ultrastructural and kinetic studies of copper metabolism in Bedlington terrier dogs. *Vet Pathol* **39**: 747-750

244. SU, L.C., OWEN, C.A.J., ZOLLMAN, P.E. and HARDY, R.M. (1982) A defect of biliary excretion in copper-laden Bedlington terriers. *Am J Physiol* **243**: 231-236

245. SATO, M., HACHIYA, N., YAMAGUCHI, Y., et al. (1993) Deficiency of holo-, but not apo-, ceruloplasmin in genetically copper- intoxicated LEC mutant rat. *Life Sci* **53**: 1411-1416

246. JOHNSON, G.F., STERNLIEB, I., TWEDT, D.C., GRUSHOFF, P.S. and SCHEINBERG, I. (1980) Inheritance of copper toxicosis in Bedlington terriers. *Am J Vet Res* **41**: 1865-1866

247. YUZBASIYAN-GURKAN, V., WAGNITZ, S., BLANTON, S.H. and BREWER, G.J. (1993) Linkage studies of the esterase D and retinoblastoma genes to canine copper toxicosis: a model for Wilson disease. *Genomics* **15**: 86-90

248. YUZBASIYAN-GURKAN, V., BLANTON, S.H., CAO, Y., et al. (1997) Linkage of a microsatellite marker to the canine copper toxicosis locus in Bedlington terriers. *Am J Vet Res* **58**: 23-27

249. VAN DE SLUIS, B.J.A., BREEN, M., NANJI, M., et al (1999) Genetic mapping of the copper toxicosis locus in Bedlington terriers to dog chromosome 10, in a region syntenic to human chromosome region 2p13- p16. *Hum Mol Genet* **8**: 501-507

250. DAGENAIS, S.L., GUEVARA-FUJITA, M., LOECHEL, R., et al. (1999) The canine copper toxicosis locus is not syntenic with ATP7B or ATX1 and maps to a region showing homology to human 2p21. *Mamm Genome* **10**: 753-756

251. VAN DE SLUIS, B., ROTHUIZEN, J., PEARSON, P.L., VAN OOST, B.A. and WIJMENGA, C. (2002) Identification of a new copper metabolism gene by positional cloning in a purebred dog population. *Hum Mol Genet* **11**: 165-173

252. GOOD, P.F., WERNER, P., HSU, A., OLANOW, C.W. and PERL, D.P. (1996) Evidence of neuronal oxidative damage in Alzheimer's disease. *Am J Pathol* **149**: 21-28

253. JENNER, P. and OLANOW, C.W. (1996) Oxidative stress and the pathogenesis of Parkinson's disease. *Neurology* **47**: S161-S170

254. COOKSON, M.R. and SHAW, P.J. (1999) Oxidative stress and motor neuron disease. *Brain Pathol* **9**: 165-186

255. LOVELL, M.A., ROBERTSON, J.D., TEESDALE, W.J., CAMPBELL, J.L. and MARKESBERY, W.R. (1998) Copper, iron and zinc in Alzheimer's disease senile plaques. *J Neurol Sci* **158**: 47-52

256. ATWOOD, C.S., SCARPA, R.C., HUANG, X., et al. (2000) Characterization of copper interactions with alzheimer amyloid beta peptides: identification of an attomolar-affinity copper binding site on amyloid beta1-42. *J Neurochem* **75**: 1219-1233

257. COX, D.W. and ROBERTS, E.A. (1998) Wilson disease. In: *Sleisenger and Fordtran's Gastrointestinal and Liver Disease*, 6th Edition. Feldman, M., Scharschmidt, B.F. and Sleisenger, M.H. Eds. W.B.Saunders, pp. 1104-1111.

258. MICHALCZYK, A.A., RIEGER, J., ALLEN, K.J., MERCER, J.F. and ACKLAND, M.L. (2000) Defective localization of the Wilson disease protein (ATP7B) in the mammary gland of the toxic milk mouse and the effects of copper supplementation. *Biochem J* **352**: 565-571

259. SWEET, H.O. and DAVISSON, M.T. (1989) Research News. *Mouse News Lett* **84**: 89-90

260. BRONSON, R.T., SWEET, H.O. and DAVISSON, M.T. (1995) Acute cerebral neuronal necrosis in copper deficient offspring of female mice with the toxic milk mutation. *Mouse Genome* **93**: 152-154

261. HA-HAO, D., HEFTER, H., STREMMEL, W., et al. (1998) His1069Gln and six novel Wilson disease mutations: analysis of relevance for early diagnosis and phenotype. *Eur J Hum Genet* **6**: 616-623

262. WALDENSTROM, E., LAGERKVIST, A., DAHLMAN, T., WESTERMARK, K. and LANDEGREN, U. (1996) Efficient detection of mutations in Wilson disease by manifold sequencing. *Genomics* **37**: 303-309

263. LOUDIANOS, G., DESSI, V., ANGIUS, A., et al. (1996) Wilson disease mutations associated with uncommon haplotypes in Mediterranean patients. *Hum Genet* **98**: 640-642

264. BREWER, G.J., DICK, R.D., SCHALL, W., et al. (1992) Use of zinc acetate to treat copper toxicosis in dogs. *J Am Vet Med Assoc* **201**: 564-568

265. VALENTINE, J.S. and GRALLA, E.B. (1997) Delivering copper inside yeast and human cells. *Science* **278**: 817-818

266. NANJI, M.S. and COX, D.W. (1999) The copper chaperone Atox1 in canine copper toxicosis in Bedlington terriers. *Genomics* **62**: 108-112

267. PRIAT, C., HITTE, C., VIGNAUX, F., et al (1998) A whole-genome radiation hybrid map of the dog genome. *Genomics* **54**: 361-378

268. LUDWIG, J., KERSCHER, S., BRANDT, U., et al. (1998) Identification and characterization of a novel 9.2 kDa membrane sector-associated protein of vacuolar proton-ATPase from chromaffin granules. *J Biol Chem* **273**: 10939-10947

269. SZCZYPKA, M.S., ZHU, Z., SILAR, P. and THIELE, D.J. (1997) *Saccharomyces cerevisiae* mutants altered in vacuole function are defective in copper detoxification and iron-responsive gene transcription. *Yeast* **13**: 1423-1435

270. VAN DE SLUIS, B., KOLE, S., VAN WOLFEREN, M., et al. (2000) Refined genetic and comparative physical mapping of the canine copper toxicosis locus. *Mamm Genome* **11**: 455-460

271. MILLER, S.A., DYKES, D.D. and POLESKY, H.F. (1988) A simple salting out procedure for extracting DNA from human nucleated cells. *Nucleic Acids Res* **16**: 1215

272. LI, R., MIGNOT, E., FARACO, J., et al. (1999) Construction and characterization of an eightfold redundant dog genomic bacterial artificial chromosome library. *Genomics* **58**: 9-17

273. MAESTRE, J., TCHENIO, T., DHELLIN, O. and HEIDMANN, T. (1995) mRNA retroposition in human cells: processed pseudogene formation. *EMBO J* **14**: 6333-6338

274. MCCARREY, J.R. and THOMAS, K. (1987) Human testis-specific PGK gene lacks introns and possesses characteristics of a processed gene. *Nature* **326**: 501-505

275. COX, D.W. (1995) Genes of the copper pathway. *Am J Hum Genet* **56**: 828-834

276. HARDY, R.M. and STEVENS, J.B. (1978) Chronic progressive hepatitis in Bedlington terriers. *Proc AAHA* **45**: 187-190

277. ROTHUIZEN, J., UBBINK, G.J., VAN ZON, P., TESKE, E., VAN DEN INGH, T.S. and YUZBASIYAN-GURKAN, V. (1999) Diagnostic value of a microsatellite DNA marker for copper toxicosis in West-European Bedlington terriers and incidence of the disease. *Anim Genet* **30**: 190-194

278. HOLMES, N.G., HERRTAGE, M.E., RYDER, E.J. and BINNS, M.M. (1998) DNA marker C04107 for copper toxicosis in a population of Bedlington terriers in the United Kingdom. *Vet Rec* **142**: 351-352

279. DANCIS, A., YUAN, D.S., HAILE, D., et al. (1994) Molecular characterization of a copper transport protein in *S. cerevisiae*: An unexpected role for copper in iron transport. *Cell* **76**: 393-402

280. KAMPFENKEL, K., KUSHNIR, S., BABIYCHUK, E., INZE, D. and VAN MONTAGU, M. (1995) Molecular characterization of a putative *Arabidopsis thaliana* copper transporter and its yeast homologue. *J Biol Chem* **270**: 28479-28486

281. KOSKINEN, M.T. and BREDBACKA, P. (1999) A convenient and efficient microsatellite-based assay for resolving parentages in dogs. *Anim Genet* **30**: 148-149

282. NABETANI, A., HATADA, I., MORISAKI, H., OSHIMURA, M. and MUKAI, T. (1997) Mouse *U2af1-rs1* is a neomorphic imprinted gene. *Mol Cell Biol* **17**: 789-798

283. ZHANG, Y., AKILESH, S. and WILCOX, D.E. (2000) Isothermal titration calorimetry measurements of Ni(II) and Cu(II) binding to His, GlyGlyHis, HisGlyHis, and bovine serum albumin: a critical evaluation. *Inorg Chem* **39**: 3057-3064

284. JOHNSON, G.F., GILBERTSON, S.R., GOLDFISCHER, S., GRUSHOFF, P.S. and STERNLIEB, I. (1984) Cytochemical detection of inherited copper toxicosis of Bedlington terriers. *Vet Pathol* **21**: 57-60

285. HAYWOOD, S., FUENTEALBA, I.C., KEMP, S.J. and TRAFF[illegible]D, J. (2001) Copper toxicosis in the Bedlington terrier: a diagnostic dilemma. *J Small Anim[illegible]act* **42**: 181-185

286. PROSCHOWSKY, H.F., JEPSEN, B., JENSEN, H.E., JENSEN, A.L. and FREDHOLM, M. (2000) Microsatellite marker C04107 as a diagnostic marker for copper toxicosis in the Danish population of Bedlington terriers. *Acta Vet Scand* **41**: 345-350

287. BREATHNACH, R., BENOIST, C., O'HARE, K., GANNON, F. and CHAMBON, P. (1978) Ovalbumin gene: evidence for a leader sequence in mRNA and DNA sequences at the exon-intron boundaries. *Proc Natl Acad Sci USA* **75**: 4853-4857

288. THORNBURG, L.P., SHAW, D., DOLAN, M., et al. (1986) Hereditary copper toxicosis in West Highland white terriers. *Vet Pathol* **23**: 148-154

289. SPEE, B., MANDIGERS, P.J., ARENDS, B., et al. (2005) Differential expression of copper-associated and oxidative stress related proteins in a new variant of copper toxicosis in Doberman pinschers. *Comp Hepatol* **4**: 3

290. COOPER, V.L., CARLSON, M.P., JACOBSON, J. and SCHNEIDER, N.R. (1997) Hepatitis and increased copper levels in a dalmatian. *J Vet Diag Invest* **9**: 201-203

291. NOAKER, L.J., WASHABAU, R.J., DETRISAC, C.J., HELDMANN, E. and HENDRICK, M.J. (1999) Copper associated acute hepatic failure in a dog. *J Am Vet Med Assoc* **214**: 1502-1506

292. MANDIGERS, P.J., VAN DEN INGH, T.S., SPEE, B., PENNING, L.C., BODE, P. and ROTHUIZEN, J. (2004) Chronic hepatitis in Doberman pinschers. A review. *Vet Q* **26**: 98-106

293. SPEETI, M., ERIKSSON, J., SAARI, S. and WESTERMARCK, E. (1998) Lesions of subclinical doberman hepatitis. *Vet Pathol* **35**: 361-369

294. WEBB, C.B., TWEDT, D.C. and MEYER, D.J. (2002) Copper-associated liver disease in Dalmatians: a review of 10 dogs (1998-2001). *J Vet Intern Med* **16**: 665-668

295. CORONADO, V.A., DAMARAJU, D. and COX, D.W. (2003) New haplotypes in the Bedlington terrier indicate complexity in copper toxicosis. *Mamm Genome* **14 (7)**: 483-493

296. HYUN, C., LAVULO, L.T. and FILIPPICH, L.J. (2004) Evaluation of haplotypes associated with copper toxicosis in Bedlington Terriers in Australia. *Am J Vet Res* **65**: 1573-1579

297. TAO, T.Y., LIU, F., KLOMP, L., WIJMENGA, C. and GITLIN, J.D. (2003) The copper toxicosis gene product MURR1 directly interacts with the Wilson disease protein. *J Biol Chem* **278**: 41593-41596

298. DEN DUNNEN, J.T. and ANTONARAKIS, S.E. (2001) Nomenclature for the description of human sequence variations. *Hum Genet* **109**: 121-14

299. ARORA, R.G., ANDERSSON, L., BUCHT, R.S., FRANK, A. and KRONEVI, T. (1977) Chronic copper toxicosis in sheep. *Nord Vet Med* **29**: 181-187

300. SOLI, N.E. (1980) Chronic copper poisoning in sheep. A review of the literature. *Nord Vet Med* **32**: 75-89

301. LOCKHART, P.J., WILCOX, S.A., DAHL, H.M. and MERCER, J.F. (2000) Cloning, mapping and expression analysis of the sheep Wilson disease gene homologue. *Biochim Biophys Acta* **1491**: 229-239

302. NG, P.C. and HENIKOFF, S. (2003) SIFT: Predicting amino acid changes that affect protein function. *Nucleic Acids Res* **31**: 3812-3814

303. GUYON, R., LORENTZEN, T.D., HITTE, C., et al. (2003) A 1-Mb resolution radiation hybrid map of the canine genome. *Proc Natl Acad Sci USA* **100**: 5296-5301

304. HOLCIK, M. and KORNELUK, R.G. (2001) XIAP, the guardian angel. *Nat Rev Mol Cell Biol* **2**: 550-556

305. BURSTEIN, E., GANESH, L., DICK, R.D., et al. (2004) A novel role for XIAP in copper homeostasis through regulation of MURR1. *EMBO J* **23**: 244-254

306. BURSTEIN, E., HOBERG, J.E., WILKINSON, A.S., et al. (2005) COMMD proteins: A novel family of structural and functional homologs of MURR1. *J Biol Chem* **280**: 22222-22232

307. STUEHLER, B., REICHERT, J., STREMMEL, W. and SCHAEFER, M. (2004) Analysis of the human homologue of the canine copper toxicosis gene *MURR1* in Wilson disease patients. *J Mol Med* **82**: 629-634

308. COX, D.W. and KENNEY, S. (2004) Wilson disease mutation on-line database: http://www.uofa-medical-genetics.org/wilson/index.php

309. STEINDL, P., FERENCI, P., DIENES, H.P., et al. (1998) Wilson's disease in patients with liver disease: A diagnostic challenge. *Gastroenterology* **113**: 212-218

310. GANESH, L., BURSTEIN, E., GUHA-NIYOGI, A., et al. (2003) The gene product MURR1 restricts HIV-1 replication in resting CD4+ lymphocytes. *Nature* **426**: 853-857

311. BIASIO, W., CHANG, T., MCINTOSH, C.J. and MCDONALD, F.J. (2003) Identification of MURR1 as a regulator of the human delta epithelial sodium channel. *J Biol Chem* **279**: 5429-5434

312. CORONADO, V.A., BONNEVILLE, J.A., NAZER, H., ROBERTS, E.A. and COX, D.W. (2005) *COMMD1 (MURR1)* as a candidate in patients with copper storage disease of undefined etiology. *Clin Genet* **68**: 548-551

313. WU, Z.Y., ZHAO, G.X., CHEN, W.J., et al. (2006) Mutation analysis of 218 Chinese patients with Wilson disease revealed no correlation between the canine copper toxicosis gene MURR1 and Wilson disease. *J Mol Med* **84**: 438-442

314. AUSUBEL, F.M., BRENT, R., KINGSTON, R.E., et al. (1998) *Current Protocols in Molecular Biology*. New York: John Wiley and Sons, Inc.

315. GNOATTO, N., LOTUFO, R.F., TOFFOLETTO, O. and MARQUEZINI, M.V. (2003) Gene expression of extracellular matrix proteoglycans in human cyclosporin-induced gingival overgrowth. *J Periodontol* **74**: 1747-1753

316. KLOMP, A.E., VAN DE SLUIS, B., KLOMP, L.W. and WIJMENGA, C. (2003) The ubiquitously expressed MURR1 protein is absent in canine copper toxicosis. *J Hepatol* **39**: 703-709

317. LA FONTAINE, S., THEOPHILOS, M.B., FIRTH, S.D., GOULD, R., PARTON, R.G. and MERCER, J.F. (2001) Effect of the toxic milk mutation (*tx*) on the function and intracellular localization of Wnd, the murine homologue of the Wilson copper ATPase. *Hum Mol Genet* **10**: 361-370

318. SEN, A., STEELE, R., GHOSH, A.K., BASU, A., RAY, R. and RAY, R.B. (2003) Inhibition of hepatitis C virus protein expression by RNA interference. *Virus Res* **96**: 27-35

319. ZHANG, Z., JOH, K., YATSUKI, H., et al. (2006) Comparative analyses of genomic imprinting and CpG island-methylation in mouse *Murr1* and human *MURR1* loci revealed a putative imprinting control region in mice. *Gene* **366**: 77-86

320. WANG, Y., JOH, K., MASUKO, S., et al (2004) The mouse *Murr1* gene is imprinted in the adult brain, presumably due to transcriptional interference by the antisense-oriented *U2af1-rs1* gene. *Mol Cell Biol* **24**: 270-279

321. WANG, Y., JOH, K. and MUKAI, T. (2002) Identification of a novel isoform of *Murr1* transcript, *U2mu*, which is transcribed from the portions of two closely located but oppositely oriented genes. *Genes Genet Syst* **77**: 377-381

322. DE BIE, P., VAN DE SLUIS, B., BURSTEIN, E., et al. (2006) Characterization of COMMD protein-protein interactions in NF-kappaB signalling. *Biochem J* **398**: 63-71

323. DE BIE, P., VAN DE SLUIS, B., KLOMP, L. and WIJMENGA, C. (2005) The many faces of the copper metabolism protein MURR1/COMMD1. *J Hered* **96**: 803-811

324. MCDONALD, F.J., PRICE, M.P., SNYDER, P.M. and WELSH, M.J. (1995) Cloning and expression of the beta- and gamma-subunits of the human epithelial sodium channel. *Am J Physiol* **268**: C1157-C1163

325. CANESSA, C.M., SCHILD, L., BUELL, G., et al. (1994) Amiloride-sensitive epithelial Na+ channel is made of three homologous subunits. *Nature* **367**: 463-467

326. WALDMANN, R., CHAMPIGNY, G., BASSILANA, F., VOILLEY, N. and LAZDUNSKI, M. (1995) Molecular cloning and functional expression of a novel amiloride-sensitive Na+ channel. *J Biol Chem* **270**: 27411-27414

327. SNYDER, P.M. (2005) Minireview: regulation of epithelial Na+ channel trafficking. *Endocrinology* **146**: 5079-5085

328. SUZUKI, Y., NAKABAYASHI, Y. and TAKAHASHI, R. (2001) Ubiquitin-protein ligase activity of X-linked inhibitor of apoptosis protein promotes proteasomal degradation of caspase-3 and enhances its anti-apoptotic effect in Fas-induced cell death. *Proc Natl Acad Sci USA* **98**: 8662-8667

329. MACFARLANE, M., MERRISON, W., BRATTON, S.B. and COHEN, G.M. (2002) Proteasome-mediated degradation of Smac during apoptosis: XIAP promotes Smac ubiquitination in vitro. *J Biol Chem* **277**: 36611-36616

330. MUFTI, A.R., BURSTEIN, E., CSOMOS, R.A., et al. (2006) XIAP Is a Copper Binding Protein Deregulated in Wilson's Disease and Other Copper Toxicosis Disorders. *Mol Cell* **21**: 775-785

331. MOYNAGH, P.N. (2005) The NF-kappaB pathway. *J Cell Sci* **118**: 4589-4592

332. HOFER-WARBINEK, R., SCHMID, J.A., STEHLIK, C., BINDER, B.R., LIPP, J. and DE MARTIN, R. (2000) Activation of NF-kappa B by XIAP, the X chromosome-linked inhibitor of apoptosis, in endothelial cells involves TAK1. *J Biol Chem* **275**: 22064-22068

333. SUN, Q., MATTA, H. and CHAUDHARY, P.M. (2005) Kaposi's sarcoma associated herpes virus-encoded viral FLICE inhibitory protein activates transcription from HIV-1 Long Terminal Repeat via the classical NF-kappaB pathway and functionally cooperates with Tat. *Retrovirology* **2**: 9

334. MALEK, S., CHEN, Y., HUXFORD, T. and GHOSH, G. (2001) IkappaBbeta, but not IkappaBalpha, functions as a classical cytoplasmic inhibitor of NF-kappaB dimers by masking both NF-kappaB nuclear localization sequences in resting cells. *J Biol Chem* **276**: 45225-45235

335. HUSTER, D., HOPPERT, M., LUTSENKO, S., et al. (2003) Defective cellular localization of mutant ATP7B in Wilson's disease patients and hepatoma cell lines. *Gastroenterology* **124**: 335-345

336. ROELOFSEN, H., BALGOBIND, R. and VONK, R.J. (2004) Proteomic analyzes of copper metabolism in an in vitro model of Wilson disease using surface enhanced laser desorption/ionization-time of flight-mass spectrometry. *J Cell Biochem* **93**: 732-740

337. RADYUK, S.N., SOHAL, R.S. and ORR, W.C. (2003) Thioredoxin peroxidases can foster cytoprotection or cell death in response to different stressors: over- and under-expression of thioredoxin peroxidase in Drosophila cells. *Biochem J* **371**: 743-752

338. HARRAR, Y., BELLINI, C. and FAURE, J.D. (2001) FKBPs: at the crossroads of folding and transduction. *Trends Plant Sci* **6**: 426-431

339. SANCHEZ, E.R. (1990) Hsp56: a novel heat shock protein associated with untransformed steroid receptor complexes. *J Biol Chem* **265**: 22067-22070

340. BOSE, S., WEIKL, T., BUGL, H. and BUCHNER, J. (1996) Chaperone function of Hsp90-associated proteins. *Science* **274**: 1715-1717

341. SANOKAWA-AKAKURA, R., DAI, H., AKAKURA, S., et al. (2004) A novel role for the immunophilin FKBP52 in copper transport. *J Biol Chem* **279**: 27845-27848

342. CZAR, M.J., OWENS-GRILLO, J.K., YEM, A.W., et al. (1994) The hsp56 immunophilin component of untransformed steroid receptor complexes is localized both to microtubules in the cytoplasm and to the same nonrandom regions within the nucleus as the steroid receptor. *Mol Endocrinol* **8**: 1731-1741

343. GALIGNIANA, M.D., MORISHIMA, Y., GALLAY, P.A. and PRATT, W.B. (2004) Cyclophilin-A is bound through its peptidylprolyl isomerase domain to the cytoplasmic dynein motor protein complex. *J Biol Chem* **279**: 55754-55759

344. SCHROER, T.A. (2004) Dynactin. *Annu Rev Cell Dev Biol* **20**: 759-779

345. LIM, C.M., CATER, M.A., MERCER, J.F. and LA FONTAINE, S. (2006) Copper-dependent interaction of dynactin subunit p62 with the N terminus of ATP7B but not ATP7A. *J Biol Chem* **281**: 14006-14014

346. OWENS-GRILLO, J.K., CZAR, M.J., HUTCHISON, K.A., HOFFMANN, K., PERDEW, G.H. and PRATT, W.B. (1996) A model of protein targeting mediated by immunophilins and other proteins that bind to hsp90 via tetratricopeptide repeat domains. *J Biol Chem* **271**: 13468-13475

347. COX, D.W., PRAT, L., WALSHE, J.M., HEATHCOTE, J. and GAFFNEY, D. (2005) Twenty-four novel mutations in Wilson disease patients of predominantly European ancestry. *Hum Mut* **26**: 280.

348. PHINNEY, A.L., DRISALDI, B., LUGOWSHI, S., et al (2003) In vivo reduction of amyloid-β by a mutant copper transporter. *Proc Natl Acad Sci USA* **100**: 14193-14198

349. CHISHTI, M.A., YANG, D.S., JANUS, C., et al (2001) Early-onset amyloid deposition and cognitive deficits in transgenic mice expressing a double mutant form of amyloid precursor protein 695. *J Biol Chem* **276**: 21562-21570

350. BAYER, T.A. and MULTHAUP, G. (2005) Involvement of amyloid beta precursor protein (AbetaPP) modulated copper homeostasis in Alzheimer's disease. *J Alzheimers Dis* **8**: 201-215

351. ONO, S., KOROPATNICK, D.J. and CHERIAN, M.G. (1997) Regional brain distribution of metallothionein, zinc and copper in toxic milk mutant and transgenic mice. *Toxicology* **124**: 1-10

352. NADEAU, J.H. (2001) Modifier genes in mice and humans. *Nat Rev Genet* **2**: 165-174

353. CZACHOR, J.D., CHERIAN, M.G. and KOROPATNICK, J. (2002) Reduction of copper and metallothionein in toxic milk mice by tetrathiomolybdate, but not deferiprone. *J Inorg Biochem* **88**: 213-222

354. ALLEN, K.J., CHEAH, D.M., LEE, X.L., et al. (2004) The potential of bone marrow stem cells to correct liver dysfunction in a mouse model of Wilson's disease. *Cell Transplant* **13**: 765-773

355. ALLEN, K.J., CHEAH, D.M., WRIGHT, P.F., et al. (2004) Liver cell transplantation leads to repopulation and functional correction in a mouse model of Wilson's disease. *J Gastroenterol Hepatol* **19**: 1283-1290

356. SHI, Z., LIANG, X.L., LU, B.X., et al. (2005) Diminution of toxic copper accumulation in toxic milk mice modeling Wilson disease by embryonic hepatocyte intrasplenic transplantation. *World J Gastroenterol* **11**: 3691-3695

357. FAVIER, R.P., SPEE, B., PENNING, L.C., BRINKHOF, B. and ROTHUIZEN, J. (2005) Quantitative PCR method to detect a 13-kb deletion in the *MURR1* gene associated with copper toxicosis and HIV-1 replication. *Mamm Genome* **16**: 460-463

358. FORMAN, O.P., BOURSNELL, M.E., DUNMORE, B.J., et al. (2005) Characterization of the *COMMD1 (MURR1)* mutation causing copper toxicosis in Bedlington terriers. *Anim Genet* **36**: 497-501

359. VAN DE SLUIS, B., PETER, A.T. and WIJMENGA, C. (2003) Indirect molecular diagnosis of copper toxicosis in Bedlington terriers is complicated by haplotype diversity. *J Hered* **94**: 256-259

360. DIXON, J.W. and SARKAR, B. (1972) Absence of a specific copper(II) binding site in dog albumin is due to amino acid mutation in position 3. *Biochem Biophys Res Commun* **48**: 197-200

361. WEISS, K.H., MERLE, U., SCHAEFER, M., FERENCI, P., FULLEKRUG, J. and STREMMEL, W. (2006) Copper toxicosis gene *MURR1* is not changed in Wilson disease patients with normal blood ceruloplasmin levels. *World J Gastroenterol* **12**: 2239-2242

362. HANDY, R.D., EDDY, F.B. and BAINES, H. (2002) Sodium-dependent copper uptake across epithelia: a review of rationale with experimental evidence from gill and intestine. *Biochim Biophys Acta* **1566**: 104-115

363. TERHEGGEN-LAGRO, S.W., RIJKERS, G.T. and VAN DER ENT, C.K. (2005) The role of airway epithelium and blood neutrophils in the inflammatory response in cystic fibrosis. *J Cyst Fibros* **4S-2**: 15-23

364. LEBOWITZ, J., EDINGER, R.S., AN, B., et al (2004) Ikappab kinase-beta (ikkbeta) modulation of epithelial sodium channel activity. *J Biol Chem* **279**: 41985-41990

365. ISEKI, A., KAMBE, F., OKUMURA, K., et al. (2000) Pyrrolidine dithiocarbamate inhibits TNF-alpha-dependent activation of NF-kappaB by increasing intracellular copper level in human aortic smooth muscle cells. *Biochem Biophys Res Commun* **276**: 88-92

366. CISTERNAS, F.A., TAPIA, G., ARREDONDO, M., et al. (2005) Early histological and functional effects of chronic copper exposure in rat liver. *Biometals* **18**: 541-551

367. YE, J., DING, M., ZHANG, X., et al. (1999) Induction of TNFalpha in macrophages by vanadate is dependent on activation of transcription factor NF-kappaB and free radical reactions. *Mol Cell Biochem* **198**: 193-200

368. SCHWABE, R.F. and BRENNER, D.A. (2006) Mechanisms of liver injury. I. TNF-alpha-induced liver injury: role of IKK, JNK, and ROS pathways. *Am J PhysiolGastrointestLiver Physiol* **290**: G583-G589

369. FONG, R.N., GONZALEZ, B.P., FUENTEALBA, I.C. and CHERIAN, M.G. (2004) Role of tumor necrosis factor-alpha in the development of spontaneous hepatic toxicity in Long-Evans Cinnamon rats. *Toxicol Appl Pharmacol* **200**: 121-130

370. LINDBLAD-TOH, K., WADE, C.M., MIKKELSEN, T.S., et al. (2005) Genome sequence, comparative analysis and haplotype structure of the domestic dog. *Nature* **438**: 803-819

371. CONKLIN, D.C. and GAO, Z. (2001) Helical polypeptide zalpha29. *WIPO patent WO/2002/000831*

372. WIJMENGA, C. and KLOMP, L.W. (2004) Molecular regulation of copper excretion in the liver. *Proc Nutr Soc* **63**: 31-39